

**Intersubunit Cross-talk in the Betaine Permease
BetP from
*Corynebacterium glutamicum***

**Inaugural-Dissertation
zur Erlangung des Doktorgrades**
der Mathematisch-Naturwissenschaftlichen Fakultät
der Universität zu Köln
vorgelegt von

Markus Christian Becker
aus Daun

Copy-Star Druck und Werbung GmbH
Köln 2013

Diese Arbeit wurde am Institut für Biochemie der Universität zu Köln unter Anleitung von Herrn Professor Dr. R. Krämer durchgeführt.

Berichtersteller: Professor Dr. R. Krämer
Professor Dr. U.- I. Flügge
Professor Dr. C. Ziegler

Tag der mündlichen Prüfung: 23.Mai 2013

„Unsere größte Schwäche liegt im Aufgeben. Der sichere Weg zum Erfolg ist immer es doch noch einmal zu versuchen.“

(Thomas Alva Edison)

Contents

Contents	I
Abbreviations	IV
1 Introduction	1
1.1 Osmotic stress	1
1.2 Osmosensors	2
1.3 The betaine permease BetP	3
1.4 The LeuT family of transporters	6
1.5 Transport mechanism of LeuT type carriers	7
1.6 Transport mechanism of BetP	9
1.7 Quarternary structure of BetP and its implications for cross-talk.....	10
1.8 Cross-talk in transport proteins and methods for its analysis	13
1.9 The osmo-transportome of <i>C. glutamicum</i>	15
2 Experimental procedures	17
2.1 Bacterial strains, plasmids and oligonucleotids	17
2.1.1 Bacterial strains	17
2.1.2 Plasmids.....	17
2.1.3 Oligonucleotides.....	20
2.1.4 Growth media and cultivation conditions	23
2.2 Molecular biology.....	24
2.2.1 Preparation of competent <i>E. coli</i> cells and transformation	24
2.2.2 Preparation of electrocompetent <i>C. glutamicum</i> cells and transformation.....	24
2.2.3 DNA techniques	25
2.2.3.1 Isolation of plasmid DNA from <i>E. coli</i>	25
2.2.3.2 Gel electrophoresis and extraction of DNA from agarose gels.....	25
2.2.3.3 Polymerase chain reaction (PCR)	25
2.2.3.4 Restriction, ligation, and sequencing of DNA	26
2.2.3.5 Site directed mutagenesis.....	26
2.2.3.6 DNA sequencing:.....	27
2.3 Analytical methods.....	27

2.3.1	Protein concentration measurements	27
2.3.2	Sodium-dodecyl-sulphate-polyacrylamid-gel-elektrophoresis (SDS-PAGE)	27
2.3.3	Blue-native-polyacrylamid-gel-elektrophoresis (BN-PAGE).....	27
2.3.4	Western-Blot	28
2.3.5	Gel-Permeation-Chromatography	28
2.3.6	Estimation of osmolalities.....	28
2.3.7	Fluorescence microscopy.....	28
2.4	Biochemical Methods	29
2.4.1	Heterologous expression	29
2.4.1.1	Heterologous expression in <i>E. coli</i> in shaker flasks.....	29
2.4.1.2	Heterologous expression in <i>E. coli</i> in bioreactor cultures	29
2.4.1.3	Heterologous expression of proteins in <i>C. glutamicum</i>	30
2.4.2	Isolation of membrane proteins.	30
2.4.2.1	Isolation of membrane proteins via bead mill.....	30
2.4.2.2	Isolation of membrane proteins via french press.....	31
2.4.3	Purification of membrane proteins via affinity tags	31
2.4.3.1	Solubilisation of membrane proteins	31
2.4.3.2	Purification of Strep tagged proteins:	31
2.4.3.3	Purification of His tagged proteins:	32
2.4.3.4	Purification of Flag tagged proteins.....	32
2.4.3.5	Purification of MBP tagged proteins.....	32
2.4.4	Chemical protein modifications	33
2.4.4.1	Protein labeling with Bodipy dye.....	33
2.4.4.2	Protein labeling with Biotin	33
2.4.5	Reconstitution of Proteins	33
2.4.5.1	Preparation of liposomes	33
2.4.5.2	Reconstitution of proteins.....	34
2.4.6	Radiochemical transport measurements.....	34
2.4.6.1	Betaine uptake measurements of BetP and LcoP in proteoliposomes	34
2.4.6.2	Betaine uptake measurements in <i>E. coli</i> MKH13 cells.....	35
2.4.6.3	Betaine uptake measurements in <i>C. glutamicum</i> DHPF cells.....	36
3	Results.....	37
3.1	Genetic fusion of BetP trimers	37
3.1.1	Fusion BetP: a. pFus	37

3.1.2	Fusion BetP: b. pFel	40
3.2	Individually tagged BetP	46
3.2.1	N-terminal affinity tags.....	46
3.3	Stability of BetP trimers	54
3.4	C-terminal affinity tags.....	55
3.5	Co-expression and purification of BetP heteromers.....	58
3.6	Cross-talk in BetP heteromers	62
3.6.1	Catalytical cross-talk in BetP.....	62
3.6.2	Regulatory cross-talk in BetP.....	65
3.7	Re-analysis of monomeric BetP	67
3.8	BetP dynamics via single molecule fluorescence.....	72
3.9	Analysis of the osmo-transportome of <i>C. glutamicum</i>	75
4	Discussion.....	80
4.1	LcoP is an osmo-sensor	80
4.2	Monomeric BetP ?.....	82
4.3	Genetic fusion of BetP trimers	84
4.4	The N-terminal domain is sensitive to alterations.....	88
4.5	State of art in the hetero-trimeric BetP production: applications in single molecule approaches and limitations	89
4.6	The nature of cross-talk in BetP	90
5	Abstract	95
6	Zusammenfassung	96
7	References	97
	Danksagung.....	107
	Erklärung	108

Abbreviations

AHT	Anhydrotetracycline
APS	Ammoniapersulfat
BCCT	Betaine-Choline-Carnitine-Transporter
BHI	Brain-Heart-Infusion
Carb	Carbenicillin
CBD	Chitin-Binding-Domain
CBP	Calmodlin-Binding-Pepitde
Cdw	cellular dry weight
Cm	Chloramphenicol
DDM	Dodecylmaltoside
DNA	Deoxyribonucleicacid
EDTA	Ethylendiaminetetramin
EAAT	Excitatory-Amino-Acid-Transporter
GST	Glutathione-S-Transferase
IPTG	Isopropyl-b-Thiogalactoside
LB	Lysogeny-Broth
LDAO	Lauroyl-Dimethyl-Amineoxide
MBP	Maltose-Binding-Protein
MFS	Major-Faciliator-Superfamily
NCS1	Nucleobase-Cation-Symporter
Rpm	rounds per minute
SEC	Size Exclusion Chromatography
TEV	Tobacco Etch Virus

1 Introduction

1.1 Osmotic stress

Unicellular organisms face rapid and severe changes in the external osmolality. Due to the permeability of the cell membrane for water, its activity equilibrates fast through the membrane between medium and cytoplasm (Wood 1999). Under physiological conditions the water activity in the cytoplasm is lower than in the surrounding medium so that the turgor can be established. Turgor describes the pressure with which the plasma membrane is pushed against the cell wall. This pressure was shown to be necessary for cell division and growth in bacteria (Koch 2000). Cells may have to encounter generally to different osmotic stress conditions in which water permeates the cell membrane, due to lowered (hyper-osmotic stress) or enlarged (hypo-osmotic stress) external water activity.

Cell integrity under hypo-osmotic stress is achieved by mechanosensitive channels. These proteins can be activated *in vitro* by pressure gradients indicating that they percept directly raising membrane tension as indicator for cell swelling. Upon opening, these channels release a broad spectrum of low molecular weight compounds thereby increasing the water activity in the cytoplasm (Sukharev et al., 1997).

Upon hyper-osmotic stress the cells take up or synthesise solutes to lower the internal water activity without cytoplasm shrinkage. Not every compound is equally well suited for this purpose. Solutes utilised for lowering the water activity should exhibit no detrimental interference with cytoplasmic compounds e.g. proteins, DNA, etc.

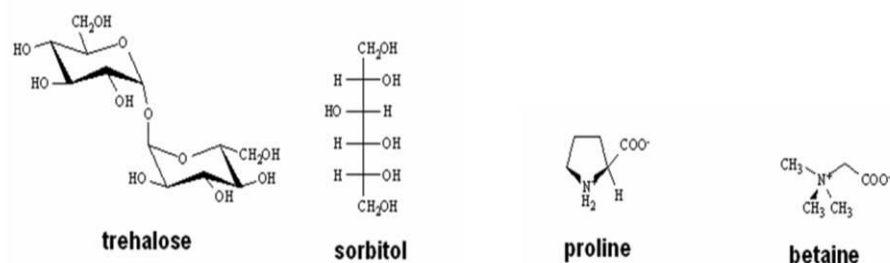


Fig. 1-1: Chemical structure representation of different compatible solutes.

Such compounds are called compatible solutes. The main compatible solutes utilised by bacteria are amino acids and derivatives like proline and betaine, or sugars and polyols like trehalose and sorbitol (Fig. 1-1). The common feature of those compounds is that they form thermodynamically unfavorable interactions with unfolded proteins thereby stabilising the native folded state (Rösgen et al., 2005).

The temporal organisation of adaption to hyper-osmotic stress is very common in all mesophiles for which it was investigated. First the cells take up potassium to maintain turgor. Interestingly it is still not clear how the influx of positive charges is compensated. Potassium ions are then replaced by compatible solutes taken up from the medium or synthesised in the cytoplasm. In the late state of adaption the gene expression is re-modeled by mainly two-component systems perceiving the osmotic stress (Wood 1999).

Solute synthesis is normally much more energy intensive than uptake. Therefore bacteria have evolved a variety of solute uptake systems. The systems for both solute uptake and synthesis are usually redundant. Interestingly the different solute transporters belong to completely different transport protein families suggesting the independent evolution of different uptake systems and thus highlighting the impact of osmotic stress.

1.2 Osmosensors

Within the large group of solute transport proteins only three have been ultimately shown to sense hyper-osmotic stress without any other factor in proteoliposomes:

(i) OpuA is an ABC transporter for betaine and was described in *Lactococcus lactis*. Resembling the common bacterial ABC transporter architecture, the protein is composed out of two transmembrane domains fused to a periplasmic binding domain and two nucleotide binding domains (NBD). The NBDs carry a C-terminal extension harbouring a tandem β -cystathionine-synthase (CBS) domain followed by a short extension with a cluster of glutamate residues (Van der Heide & Poolman 2000). The transporter was shown to be activated by increasing ionic strength (Van der Heide et al., 2001). The osmo-regulation of this transporter is abolished by deletion of the CBS, whereas deletion of the anionic C-terminal domain leads to regulatory dependence on the head groups of the

membrane lipids. Mutations in exposed cationic residues also lead to deregulation of the transporter. It is likely that the C-terminal domain of OpuA senses salt stress via disturbance of ionic interaction with the membrane (Mahmood et al. 2009; Biemans-Oldehinkel et al. 2006).

(ii) ProP from *Escherichia coli* is a secondary active transporter that mediates import of betaine and prolin together with protons. The transporter belongs to the major facilitator superfamily (MFS) and consists of twelve transmembrane helices. 60 amino acids at the transporters C-terminus form a coiled coil structure in the cytosol and are shown to be important for the activation threshold of the transporter (Hillar et al., 2005). Osmoregulation of this transporter depends on the lipid environment (Romantsov et al., 2008; Tsatskis et al., 2005). Interestingly the transporter seems to co-localise with cardiolipin at the cell poles suggesting functional inhomogeneity of the cell membrane. (Romantsov et al. 2008; 2010). ProP is activated by all kinds of hyper-osmotic stress including ionic strength, concentration of neutral molecules and macromolecules. This finding suggests that this transporter senses directly its hydration state (Racher et al. 2001; Culham et al. 2003; Wood 2006).

1.3 The betaine permease BetP

The protein BetP was discovered functionally as osmoregulated betaine/Na⁺ symport carrier mediating fast (up to 110 nmol x mg_{cdw}⁻¹ x min⁻¹) and high affine (K_{m(betaine)}=8,6 μM) import of this solute in *C. glutamicum* (Farwick et al., 1995). The carrier encoding gene was identified by functional complementation of an *E. coli* mutant unable to import or synthesise betaine (Peter et al. 1996). BetP could be purified via an amino terminal StrepII™-tag (Strep-tag) out of *E. coli* and reconstituted to proteoliposomes where it retained its ability to conduct the import of Na⁺/betaine driven by the sodium motive force (Rübenhagen et al., 2000). The protein is activated exclusively by raising K⁺ (Rb⁺, Cs⁺) concentration in proteoliposomes suggesting this as being the only relevant stimulus (Schiller et al. 2004; Rübenhagen et al. 2001). However it was shown *in vivo*, that potassium is not the only stimulus (Ott 2009). BetP belongs to the betaine choline-carnithine transporter (BCCT) family characterised by these substrates. These substrates share a

positively charged quarternary nitrogen atom which is coordinated by a highly conserved motif of aromatic amino acids (Ziegler et al. 2010). It possess 12 transmembrane helices and N-, and C-terminal extensions of 59/49 amino acids. These extensions are both located in the cytoplasm (Peter et al. 1996; Rübenhagen et al. 2001). Both extensions were shown to be involved in BetP activation (Peter et al. 1998). The C-terminal domain of BetP was also identified *in vitro* to be responsible for the perception of rising K^+ concentrations (Schiller & Morbach 2004). Via site directed mutagenesis of the C-domain and functional analysis of the resultant BetP variants in *E. coli* and *C. glutamicum* it was concluded that this domain interacts with the membrane lipids and that not only its charge but also its structure is important for correct signal transduction (Schiller et al. 2006; Ott et al. 2008). The interactions of the C-domain were shown via peptide binding array experiments to occur also with the cytoplasmic loops L2, L4; L8, the N-domain and the C-domain of the adjacent protomers showing that the regulation mechanism is much more complicated (Ott et al. 2008). Because of its high stability in detergent solutions, BetP was also chosen as target for structural analysis. A 2D projection map at an resolution of 0,75 nm showed that BetP is a homotrimer where every monomer is most likely to form its own betaine translocation pathway.

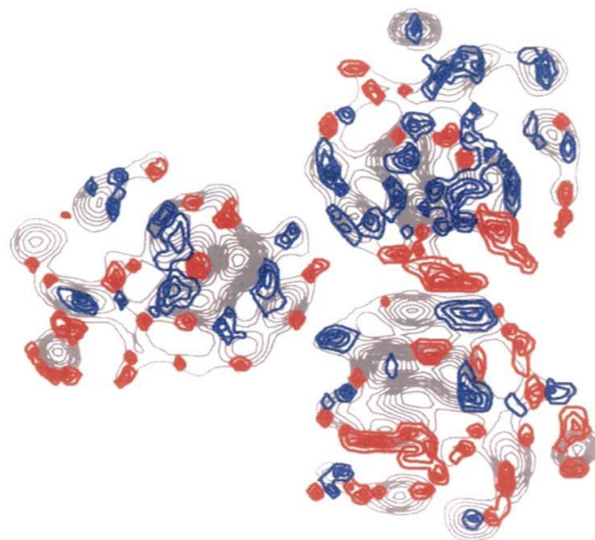


Fig. 1-2: Electron density projection map of 2D BetP crystals (Ziegler et al. 2004). Differences from the average densities are highlighted in red (additional densities) and blue (missing densities).

Interestingly the subunits were shown to be not symmetrical to each other which is a first hint for catalytical or regulative cross-talk (Fig. 1-2) (Ziegler et al. 2004; Tsai et al. 2011). The protein was also crystallised in detergent solubilised state in type II 3D crystals (Ressl et al., 2009). Many features of the solved structure are consistent with functional observations and bioinformatic predictions. Each protomer consists of twelve transmembrane helices. The substrate was found to be bound in an aromatic box build by the side chains of tryptophanes and one tyrosine (Ressl et al., 2009).

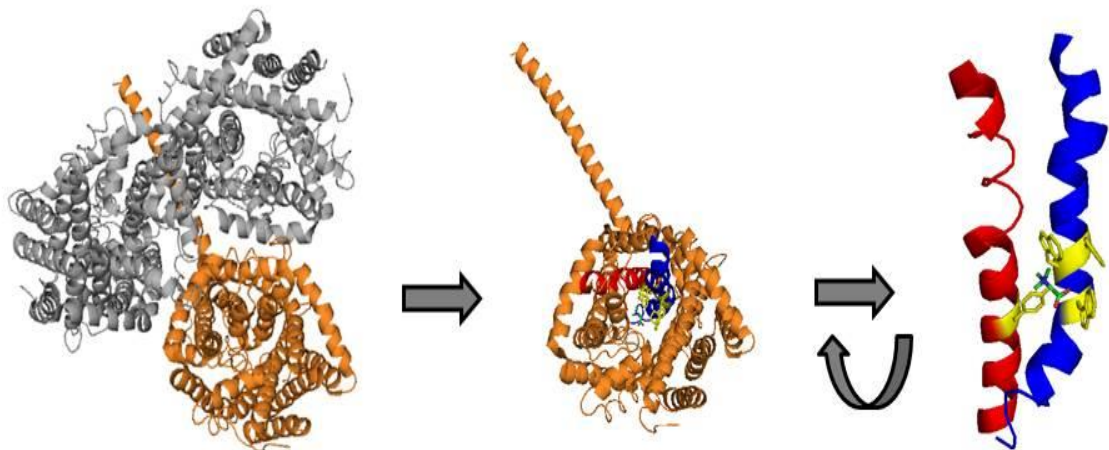


Fig. 1-3: Structure of the BetP trimer (left). One subunit shown with the residues of the betaine binding motif highlighted in yellow (middle). Structural arrangement of the tryptophane and tyrosine residues (red) contributing to betaine binding located on TM8 (blue) and TM4 (red) (right). (modified from PDB entry: 2WIT)

The two co-transported sodium ions are bound in remarkably distant sites. The first sodium binding site (Na2) is formed by backbone and sidechain carbonyl oxygens of residues in TM 7 and 3. The second sodium binding site (Na1) is formed by residues of TM 5 and 8. Mutations in the respective residues abolished sodium binding and sodium coupled transport completely (Khafizov et al., 2012). Whereas the Na2 site was found by structural alignments of BetP with the NSS type transporter LeuT, the Na1 site was established by symmetry investigations of the TM helix arrangement in BetP. The successful elaboration of the sodium binding sites was only possible, because the BetP structure exhibits a remarkable global fold that was shown in the last years to hold true for many different

secondary active transporters and was first discovered in the LeuT structure: the inverted repeat motif (Forrest et al., 2008; Krishnamurthy et al., 2009; Yamashita et al., 2005)

1.4 The LeuT family of transporters

The inverted repeat motif consists of ten transmembrane helices.

tab. 1-1: Different secondary active transport proteins all shown to comprise the inverted repeat architecture first described for the NSS-type transporter LeuT.

transporter	substrate/mechanism	family	source
LeuT	Leucine/Na ⁺ symport	NSS	(Yamashita et al., 2005)
vSglT	galactose/Na ⁺ symport	SSS	(Faham et al., 2008)
Mhp1	benzylhydantoin/Na ⁺ symport	NCS1	(Weyand et al., 2008; (Shimamura et al. 2010)
CaiT	carnithine/ γ -butyrobateine antiport	BCCT	(Tang et al., 2010)
AdiC	arginin/agmatin antiport	APC	(Gao et al., 2009)
ApcT	Amino acid/ H ⁺ symport	APC	(Shaffer et al., 2009)
Glt _{PH}	Glutamate/Na ⁺ symport	EAAT	(Yernool et. al 2005)

The first five transmembrane helices are structurally related to the following five ones by a two-fold symmetry axis in the membrane plane. This fold contains the transporter core where the transport reaction takes place (Fig. 1-4).

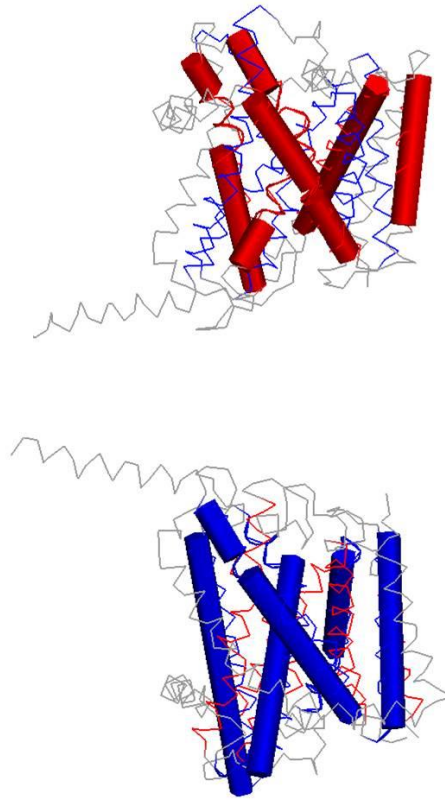


Fig. 1-4: The inverted repeat motifs in the structure of a single BetP protomer. First repeat (red) formed by TM3-TM7 and second repeat (blue) formed by TM8-TM12. The c terminal domain as well as the TM1 and 2 not taking part in the formation of the inverted repeat motif are shown in grey. (Modified from PDB entry: 2WIT)

The first two transmembrane helices of each repeat form a tight bundle, whereas the latter two of each repeat form a scaffold which is called a hash domain according to arrangement of the helices (Abramson and Wright, 2009; Krishnamurthy et al., 2009). Interestingly, this architecture was found in transporters of completely distinct families (tab.1-1).

1.5 Transport mechanism of LeuT type carriers

According to the generally accepted model of alternating access (Tanford, 1983) of a single substrate binding site mediating transport in secondary active transporters, at least three different conformations (binding site accessible from the cytoplasm C_i ; binding site accessible from the periplasm C_e and binding site not accessible from both compartments C_c) have to be realised during the transport cycle (Jardetzky 1966). The binding site is mainly build by the first helices of each repeat and located halfway across the membrane in

LeuT type transporters (Abramson and Wright, 2009). From the different available structures of LeuT type transporters in different conformations, a model for the realisation of the alternating access of the binding site during transport was proposed. This model proposes a relative rocking type movement of the 4 helix bundle against the hash domain as being responsible for the necessary accessibility change of the binding site during the catalytic cycle (Forrest and Rudnick, 2009; Shimamura et al., 2010).

Mhp1 was the first member of the LeuT family that was crystallised in the Ce; Ci and Cc conformation. From this structure the model could convincingly be extended by sub-states occluding the binding site by so-called gating residues prior to the global conformational change in the Ce-Ci transition (Shimamura et al., 2010).

Although good evidence exists for the global conformational transition of LeuT type transporters during transport, the mechanism of coupling the free enthalpy of substrate and co-substrate flux is poorly understood. Molecular dynamic simulations of the sugar transporter vSglT suggested the obligatory order of substrate release as the molecular realisation of free enthalpy coupling (Watanabe et al., 2010). The LeuT transporter itself has recently been crystallised by use of conformation specific antibodies in different conformations. From these structures it was concluded that binding of the substrate to the outward open, sodium bound conformation is the trigger for closure of the extracellular exit leading in addition to the disruption of the two sodium binding sites. It is however not clear how the substrate is released to the cytoplasm as no inward occluded structure of this transporter is available (Krishnamurthy and Gouaux, 2012).

Several substrate binding sites assigned to the structures of different LeuT type transporters lead to the assumption of regulatory involvement of additional substrate binding sites in the transport pathways of these transporters. In the structure of the BCC-type carnithin/ γ -butyrobetaine antiporter CaiT a second γ -butyrobetaine binding site near the periplasmic end of the substrate pathway was found. Mutations in this site abolished the slight cooperativity observed in binding of both substrates (Schulze et al. 2010). A possible second substrate binding site in the transporter LeuT and its functional relevance is still not clear (Zhao et al. 2011; Quick et al. 2012; Shi et al. 2008; Piscitelli et al. 2010; Krishnamurthy & Gouaux 2012). BetP comprises an exception of all LeuT-family members found so far because it is the only member of this group where transport activity is regulated on a

biochemical level which necessitates the occurrence of more substates resembling active and inactive states of the protein (Ziegler et al. 2010).

1.6 Transport mechanism of BetP

As the structure of BetP has recently been established in different conformational states (Perez et al. 2012; 2011) it was possible to assign the transport cycle according to the generally accepted alternating access model (Jardetzky 1966). The state of the art model of alternating access during the betaine/sodium co-transport in BetP mainly involves the molecular displacements of the first and last helix of each repeat, TM3; 7; 8 and 12 for realisation of the change of accessibility during the transport cycle (Perez et al., 2012). Binding and dissociation of the substrate betaine is mainly achieved by different rotamer conformations of the aromatic residues W377 and W374 located on TM8 which resembles the first (bundle) helix of the second repeat. The outward open conformation allowing for betaine binding is established by sodium binding to the Na2 site. Binding of betaine to BetP in the outward open conformation leads to the formation of the Na1 site, allowing sodium to bind to the transporter in this site. The periplasmic exit pathway is then closed by a relative movement of the periplasmic halves of TM3 and TM12. Dissociation of sodium from the Na1 site formed by residues of TM5 and TM8 leads to an opening of the intracellular exit by a remarkable displacement of the cytoplasmic half of TM3: The Na2 site and the betaine binding site are consequently disrupted leading to the dissociation of all substrate towards the cytoplasmic exit (Perez et al., 2012).

Although it was possible to assign an alternating access mechanism for BetP by the established crystal structures, the nature of coupling the substrate/co-substrate flux is not clear to date. Furthermore very few conclusions about the regulatory function of the BetP protein could be drawn from the structural analysis for several reasons. First of all it is known that the regulation of the protein strictly depends on the membrane environment (Schiller et al. 2006), a factor which is of course not present in 3D detergent crystals. The crystallisation of BetP necessitated the truncation of the N-terminus by 29 amino acids, resulting in a protein that lacks the osmoregulation in *E. coli* membranes completely (Ressl et al., 2009).

A second betaine binding site at the periplasmic entry of the protein that was only visible by cooperative betaine binding upon elevated potassium concentration was proposed. The role of this binding site is not clear yet especially as the betaine affinity measured by tryptophan fluorescence exhibited an apparent affinity two orders of magnitude lower than the apparent affinity in transport measurements (Ge et al., 2011).

1.7 Quarternary structure of BetP and its implications for cross-talk

Interestingly BetP and AdiC are the only members of the LeuT family where structural information from membrane embedded proteins in 2D crystals is available. Since the 2D structure of AdiC was solved with the application of 2 fold non-crystallographic-symmetry no asymmetry in this structure could be detected (Casagrande et al., 2008).

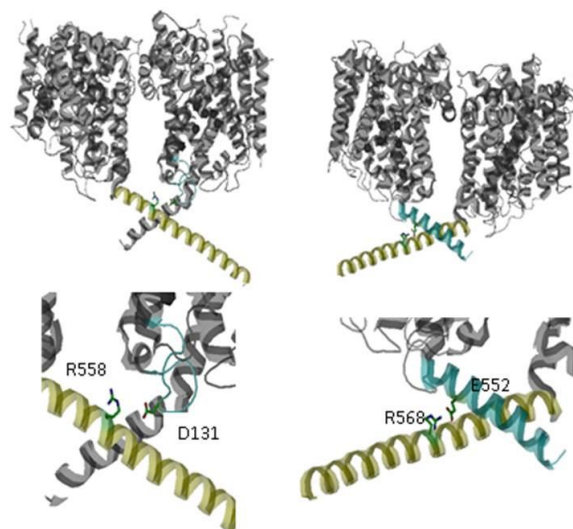


Fig. 1-5: C-terminal inter protomer contacts in the C-terminal helices. Salt-bridge between R558 and D131 in loop2 of the neighbouring protomers (left) and the interaction of R568 and E552 of the same protomers (right). (Structure from PDB entry: 2WIT)

As already mentioned, the protomers in the 2D BetP crystals do not seem to be symmetric to each other (Tsai et al. 2011; Ziegler et al. 2004) (Fig. 1-2). Homo-trimeric BetP proved to exist in conformationally asymmetric states as well in the recent 3D structures (Perez et al., 2012). Therefore it might be the case that the monomers function in a concerted manner where all three conformations (Ce, Cc and Ci) are present at the same time in the trimer. This fact would also explain why betaine could be detected in the 3D crystal structure

without supplementation of the crystallisation solution with this compound (Ressl et al., 2009). If the substrate would not be trapped in one subunit it could hardly stay bound during crystallisation for kinetic reasons. Cross-talk will most likely involve the residues mediating the monomer contacts. The protein contacts can be nicely seen in the published 3D structures. Only few residues contribute to monomer interactions. Most of the space between the monomers is occupied by non-protein density in the structure (Perez et al., 2012; Ressler et al., 2009). Two salt bridges in the C-terminal domain between R568 and E552 contribute to monomer interaction. Mutations of R568 to proline (charge and structure change) and alanine/aspartate (charge effect) were shown to strongly impair BetP function (Ott et al. 2008). The second salt bridge is formed between R558 in the C-terminal helix of one protomer and D131 of the neighbouring protomer. As this interaction links the regulatory C-terminal domain to the functional relevant first and second bundle helix of the neighbouring protomer it was suggested that this site might be involved in a regulatory crosstalk (Gärtner et al., 2011) although the regulation of the respective R558D BetP mutant is comparable to that of the wild-type protein (Ott et al. 2008). Since the BetP activity is very sensitive to mutations in the C-domain it cannot be immediately concluded that observed effects are due to impaired monomer interaction. Although the quaternary structure of these mutants was not addressed it is unlikely that trimerisation is affected here because it was shown that the deletion of the complete C-domain from Y550 on does not affect the trimerisation (Tsai et al. 2011; Perez et al. 2011). Beside the protomer interactions mediated by the C-domain, few protomer contacts were found at the membranous interfaces. Van der Waals contacts were found between TM2 and the horizontal amphipathic helix 7 of neighboring protomers (T108 and F112 in TM2, Y340, F344 and F345 in helix 7 and H192 in TM4). The main salt bridges between the neighbouring protomers were found between N331 to D356 and T351 to E425 in TM9 of the neighbouring protomer (Ressler et al., 2009).

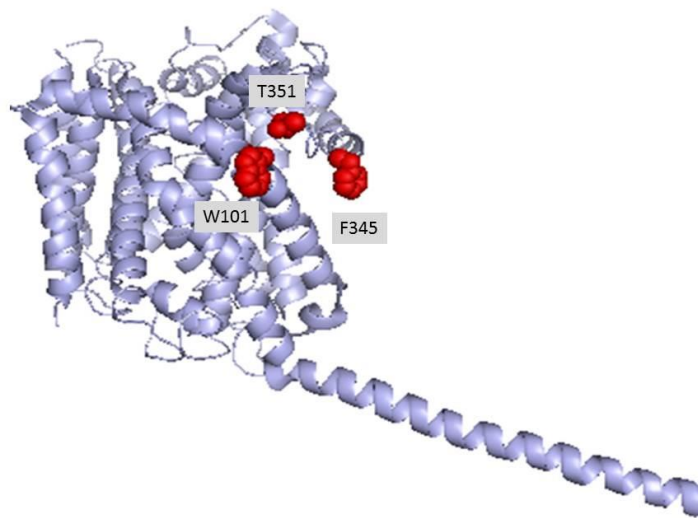


Fig. 1-6: Side view on one BetP monomer. The positions for the alanine mutations leading to monomerisation of the protein are highlighted in red. (modified from PDB entry: 2WIT)

By *in silico* alanine scanning approaches several single site mutations could be predicted to impair trimerisation of the protein. The mutant variants W101A/T351A and W101A/T351A/F345A were shown to form complexes that appear much smaller in freeze fracture analysed liposomes in comparison to the wild type protein. These variants were further shown to migrate as monomers upon native PAGE analysis whereas the wild type protein migrates at trimer size. The monomeric variants exhibit only a very low but significant uptake activity. These results suggest the functional necessity of cross-talk for the transport function. The monomeric mutant was interpreted to be non-activatable by hyperosmotic stress which also suggests a regulatory relevant cross-talk.

But it has to be taken into account that the conclusions from the monomeric BetP are hardly interpretable in terms of cross-talk because it remains unclear if the functional effects result from missing stabilisation or missing functional cross-talk. Further it is not clear if the observed activity results from monomers or from transient trimers even though strong suggestions for the absence of transient trimers could be found by cysteine crosslinking experiments (Perez et al. 2011).

Nevertheless the nature of the cross-talk remains highly speculative. The current model of BetP activation involves cross-talk as a necessity for the activation of the protein (Perez et al. 2011). In the current model of activation the interaction of the C-terminal domain with loop2 of the adjacent protomer is modulated by potassium. Raising potassium

concentration would thereby tighten this interaction and consequently be transduced to the periplasmic side of the protein were the formation of the potassium dependent second betaine binding site is then established (Ge et al., 2011b). The potassium binding at the cytoplasmic face of the membrane would thereby be transduced by TM3 to the periplasmic side of the membrane (Gärtner et al., 2011).

1.8 Cross-talk in transport proteins and methods for its analysis

Cross-talk in transport proteins, meaning that conformational changes in a single subunit affect the function of another subunit, was observed for different systems. For transporters in which the transport pathway is located at the interface between different subunits such a kind of cross-talk is quite obvious. The multidrug exporter EmrE from *E. coli* is build up by a homo-dimer of two membrane protein subunits. The transport pathway is located at the interface of the two subunits. Consequently it could early be shown by titration studies with inactivated monomers that the inactivation of a single subunit leads to inactivation of the transport function (Yerushalmi et. al 1995). This effect is named negative dominance. The same effects were observed for the phosphate carrier PIC from yeast mitochondria. Again it could be shown *in vitro*, that the inactivation of a single subunit in the dimer abolishes transport function (Schroers et al., 1998). For those proteins the negative dominance is easy to rationalise as both subunits participate in the formation of a single substrate conduit. In several studies negative dominance was observed for proteins in which one single subunit forms a transport conduit.

For the multidrug efflux pump AcrB as well as for the F_1F_0 -ATPase it is clear that impaired function of a single transporting subunit affects the function of the whole protein as in both examples three substrate binding sites are established for drug binding from the periplasm (AcrB) or the ADP/phosphate binding (F_1F_0 -ATPase) that obviously change their conformation in a concerted manner. Not only cross-talk for catalysis of transporters but also cross-talk in the regulation of a transporter has been described. The ammonium uptake carrier Amt1 from *Arabidopsis thaliana* is activated by the phosphorylation state of a threonine in the C-terminal soluble domain of this protein. By co-expression of regulation defective mutants together with mutant variants defective in transport but unaffected in

the regulatory C-domain, *in vivo* evidence could be provided for allosteric trans-activation of this domain on the neighbouring subunit (Lanquar et al. 2009; Lalonde et al. 2007).

Two principal different strategies exist to address monomer function in proteins composed of homo-oligomers. First, the protein contacts can be impaired in their flexibility by cross-linking in the interfaces. This approach relies on an in-depth structural knowledge of the protein of interest and it only enables detection of cross-talk that requires large structural rearrangements at the interface. By such an approach it was shown that the trimeric glutamate /sodium symporter Glt_{pH} (GltT) of *Pyrococcus horikoshi*, is not impaired in transport function upon oxidative crosslinking of interface cysteine residues (Groeneveld and Slotboom, 2007).

Another approach is to express artificial heteromers. Via these proteins it can be addressed if the oligomer works in a concerted manner or not. Furthermore it is possible to apply site directed mutagenesis and protein labeling for spectroscopic analyses. To construct such hetero-oligomers generally two strategies can be followed. The protein can be expressed as a fusion construct in which all monomers are located on one polypeptide chain. This strategy was successfully applied to unravel cross-talk in the homo-trimeric multidrug efflux pump AcrB (Takatsuka and Nikaido, 2009) and dimer topology of the multidrug efflux pump EmrE (Steiner-Mordoch et al., 2008). A severe drawback of this strategy is the conformational restriction of the termini in the linked subunits.

Another way to create hetero-oligomers is the sequential affinity purification of oligomers with differently tagged monomers of the protein. This approach was successfully applied to unravel functional cross-talk of the phosphate carrier from yeast mitochondria (Schroers et al., 1998). So far no study published the co-expression and sequential affinity purification of a homo-oligomeric protein by this approach with more than two subunits. The great advantage of this approach for BetP heterotrimer purification would be in that the termini remain their flexibility. The two major drawbacks of this approach are that for stochastic reasons only a maximum of 20% of the protein will comprise correct hetero-trimeric composition and that no *in vivo* studies with this protein would be possible.

Establishing the heterotrimeric BetP complexes is not only a pre-requisite for the in-depth analysis of protomer cross-talk but also for spectroscopic analysis of this protein via labels attached to engineered cysteine residues. Labeling of engineered cysteines in the

homotrimeric protein will always lead to hardly interpretable results, due to the fact that already one cysteine residue labeled in every subunit leads to at least two different distances of the labels. The situation would be even much more difficult if photofluorescent labels are introduced than for the EPR analysis (Nicklisch, 2008).

1.9 The osmo-transportome of *C. glutamicum*

C. glutamicum is equipped with at least five different secondary active osmolyte transporters (Peter et al. 1998; Steger et al. 2004).

tab. 1-2: Osmo-regulated transport systems in *C. glutamicum* and their kinetic properties. (Peter et al. 1996; Peter et al. 1998; Steger et al. 2004; Krämer & Morbach 2004). **Classification of these systems according to** (Saier, 2000; Saier et al., 1999)

Transporter	Substrate	co-substrate	KM [μ M]	Vmax [nmol x mgcdw- 1 x min ⁻¹]	Transport protein family
BetP	Betaine	Na ⁺	8,6	110	BCCT
EctP	Ectoine	Na ⁺	53	27	BCCT
	Betaine		333	34	
	Prolin		1200	34	
ProP	Prolin	H ⁺	48	8,5	MFS
	Ectoine		132	8,6	
LcoP	Betaine	Na ⁺	154	71	BCCT
	Ectoine		539	129	

Four of those, namely BetP; ProP; EctP and LcoP were shown to be regulated by the external osmolality *in vivo*. It was shown that the activity of BetP, ProP and LcoP is further controlled on the level of transcription by the MtrBA two component system whereas the EctP coding gene is constitutively transcribed (Möker et al., 2004). BetP as well as LcoP were additionally shown to be activated *in vivo* by chill stress, whereas the activity of the other osmolyte transporter was not enhanced by low temperatures (Özcan et al., 2005). The only osmolyte transport system of *C. glutamicum* for which the osmoregulatory function is proven to be an intrinsic protein function *in vitro* is the betaine permease BetP

(Rübenhagen et al., 2000). Any kind of cross-talk in BetP would raise the question about the universality of the underlying mechanism. Most of the recently elucidated structures of secondary active transport proteins from completely distinct families suggested that the underlying mechanisms of transport are remarkably similar (Forrest, 2013; Forrest and Rudnick, 2013). The osmo-regulatory function of secondary osmolyte transporters might also be conserved. For BetP and EctP, both being BCC-Transporters from *C. glutamicum* it was shown that C-terminal soluble domains are crucial for the osmoregulation of the transport activity *in vivo* (Peter et al. 1998)(Steger 2002). As BetP appeared to be easily accessible for functional studies *in vitro* as well as for structural analyses it had become the major target for studying the osmoregulation and the transport mechanism of osmolyte transporters. None of the attempts carried out in earlier studies to examine the regulation of EctP *in vitro* was successful due to the fact that this protein appeared to be not expressed in *E. coli* cells. None of the other osmolyte transporters of *C. glutamicum* were subjected to heterologous expression and activity studies so far.

2 Experimental procedures

2.1 Bacterial strains, plasmids and oligonucleotids

2.1.1 Bacterial strains

C. glutamicum and *E. coli* strains used in this study are listed in tab. 2-1

tab. 2-1: Bacterial strains used in this study

Strain	Genotype	Reference
<i>E. coli</i> DH5 α	endA1 supE44 thi-1 λ - recA1 gyrA96 relA1 Δ eoR Δ (lacZYA- argF) U169 Φ 80dlacZ Δ M15 mcrA Δ (mrr hsdRMS mcrBC)	(Grant et al., 1990)
<i>E. coli</i> MKH13	ara Δ 39 (argF-lac) U169 relA51 rps150 flbB5301 deoC ptsF25 Δ (putPA)101 V(proP)2 Δ (proU)	(Haardt et al., 1995)
<i>C. glutamicum</i> DHPF	ATCC 13032 (Δ betP, Δ proP, Δ putP, Δ ectP, Δ lcoP)	(Steger et al., 2004)

2.1.2 Plasmids

Plasmids used in this work are listed in tab. 2-2. The listed plasmids were used for the expression of the respective construct in *E. coli*. For the expression of those in *C. glutamicum* the coding sequences were cut via Xba1/Nae1 and subcloned to the Xba1/Xma1 cut pXMJ19 vector. pD vectors used for the co-expression of the different constructs were subcloned from the single vectors and are not listed.

tab. 2-2: Plasmids used in this study

Plasmid	Description/coding sequence (cds)	Reference
pASK-IBA5	ColE1;ApR;pTET expression vector	(Skerra, 1994)
pXMJ19	CmR,lacl,pTac expression vector	(Jakobi et. al 1999)
pASK-IBA5_BetP	pASK-IBA5 derivative encoding for StrepII_tagged BetP_C252T	(Rübenhagen et al., 2000)
pEX	pASK-IBA5 derivative with an TEV recognition element between Nhe1 and Kas1 site	this study
pEX_His_BetP	cds: His10_TEV_BetP	this study
pEX_Strep_BetP	cds: StrepII_TEV_BetP	this study
pEX_Flag_BetP	cds: Flag_TEV_BetP	this study
pEX_MBP_BetP	cds: maltose-binding-protein_TEV_BetP	this study
pEX_CBP_BetP	cds: Calmodulin-binding-peptide_TEV_BetP	this study
pEX_CBD_BetP	cds: Chitin-binding-domain_TEV_BetP	this study
pEX_R6_BetP	cds: Arginine6_TEV_BetP	this study
pEX_D6_BetP	cds: Aspartate6_TEV_BetP	this study
pEX_GST_BetP	cds: Glutathione-S-transferase_TEV_BetP	this study
pEX_HIS_SSG6_BetP	cds: His10_(SerSerGly)6_TEV_BetP	this study
pEX_mVenus_BetP	cds: mVenus_TEV_BetP	this study
pEX_His_mVenus_BetP	cds: His10_mVenus_TEV_BetP	this study
pEX_HAT_BetP	cds: Lysozyme-chelating-peptide_TEV_BetP	this study
pEX_HQ_BetP	cds: (HistidineGlutamine)3_TEV_BetP	this study
pEX_myc_BetP	cds: myc_TEV_BetP	this study
pEX_Flag_BetP	cds: Flag_TEV_BetP	this study
pEX_S_BetP	cds: RNase1-S-fragment_TEV_BetP	this study
pEXT_Strep_BetP	cds: Strep_Thrombin_BetP	this study
pEXF_Strep_BetP	cds:Strep_FactorXa_BetP	this study
pFus	cds:fusion BetP trimers with TEV cleavable linkers	this study
pFus_mon1_W141A	pFus with W141A mutation in the first protomer	this study
pFus_mon2_W141A	pFus with W141A mutation in the second protomer	this study
pFus_mon3_W141A	pFus with W141A mutation in the third protomer	this study
pFus_mon1&2_W141A	pFus with W141A mutation in the first and second protomer	this study
pFus_mon1&3_W141A	pFus with W141A mutation in the first and third protomer	this study
pFus_mon2&3_W141A	pFus with W141A mutation in all three protomers	this study
pFel	cds: fusion BetP with elongatable linkers	this study
pFel17	pFel with 17 mer SSG linker	this study
pFel28	pFel with 17 mer SSG linker	this study

EXPERIMENTAL PROCEDURES

pFel39	pFel wiht 17 mer SSG linker	(Salman 2012)
pFel50	pFel wiht 17 mer SSG linker	(Salman 2012)
pFel61	pFel wiht 17 mer SSG linker	(Salman 2012)
pFel17a	pFel wiht 17 mer poly-A linker	this study
pFel28a	pFel wiht 17 mer poly-A linker	(Salman 2012)
psFel	cds: fusion BetP_DC12 with elongatable linkers	this study
psFel17	psFel with 17 mer SSG linker	(Salman 2012)
psFel17a	psFel with 17 mer poly-A linker	(Salman 2012)
pFel_mon1_W141A	pFel with W141A mutation in the first protomer	this study
pFel_mon3_W141A	pFel with W141A mutation in the first protomer	this study
pFel_mon1&2_W141A	pFel with W141A mutation in the first and second protomer	this study
pFel_mon1&3_W141A	pFel with W141A mutation in the first and second protomer	this study
pFel_mon2&3_W141A	pFel with W141A mutation in the first and second protomer	this study
pFel_mon1&2&3_W141A	pFel with W141A mutation in all protomers	this study
pC17_Strep_BetP_His	cds: Strep_BetP_17merSSG_His	this study
pC28_Strep_BetP_His	cds: Strep_BetP_28merSSG_His	this study
pC39_Strep_BetP_His	cds: Strep_BetP_39merSSG_His	this study
pC9_Strep_BetP_DC12_His	cds: Strep_BetP_DC12_17merSSG_TEV_His	this study
pC9_Strep_BetP_DC12_Flag	cds: Strep_BetP_DC12_17merSSG_TEV_Flag	this study
pC9_Strep_BetP_DC12_MBP	cds: Strep_BetP_DC12_17merSSG_TEV_MBP	this study
pC9_Strep_BetP_Y197L/W377L/T467A/S468A_DC12_His	pC9_Strep_BetP_DC12_His with indicated mutations in BetP	this study
pC9_Strep_BetP_Y197L/W377L/T467A/S468A_DC12_Flag	pC9_Strep_BetP_DC12_Flag with indicated mutations in BetP	this study
pC9_Strep_BetP_Y197L/W377L/T467A/S468A/A564P_DC12_His	pC9_Strep_BetP_DC12_His with indicated mutations in BetP	this study
pC9_Strep_BetP_Y197L/W377L/T467A/S468A/A564P_DC12_Flag	pC9_Strep_BetP_DC12_Flag with indicated mutations in BetP	this study
pC2_Strep_BetP_Y197L/W377L/T467A/S468A_DC45_His	pC9_Strep_BetP_DC12_His with indicated mutations in BetP	this study
pC2_Strep_BetP_Y197L/W377L/T467A/S468A_DC45_Flag	pC9_Strep_BetP_DC12_Flag with indicated mutations in BetP	this study
pC2_Strep_BetPR129A/I130A/D131S/E132G/A133G/P134A/DE135/Y197L/W377L/T467A/S468A/A564P__DC45_His	pC2_Strep_BetP with c-terminal His tag and the indicated mutations	this study
pC2_Strep_BetPR129A/I130A/D131S/E132G/A133G/P134A/DE135/Y197L/W377L/T467A/S468A/A564P__DC45_Flag	pC2_Strep_BetP with c-terminal Flag tag and the indicated mutations	this study

77L/T467A/ S468A/A564P __DC45_Flag		
pC2_Strep_BetP_eGFP	cds: Strep_BetP_6merSSG_eGFP	this study
pASK-IBA5_Strep_BetP_A564P	cds: Strep_BetP with indicated mutation	(Ott et al. 2008)
pASK-IBA5_Strep_BetP_Y197L	cds: Strep_BetP with indicated mutation	(Ressl et al., 2009)
pASK-IBA5_Strep_BetP_W377L	cds: Strep_BetP with indicated mutation	(Ressl et al., 2009)
pASK-IBA5_Strep_BetP_Y197L/W377L	cds: Strep_BetP with indicated mutation	this study
pASK-IBA5_Strep_BetP_T467A/S468A	cds: Strep_BetP with indicated mutation	this study
pASK-IBA5_Strep_BetP_Y197L/W377L/ T467A/S468A	cds: Strep_BetP with indicated mutation	this study
pASK-IBA5_Strep_BetP_E577C	cds: Strep_BetP with indicated mutation	this study
pASK-IBA5_Strep_BetP_A564P/E577C	cds: Strep_BetP with indicated mutation	this study
pASK-IBA5_Strep_BetP_G510C	cds: Strep_BetP with indicated mutation	this study
pASK-IBA5_Strep_BetP_G511C	cds: Strep_BetP with indicated mutation	this study
pASK-IBA5_Strep_BetP_D512C	cds: Strep_BetP with indicated mutation	this study
pASK-IBA5_Strep_BetP_N513C	cds: Strep_BetP with indicated mutation	this study
pASK-IBA5_Strep_BetP_E175C	cds: Strep_BetP with indicated mutation	this study
pASK-IBA5_Strep_BetP_L447C	cds: Strep_BetP with indicated mutation	this study
pASK-IBA5_Strep_BetP_Q451C	cds: Strep_BetP with indicated mutation	this study
pASK-IBA5_Strep_BetP_W101A/T351A	cds: Strep_BetP with indicated mutation	(Perez et al. 2011)
pASK-IBA5_Strep_BetP_W101A/ F345A/T351A	cds: Strep_BetP with indicated mutation	(Perez et al. 2011)
pASK-IBA5_Strep_BetP_D97C/W101A/ S328C/T351A	cds: Strep_BetP with indicated mutation	(Perez et al. 2011)
pASK-IBA5_Strep_BetP_D97C/W101A/ S328C/F345A/T351A	cds: Strep_BetP with indicated mutation	this study
pC2_Strep_LcoP	cds: Strep_LcoP_GT	this study
pC2_Strep_LcoP_C483T	cds: Strep_LcoP_C483T_GT	this study
pEX_Strep_ProP	cds: Strep_TEV_ProP	this study
pC2_Strep_LcoP_DN20	cds: Strep_DN20_LcoP_C483T_GT	this study
pC2_Strep_LcoP_DN40	cds: Strep_DN_40_LcoP_C483T_GT	this study
pC2_Strep_LcoP_DC40	cds: Strep_LcoP_C483T_DC40_GT	this study
pC2_Strep_LcoP_DC70	cds: Strep_LcoP_C483T_DC70_GT	this study

2.1.3 Oligonucleotides

Oligonucleotides used in this study are listed in table 2.3.

tab. 2-3: oligonucleotides used in this study

oligonucleotide	sequence
-----------------	----------

EX_TEV_sense	CGCGCCGGGCGGTAGCGAAAACCTCTACTTCCAGG
EX_TEV_anti	GCGCCCTGGAAGTAGAGTTTTTCGCTACCGCCCCG
EX_Thrombin_sense	CGCGCCGCTGGTTCGCGTGGTTCTG
EX_Thrombin_anti	GCGCCAGAACCACGCGGAACCAGCGG
EX_FXa_sense	CGCGCCGATCGAAGGCCGTACCG
EX_FXa_anti	GCGCCGGTACGGCCTTCGATCGG
EX_SSG6_sense	CGCGCCGGGCGGTAGCTCTGGTCTTCCGGCTCCAGCGGTTCTAGCGGCTCCA GCGGTTCTAGCGGTGAAAACCTCTACTTCCAGG
EX_SSG6_anti	GCGCCCTGGAAGTAGAGTTTTACCGCTAGAACCCTGGAGCCGCTAGAAC CGCTGGAGCCGGAAGAACCAGAGCTACCGCCCCG
EX_Strep_sense	CTAGCGTCGACGGAGATCTTTGGAGCCACCCGAGTTCGAAAAGGG
EX_Strep_anti	CGCGCCCTTTTCGAACTGCGGGTGGCTCAAAGATCTCCGTCGACG
EX_His_sense	CTAGCCATCACCATCATCACCACCATCACCATCATGG
EX_His_anti	CGCGCCATGATGGTGTGGTGGTGTGGTGTGGTGTGG
EX_Flag_sense	CTAGCGATTATAAAGATGATGATGATAAAGG
EX_Flag_anti	CGCGCCTTTATCATCATCTTTATAATCG
EX_HQ_sense	CTAGCCATCAACATCAGCACCAAGG
EX_HQ_anti	CGCGCCTTGGTGCTGATGTTGATGG
EX_HAT_sense	CTAGCAAGGATCATCTCATCCACAATGTCCACAAAGAGGAGCACGCTCATGCC CACAACAAGGG
EX_HAT_anti	CGCGCCCTTGTGTGGGCATGAGCGTGCTCCTCTTTGTGGACATTGTGGATGA GATGATCCTTG
EX_myc_sense	CTAGCGAACAGAAACTGATCTCTGAAGAAGATCTGGG
EX_myc_anti	CGCGCCAGATCTTCTTCAGAGATCAGTTTCTGTTCCG
EX_S_sense	CTAGCAAAGAAACCGCTGCTGCGAAATTTGAACGCCAGCACATGGACTCGGG
EX_S_anti	CGCGCCCGAGTCCATGTGCTGGCGTTCAAATTCGCAGCAGCGGTTTCTTTG
EX_D6_sense	CTAGCGATGACGATGACGATGACGG
EX_D6_anti	CGCGCCGTCATCGTCATCGTCATCG
EX_R6_sense	CTAGCCGCGTCGCGTCGCGGTGG
EX_R6_anti	CGCGCCACGGCGACGGCGACGGCGG
EX_CBP_sense	CTAGCAAGCGACGATGGA AAAAAGAATTCATAGCCGTCTCAGCAGCCAACCGC TTTAAGAAAATCTCATCTCCGGGGCACTTGG
EX_CBP_anti	CGCGCCAAGTGCCCGGAGGATGAGATTTTCTTAAGCGGTTGGCTGCTGAG ACGGCTATGAAATCTTTTTCCATCGTCGCTTG
EX_mVen_sense	ATGAGGCGCCATCGGAGGGCTAGCTGTGAA
EX_mVen_anti	GCGCGAATTCTAAAACCACCACCTCCGGAACCA
EX_CBD_sense	GCAGCTAGCACAAATCCTGGTGTATCCGCTTGG
EX_CBD_anti	ATTGGCGCGCCTTGAAGCTGCCACAAGGCAGGAAC
EX_GST_sense	GAGCGCTAGTCCCCTATACTAGGTTATTGG
EX_GST_anti	GAGCGCTAGTCCCCTATACTAGGTTATTGG
EX_MBP_sense	GCAGCTAGCAAATCGAAGAAGGTA AACTG
EX_MBP_anti	CCGTTTCGAGCTCGAATTAGTCTGCGGTCT
pC_MBP_sense	GATCACCGGTGAAAACCTCTACTTCCAGGGCGGGGGCTAGCAAATCGAA GAAGGTAAA
pC_MBP_anti	GATCAAGCTTATTTAGTCTGCGGTCTTTCCAGGGCTTCATCGACAG
pC_Flag_sense	CCGGTGAAAACCTCTACTTCCAGGGCGATTATAAAGATGATGATGATAAATAA A
pC_Flag_anti	AGCTTTTATTTATCATCATCATCTTTATAATCGCCCTGGAAGTAGAGGTTTTCA
pC_His_sense	CCGGTGAAAACCTCTACTTCCAGGGCCATCACCATCATCACCACCATCAACATC

pEX&pC_LcoP_sense	GAATGGCGCCTCCACCAACTCTGGCAATAA
pEX&pC_LcoP_anti	GCGCAAGCTTTTAACCGGTATCCTTTTTCGCGTCCACTTCGCCTTC
pEX&pC_ProP_sense	GATAGGCGCCAGCCCCGATTCGCTCAAAAAAG
pEX&pC_ProP_anti	GCGCAAGCTTTTATGCGTTTTGCTTTTCAGCACCTAC
LcoP_-Kas1_sense	TGCGATGATGTTTCGGTGCCGGCATCGGTGT
LcoP_-Kas1_anti	ACACCGATGCCGGCACCGAACATCATCGCA
LcoP_DN20_sense	GACGGCGCCCCTCACGACACCCACCCAGGCCTAG
LcoP_DN40_sense	GACGGCGCCTTCGGACTCGACAAAACCGTTTT
LcoP_DC40_sense	GATACCGGTGTCGGTGATGTGATCAGCGGTGGAAT
LcoP_DC70_sense	GATACCGGTGTTCTTCCAAGCCACGAACCACCGCGTTAG
Loop2_5'_anti	GATTCCGGAGCCGGCGCCTAAGCGAATCGTGCCGAATTTAC
Loop2_3'_sense	GATTCCGGAGGGGCGTTTTGCACGGTGTTCATGGAT

2.1.4 Growth media and cultivation conditions

The growth media used in these studies are listed in tab. 2-4. For agar plates 15 g/L Bacto-Agar (Difco, Detroit, USA) were added. If appropriate, the antibiotics chloramphenicol (Cm) or carbenicillin (Carb) were added to the growth media with a final concentration of 34 µg/mL (Cm) and 100 µg/ml (Carb). *E. coli* strains were generally cultivated in LB- (Lysogeny Broth) medium (tab. 2-4). During expression in fermenter cultures *E. coli* was cultivated in LB+ medium. *C. glutamicum* was grown in BHI complex medium.

tab. 2-4: Cultivation media used in this study.

Medium	Ingredients
LB	NaCl 10 g/L; yeast extract 5 g/L; tryptone 10 g/L
BHI	Brain-Heart-Infusion 37g/L
LB+	NaCl 10 g/L; yeast extract 5 g/L; tryptone 10 g/L; 20 mM KH ₂ PO ₄ /K ₂ HPO ₄ (pH 7,5); Glucose 2%
BHIS	Brain-Heart-Infusion 37g/L 0,6 M Sorbitol sterilized by filtration
SOB	20 g/L Tryptone, 5 g/L yeast extract, 0.5 g/L NaCl, 2.5 mM KCl. After heat sterilization, 5 mL 2 M MgCl ₂ were added.

--	--

2.2 Molecular biology

2.2.1 Preparation of competent *E. coli* cells and transformation

Preparation of chemically competent *E. coli* DH5 α was carried out according to (Inoue et al., 1990). In brief 200 ml SOB medium were inoculated with 1 ml *E. coli* culture grown in LB to stationary phase. After growth for additional 18 h at 18°C and 200 rpm cells were soiled on ice for 10 min. Cells were harvested by centrifugation (4000 g 10 min 4°C) and washed once in 80 ml TB buffer. After resuspension in 20 ml TB the cell suspension was supplemented with 1,4 ml DMSO and incubated for 10 min on ice. After aliquoting to 200 μ l cells were flash frozen in liquid N₂ and stored at -80°C until use. For transformation one aliquot was supplemented with plasmid DNA and stored on ice for 1h. Hereafter the cells were heat-shocked by insertion of the tube to an incubator set to 42°C for 45 s. The cells were chilled on ice for 5 min and supplemented with 600 μ l LB. After incubation at 37°C for 1h at vigorous shaking the cells were streaked out on LB-Agar plates containing the appropriate antibiotics.

TB buffer: 10 mM Pipes, 15 mM CaCl₂, 250 mM KCl, pH (KOH) = 6.7. After adjustment of pH, 55 mM MnCl₂ were added. The buffer was sterilised by filtration.

E. coli MKH13 cells were transformed according to (Chung et al., 1989). 1 ml *E. coli* culture was grown to OD₆₀₀ ~0,4. Cells were harvested and resuspended in 100 μ l buffer TSS (LB; 50 mM MgCl₂; 2% DMSO). Plasmid DNA was added and the cells were heat-shocked at 42°C for 45 s after incubation for 1 h on ice. The cells were chilled on ice for 5 min and supplemented with 600 μ l LB. After incubation at 37°C for 1h at vigorous shaking the cells were streaked out on LB-Agar plates containing the appropriate antibiotics.

2.2.2 Preparation of electrocompetent *C. glutamicum* cells and transformation

Competent *C. glutamicum* cells were prepared according to (Liebl et al. 1989). Electrocompetent *C. glutamicum* cells were transformed with approx. 400 ng plasmid DNA

by a 2,5 kV pulse applied with a half-value-period of typically 5 ms. Subsequently the cells were immediately supplemented with 1 BHIS medium and streaked out on BHI-agar plates after incubation at 30°C for 2h.

2.2.3 DNA techniques

2.2.3.1 Isolation of plasmid DNA from *E. coli*

The isolation of plasmid DNA from *E. coli* cells was performed following the principle of alkaline lysis. For the isolation of plasmid DNA from these cultures, the NucleoSpin® Plasmid DNA Purification kit (Macherey-Nagel, Düren) was used as recommended by the supplier.

2.2.3.2 Gel electrophoresis and extraction of DNA from agarose gels

Gel electrophoresis of DNA was performed using 0.8 to 2 % agarose gels in 1X TAE buffer (40 mM TRIS/Acetate pH7,9; 0,5 mM EDTA) as described by (Sambrook et al. 1989). For this purpose, DNA samples were mixed with 5X Loading Dye (MBI Fermentas, St. Leon-Roth). After electrophoresis, DNA was stained with ethidium bromide (Biosciences, Freiburg). DNA was isolated from agarose gels using the NucleoSpion® Extract kit (Macherey-Nagel, Düren) as recommended by the supplier.

2.2.3.3 Polymerase chain reaction (PCR)

The *in vitro* amplification of specific DNA fragments was performed by the polymerase chain reaction using the Phusion polymerase (MBI Fermentas, St. Leon-Roth) as recommended by the supplier. For this purpose, two oligonucleotides were used, flanking the DNA region to be amplified. Oligonucleotides were diluted to a concentration of 10 pmol/μL. The annealing temperature was chosen with respect to the forward and reverse oligonucleotides. For each guanine and cytosine 4 °C, for each adenine and thymine 2 °C are required to separate the hydrogen bonds. As template, total DNA, plasmid DNA, or a cell suspension, which was diluted in H₂O_{dd} and incubated for 10 min at 95 °C, could be used. The PCR reaction was performed using the thermocycler Mastercycler® personal or Mastercycler® gradient (Eppendorff, Hamburg). A 50 μL PCR reaction mixture was prepared as follows:

10 μL 5x HQ Buffer Phusion

2 µl dNTPs 5 µM each
1,5 µl DMSO
2,5 µL oligonucleotides forward [10 µM]
2,5µL oligonucleotides reverse [10 µM]
0,01-1 µL template
0,5 µl Phusion polymerase
H₂O_{dd} add 50 µL

The amplification reaction was initiated by denaturing the template for 4 min at 95 °C. The following steps were performed in 30 cycles: Denaturing the DNA for 30 seconds at 95°C, hybridisation of the primers for 30 seconds at the specific annealing temperature, and polymerisation for 1 min per kb at 72 °C. After a final incubation for 10 min at 72 °C, the samples were kept at 4 °C or -20 °C. If appropriate, the PCR product was purified either with the NucleoSpin® Extract Kit (Macherey-Nagel, Düren) as recommended by the supplier, or by gel electrophoresis.

2.2.3.4 Restriction, ligation, and sequencing of DNA

For restriction of DNA, restriction enzymes were used as recommended by the suppliers (MBI Fermentas, St. Leon-Roth). After restriction DNA was purified either with the NucleoSpin® Extract kit (Macherey-Nagel, Düren) following the suppliers recommendations or by gel electrophoresis. Ligations were carried out with the use of T4-DNA-Ligase (MBI Fermentas, St. Leon-Roth) as recommended by the supplier.

For the cloning of small fragments (<80 bp) the respective 3'-5' and 5'-3' DNA fragments were purchased from MWG Operon and ligated immediately after annealing reaction. The annealing reaction was carried out by mixture of the two oligonucleotides and heating to 95°C with subsequent chilling in steps of 5°C for each 1min.

2.2.3.5 Site directed mutagenesis

For site directed mutagenesis oligonucleotides containing the appropriate mutations flanked by 15 bp of correct template sequence were ordered and the whole plasmid template sequence was amplified in a common PCR reaction. After digest of the parental methylated DNA via Dpn1 (MBI Fermentas, St. Leon-Roth) the amplified vectors were

immediately transformed to *E. coli* DH5 α . To reduce the appearance of mutations in the vector backbone, the sequenced, mutated genes were recloned to vectors that had not been amplified by PCR.

2.2.3.6 DNA sequencing:

DNA was sequenced via the Sanger-sequencing (GATC Biotech, Konstanz). Sequences were analysed by the SE-Central Clone Manager5 software.

2.3 Analytical methods

2.3.1 Protein concentration measurements

The concentration of protein in any sample was measured by amido black staining (Schaffner and Weissmann, 1973) with BSA solutions of different concentration as reference.

2.3.2 Sodium-dodecyl-sulphate-polyacrylamid-gel-elektrophoresis (SDS-PAGE)

For the analysis of homogeneity and rough estimates of molecular mass of purified proteins those were analysed on SDS-PAGE (Laemmli 1970). Separation gels were casted with 12% (20-100 kDa proteins) or 8% acrylamide (>100kDa proteins). Protein samples were mixed 4:1 with sample buffer (glycerol 20%; SDS 8%, Tris/HCl (pH 6,8) 400 mM; 10 mM EDTA, 100 μ M β -mercaptoethanol, bromo-phenol-blue). Protein bands were visualised by staining the gel with Coomassie brilliant blue dye.

2.3.3 Blue-native-polyacrylamid-gel-elektrophoresis (BN-PAGE)

For the detection of aggregation and oligomerisation solubilised proteins were separated on 4-16% acrylamide gels after partial replacement of the solubilising detergent via Coomassie brilliant blue dye (Schägger and Von Jagow, 1987). The NativePAGE™ Bis-Tris Gel System (Invitrogen, Carlsbad,CA,USA) was used for this purpose according to the manufacturers recommendations. 100 μ L solubilised protein (1-10 μ g total protein) were mixed with 10 μ L coomassie additive and 35 μ L 4x native PAGE sample buffer (Invitrogen, Carlsbad,CA,USA).

2.3.4 Western-Blot

Proteins separated on SDS-PAGE and native PAGE gels were identified by immunoblotting (Towbin et al., 1979) against either protein sequences (polyclonal BetP antibody) or various epitope tags against which monoclonal antibodies were commercially available. Proteins were transferred on methanol activated PVDF membranes by semi-dry blotting (Kyhse-Andersen, 1984). After transfer of the proteins free binding sites on the membrane were blocked by 3% skin milk powder (Carl-Roth, Karlsruhe) in TBS buffer (50 mM TRIS/Cl pH 7,4; 0,9% NaCl). The membrane was incubated with TBS+3% milk powder + antibodies (1:10000) for 1 h at room temperature. Epitope bands were visualised by the formation of diformazan and Indigo out of NBT and BCIP catalysed by an alkaline phosphatase conjugated to the secondary antibody.

2.3.5 Gel-Permeation-Chromatography

For the purification of proteins after labeling with thiol reactive fluorescent dye (2.4.4.1), the reaction assay was subjected to GPC on gravity flow columns equilibrated in Buffer HA (2.4.3.2) equilibrated 5 ml gravity flow columns containing sehadex G25 medium (PD10 column GE-Healthcare). Samples up to 700 µl volume were loaded to the column and eluted via Buffer HA. For the analysis of the apparent molecular mass of purified proteins those were subjected to GPC on a 24 ml Superose6 column run by an AEKTA FPLC system (GE-Healthcare, Freiburg). The separation of the proteins on the column was carried out by washing with Buffer HA at a flow rate of 0,3 ml/min.

2.3.6 Estimation of osmolalities

To determine the osmolality in any buffer it was directly measured by the determination of the melting temperature. Measurements were carried out with an osmometer (Osmomat 030, Gonotec, Berlin) according to the manufacturer's recommendations.

2.3.7 Fluorescence microscopy

For phase contrast and fluorescence microscopy, 1-3 µl of a culture sample was placed on a microscope slide coated with a thin 1 % agarose layer and covered by a cover slip. Images were taken on a Zeiss AxioImager M1 equipped with a Zeiss AxioCam HRm camera. GFP fluorescence was monitored using filter set 38 HE. An EC Plan-Neofluar 100x/1.3 Oil Ph3

objective was used. Digital images were acquired and analysed with the AxioVision 4.6 software (Carl Zeiss Jena).

2.4 Biochemical Methods

2.4.1 Heterologous expression

2.4.1.1 Heterologous expression in *E. coli* in shaker flasks

Heterologous protein expression in *E. coli* was carried out in shaker flask and in fermenter cultures. In any case a 5ml preculture was inoculated in LB with the appropriate antibiotic. After overday cultivation precultures (100 ml-3 L) LB with the appropriate antibiotic were inoculated in shaker flasks and cultivated overnight at 37°C and 110 rpm shaking. With those cultures the respective volume of expression culture was inoculated to an OD600 of 0,2 in LB medium with the respective antibiotic. After the cells reached an OD600 of 0,8-1 in those cultures expression was induced by addition of 1:10000 (v/v) AHT 2mg/ml in DMF). Expression was then carried out by further cultivation of the cells for 3 h. These cultures were harvested by centrifugation 4500 rpm at 4°C (Avanti Centrifuge J25, Beckman,Rotor JLA 10.500). After washing the cells with cold buffer $\text{KH}_2\text{PO}_4/\text{K}_2\text{HPO}_4$ (pH 7,5) 100 mM cells were frozen at -20°C.

2.4.1.2 Heterologous expression in *E. coli* in bioreactor cultures

For the expression of proteins in bioreactor cultures, precultures were prepared as for the expression in shaker flasks (2.4.1.1). The precultures were harvested by centrifugation 4500 rpm at 4°C (Avanti Centrifuge J25, Beckman,Rotor JLA 10.500) and resuspended in LB to an OD600 of 200. With those cultures bioreactors (Biostat B Sartorius Braun) containing 1,5 L LB+ and 75 mg Ampicillin, 200 µL Antifoam A (Sigma-Aldrich Taufkirchen); were inoculated to an OD600 of 2. The cells were further cultivated at 36°C; 750 rpm stirring 2,5L/min aeration. The pH in the growing cultures was kept constant at pH 6,7 by automated addition of either sulphuric acid 8% or potassium hydroxide 2M. After around 2h

the cultures reached an OD600 of 8 and expression was induced by addition of 600 μ l AHT (2mg/ml in DMF). Expression was carried out for three hours under these conditions. Following expression the cells were treated as the shaker flasks expression cultures (2.4.1.1).

2.4.1.3 Heterologous expression of proteins in *C. glutamicum*

For the heterologous expression of proteins in *C. glutamicum* a 5 ml preculture was inoculated in BHI medium with the appropriate antibiotic. Cells were cultivated overnight at 30°C and 120 rpm shaking. With this culture the expression culture containing BHI with antibiotic and 100 μ M IPTG was inoculated to an OD600 of 0,1. After 8 h of cultivation at 30°C in shaker flasks 120 rpm shaking, cells were harvested by centrifugation and either prepared for uptake measurements or frozen for later expression analysis via SDS-PAGE (2.3.2).

2.4.2 Isolation of membrane proteins.

2.4.2.1 Isolation of membrane proteins via bead mill

Small scale membrane preparation for SDS-PAGE analysis of expression in different strains was carried out by cell disruption in a bead mill (precllys24, Peqlab). The cell pellet (usually 0,1-0,2g wet weight) was resuspended in 0,5 ml disruption buffer (50 mM sodium phosphate pH 7,5; 100 mM NaCl; complete protease inhibitor (Roche, Mannheim); 1 mM EDTA). The cell suspension was transferred to a 2ml screw cap plastic tube and 250 μ l of glassbeads (150 μ M diameter (Carl Roth, Karlsruhe) were added. The cells were vigorously vortexed in the bead mill for 30s 3 times with chilling on ice for 5 min between each vortexing step. Hereafter debris was centrifuged at 10000xg 10 min 4°C. Membranes were harvested from the supernatant by ultracentrifugation at 220000xg 30 min 4°C (Beckmann TLX tabletop ultracentrifuge). After washing in disruption buffer the membranes were resuspended in disruption buffer to a final volume of typically 50 μ l. Membrane protein concentration was estimated by amido black staining (2.3.1) and the proteins were analysed by SDS-PAGE (2.3.2) and western blotting (2.3.4).

2.4.2.2 Isolation of membrane proteins via french press

Membranes of large scale expression cultures were prepared with cell disruption via french press (SLM Aminco, Rochester). Cells were thawed and resuspended 3:1 (v/v) in disruption buffer (100 mM KPi, 1mM EDTA, complete protease inhibitor (Roche Mannheim)). The resultant suspension was passed three times through the french press cell at a constant pressure of 1200 PSI. Debris was centrifuged from this suspension at 15000xg, 4°C, 20 min (Avanti Centrifuge J25, Beckman, Rotor JA25.50). Membranes were harvested from the supernatant by ultracentrifugation at 300000xg, 2h, 4°C (L90K centrifuge; Beckmann rotor 70.Ti). Membranes were resuspended 10:1 in disruption buffer without EDTA and resuspended after additional ultracentrifugation in same buffer to a protein concentration of 10 mg/ml. Membranes were then frozen in liquid nitrogen and stored at -80°C.

2.4.3 Purification of membrane proteins via affinity tags

2.4.3.1 Solubilisation of membrane proteins

For solubilisation of the proteins out of the prepared membranes (2.4.2.2), those were thawed and supplemented with glycerol, H₂O, and detergent to final concentrations of membrane proteins 5 mg/ml; potassium phosphate pH 7,5 50 mM; glycerol 8,6%; detergent usually 2%. For the solubilisation of membrane vesicles the solution was stirred gently for 30 min on ice. Hereafter debris was removed by ultracentrifugation 150000xg, 40min, 4°C (L90K centrifuge; Beckmann rotor 70.Ti). The supernatant was diluted 1:4 with the respective binding buffer and the solubilisate was loaded to the respective affinity purification matrix. Detergents used for solubilisation were LDAO, TritonX100 (Sigma-Aldrich) and DDM (Anatrace).

2.4.3.2 Purification of Strep tagged proteins:

For the purification proteins carrying the Strep tag (NH₂-WSHPQFEK-COOH (Schmidt et al., 1996)) the diluted solubilisate (2.4.3.1) or IMAC and Flag-affinity gel pre-purified protein was bound to BufferA equilibrated Strep-Tactin-sepharose (Strep-Trap 1ml/5ml (GE-Healthcare, Freiburg) by an AEKTA FPLC system (GE-Healthcare, Freiburg) at flowrate of 1 ml/min. After loading the column was washed with 2CV Buffer SA followed by a 6CV

washing step with buffer SB. After reequilibration of the column with BufferA (3CV) specifically bound proteins were eluted by buffer SE (4CV).

BufferSA: 50 mM potassium phosphate pH 7,5; 8,6% glycerol; 200 mM NaCl; 1 mM EDTA, 0,1% detergent (DDM for BetP/LDAO for LcoP).

BufferSB: BufferSA + 300 mM NaCl

BufferSE: BufferSA+ 5mM D-desthiobiotin (IBA, Göttingen)

2.4.3.3 Purification of His tagged proteins:

Proteins carrying a metal affinity tag composed of repetitive Histidin (NH₂-HHHHHHHQHH-COOH) sequences were purified by Nickel chelate affinity chromatography (Porath et al., 1975) on BufferHA equilibrated Ni-IDA-sepharose (HiTrap chelate column 1 ml / 5 ml (GE Healthcare, Freiburg) by an AEKTA FPLC system(GE-Healthcare, Freiburg). After loading diluted solubilisates (2.4.3.1), contaminating proteins were washed away by washing the column with 2CV BufferHA, 7 CV 90% BufferA/10% BufferHB and subsequently eluted by 100% BufferB. All steps were carried out at a flowrate of 2.5 ml/min.

BufferHA: 50 mM potassium phosphate pH 7,5; 8,6% glycerol; 200 mM NaCl, 10 mM Imidazol 0,1% detergent (DDM for BetP/LDAO for LcoP).

BufferHB: BufferHA+ 490 mM Imidazol

2.4.3.4 Purification of Flag tagged proteins.

Proteins carrying a Flag epitope tag (trypsinogen cleavage signal (NH₂-DYKDDDDK-COOH) sequences were purified by epitope affinity chromatography on sepharose cross-linked Flag-M2 antibodies (Sigma-Aldrich, Taufkirchen). A 2,5 ml self-cast gravity flow column was used for purifications. Proteins were bound in BufferHA (2.4.3.2). After washing with 4 CV Buffer HA the proteins were eluted by 3 CV BufferHA supplemented with Flag peptide (Sigma Aldrich, Taufkirchen.) 0,2 mg/ml.

2.4.3.5 Purification of MBP tagged proteins

Proteins carrying the maltose-binding-protein sequence were purified upon solubilisation and dilution (2.4.3.1) by binding to BufferSA (2.4.3.2) equilibrated amylose resin (NEB,

Schwalbach) A 2,5 ml self-cast gravity flow column was used for purifications. Proteins were bound in BufferSA (2.4.3.2). After washing with 4 CV Buffer SA the proteins were eluted by 3 CV BufferSA supplemented with Maltose (Sigma Aldrich, Taufkirchen.) 20 mM.

2.4.4 Chemical protein modifications

2.4.4.1 Protein labeling with Bodipy dye

Engineered single cysteine variants of BetP were labeled with the cysteine reactive Bodipy_FL_Iodoacetamide dye (Invitrogen, Carlsbad, USA). Therefore the purified protein was incubated with 2 fold molar excess Tris-carboxy-ethyl-phosphinate (TCEP, Carl-Roth, Karlsruhe) for 15 min on ice in BufferHA (2.4.3.2). Hereafter a 5 fold molar excess, usually about 20 μ M Bodipy_IA_FL was added to the reaction mixture from a 500x concentrated, freshly prepared stock solution in DMSO. After quenching of the reaction with 100 μ M β -mercaptoethanol the proteins were separated from the free dye via GPC (2.3.5).

2.4.4.2 Protein labeling with Biotin

For the covalent attachment of Biotin to cysteine containing BetP constructs those were labeled with HDPD-Biotin (Thermo Scientific, Rockford, USA). The labeling was carried out during IMAC purifications (2.4.3.3). Upon removal of contaminant proteins the column was washed with BufferHA supplemented with 4CV 500 μ M TCEP. Hereafter the column was washed with 4CV BufferHA followed by washing the column with 3CV BufferHA supplemented with 500 μ M HDPD-Biotin. After removal of the non-bound HDPD-Biotin label by washing the column with 4CV buffer HA the proteins were eluted as described (2.4.3.3).

2.4.5 Reconstitution of Proteins

2.4.5.1 Preparation of liposomes

Liposomes were prepared with *E coli* polar lipid extract (AvantiPolar Inc., USA). Lipids were dried from the Chloroform/Methanol solution by rotating under vacuum at 50°C for 3h. Dry lipids were then resuspended in Buffer (100 mM potassium phosphate pH 7,5; 2 mM β -mercaptoethanol to a final lipid concentration of 20 mg/ml by gentle stirring overnight. To prevent lipid oxidation all steps were carried out under inert nitrogen atmosphere. Lipids

were aliquoted after resuspension to 1 ml aliquots and stored at -80°C after freezing in liquid nitrogen.

2.4.5.2 Reconstitution of proteins

Membrane proteins were reconstituted according to the method of Jean-Lois Rigaud (Rigaud and Lévy, 2003). Resuspended lipids (2.4.5.1) were thawed and diluted to a lipid concentration of 5 mg/ml with potassium phosphate 100 mM pH 7,5. The lipid suspension was extruded 14 times through a 400 nm pore sized poly carbonate filter via a Miniextruder device (AvantiPolar Inc., USA). Extruded lipids were then titrated with TritonX-100 20% (Sigma-Aldrich, Taufkirchen) in steps of 1-2 µl TritonX100/ml liposome suspension. For each step the optical absorbance at 540 nm of the liposome was measured to monitor liposome enlargement. Upon saturation the protein was added at room temperature. The protein was added to yield a final ratio of lipid to protein (LPR) of 30:1 (m/m). The suspension was gently shaken for 15 min at room temperature. After addition of Biobeads (SM2-Biobeads, BioRad, München) with a wet weight corresponding to 1mg/Biobeads per µl TritonX100 20% the suspension was further gently shaken for 1 h at room temperature. Hereafter the same amount of biobeads was added and the suspension was transferred to 4°C. After addition of the double amount of Biobeads the suspension was incubated overnight at 4°C and gentle shaking. Proteoliposomes were harvested next morning by ultracentrifugation (353000xg, 20 min, 4°C) and washed 2 times with potassium phosphate 100 mM pH 7,5; 15°C). The proteoliposomes were then resuspended to a final concentration of 60 mg/ml lipid and stored at -80°C after freezing in liquid nitrogen.

2.4.6 Radiochemical transport measurements

2.4.6.1 Betaine uptake measurements of BetP and LcoP in proteoliposomes

One aliquot proteoliposomes (2.4.5.2) was thawed and diluted with potassium phosphate 100 mM pH 7,5 to a final lipid concentration of 5 mg/ml. The liposome suspension was extruded 17 times (2.4.5.2). Proteoliposomes were harvested from the suspension by ultracentrifugation and washed 2 times in potassium phosphate 100 mM pH 7,5. Finally the proteoliposomes were resuspended to a lipid concentration of 60 mg/ml in same buffer and stored at room temperature for up to 10 h. To determine the uptake activity of the

reconstituted BetP protein proteoliposome suspension was diluted 1:200 in uptake buffer (25 mM sodium phosphate pH 7,5; 20 mM NaCl, sorbitol as osmolyte and 30 μ M betaine (14 C betaine 400 cpm/ μ l) for BetP or 600 μ M betaine (14 C betaine 1000 cpm/ μ l) for LcoP and Valinomycin 1 μ M. In steps of 5 s 200 μ L of the reaction mixture were filtered through a 450 nm pore sized cellulose nitrate filter (Millipore, Schwalbach) on a vacuum filtration device (Hoefer, Pharmacia Biotech). The samples were immediately washed once with 2,5 ml LiCl 100 mM. The filter was subsequently incubated in 3,8 ml Szintillation liquid (Rotiszint; Carl-Roth, Karlsruhe). The amount of radiolabeled betaine in the bound proteoliposomes was then measured by a β -radiation counter (Beckmann, Muenchen). The increase of radioactivity under steady state conditions was used to calculate the uptake activity of the reconstituted protein.

2.4.6.2 Betaine uptake measurements in *E. coli* MKH13 cells

To estimate the *in vivo* activity of BetP and LcoP in *E. coli* the respective proteins were expressed in *E. coli* MKH13 (2.4.1.1). Cells were harvested and washed once in potassium phosphate pH7,5 25 mM; sodium chloride 100 mM at 4°C. Cells were resuspended then to an OD600 of 1-5 and supplemented with 20 mM Glucose and stored on ice for up to 3 h until the activity was measured. The uptake measurements were started by stirring 1 ml cell suspension mixed with 1 ml shock buffer (potassium phosphate pH7,5 25 mM; NaCl 100 mM; NaCl or KCl as osmolyte) for 3 min at 37°C. After this energetisation of the cells the uptake reaction was initiated by adding 10 μ l betaine 250 μ M (14 C-betaine 50 cpm/ μ L). for BetP constructs and 1 mM betaine (14 C-betaine 100 cpm/ μ L) for LcoP constructs. 200 μ l aliquots were taken at 15s, 30s, 45s,60s and 90s and immediately filtered through a glass fibre filter GF5, (Schleicher und Schuell, Dassel) on a vacuum filtration device (Hoefer, Pharmacia Biotech). The samples were immediately washed twice with 2,5 ml potassium phosphate 600 mM pH 7,5. The filter was subsequently incubated in 3,8 ml Szintillation liquid (Rotiszint; Carl-Roth, Karlsruhe). The amount of radiolabeled betaine in the cells was then measured by a β -radiation counter (Beckmann, München). The increase of radioactivity under steady state conditions was used to calculate the uptake activity of the cells. For the calculation a biomass of 0,34 mg/ml and OD600 was assumed.

2.4.6.3 Betaine uptake measurements in *C. glutamicum* DHPF cells.

To estimate the *in vivo* activity of BetP *C. glutamicum* the respective proteins were expressed in *C. glutamicum* DHPF (2.4.1.3). Cells were harvested and washed once in potassium phosphate pH7,5 25 mM; sodium chloride 100 mM at 4°C. Cells were resuspended then to an OD600 of 1-5 and supplemented with 20 mM Glucose and stored on ice for up to 3 h until the activity was measured. The uptake measurements were started by stirring 1 ml cell suspension mixed with 1 ml shock buffer (potassium phosphate pH7,5 25 mM; NaCl 100 mM; NaCl or KCl as osmolyte) for 3 min at 30°C. After this energetisation of the cells the uptake reaction was initiated by adding 10 µl betaine 250 µM (¹⁴C-betaine 50 cpm/µL). 200 µl aliquots were taken at 15s, 30s, 45s,60s and 90s and immediately filtered through a glass fibre filter (GF5, Schleicher und Schuell, Dassel) on a vacuum filtration device (Hoefer, Pharmacia Biotech). The samples were immediately washed twice with 2,5 ml LiCl 100 mM. The filter was subsequently incubated in 3,8 ml Szintillation liquid (Rotiszint; Carl Roth, Karlsruhe). The amount of radiolabeled betaine in the cells was then measured by a β-radiation counter (Beckmann, München). The increase of radioactivity under steady state conditions was used to calculate the uptake activity of the cells. For the calculation a biomass of 0,36mg/ml and OD600 was assumed.

3 Results

3.1 Genetic fusion of BetP trimers

3.1.1 Fusion BetP: a. pFus

The analysis of cross-talk relied on the ability of introduction of modifications in defined protomers. The genetically fused BetP comprised an attractive tool as such a protein would have led to the possibility of the examination of cross-talk between BetP protomers *in vivo*. Therefore the pFus vectors were constructed encoding BetP trimers in which the three protomers were linked by short TEV-cleavable amino acid linkers. These proteins exhibited a maximal betaine uptake activity of approximately $70 \text{ nmol} \times \text{mg}_{\text{cdw}}^{-1} \times \text{min}^{-1}$ in *E. coli* and *C. glutamicum* at external osmolalities of 800 mOsM (*E. coli*) or 1300 mOsM (*C. glutamicum*) (Fig. 3-1)

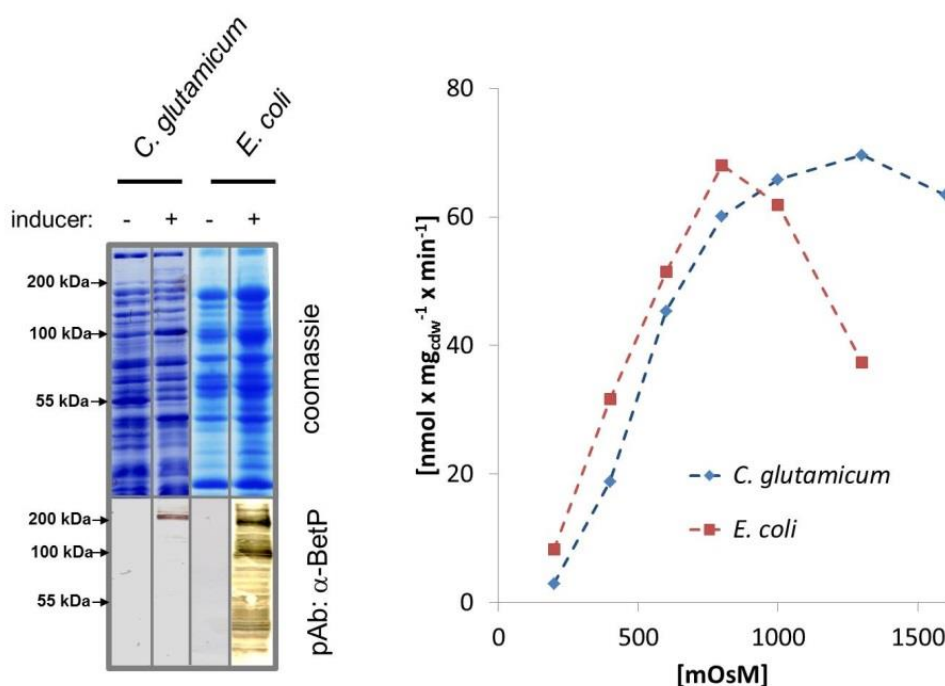


Fig. 3-1: SDS-PAGE/western blot analysis of membrane proteins prepared from *E. coli* MKH13 and *C. glutamicum* DHPF cells that had expressed genetically fused BetP trimers encoded by the pFus (*E. coli*) and the pXMJ19_Fus (*C. glutamicum*) (left). *In vivo* betaine uptake activity in dependence of the external osmolality of the respective strains (right). Fusion BetP protein visible in the upper band at the expected apparent molecular weight of 200 kDa.

Therefore both activity and regulation of the genetically fused BetP trimers appeared to be very similar to wildtype BetP in both organisms. SDS-PAGE revealed severe degradation of the fusion trimers taking place in the *E. coli* cell whereas the same construct expressed in *C. glutamicum* cells appeared to be physically stable. The degradation pattern observed for the pFus encoded protein in *E. coli* suggested a proteolytic cleavage in the linker regions as the apparent molecular weights were close to that of monomeric (~65 kDa), dimeric (~130 kDa) and trimeric (~200 kDa) BetP proteins. As expected, purification of the the genetically fused BetP trimers, expressed in *E. coli*, led to a preparation in which huge amounts of degraded protein could be detected by SDS-PAGE and westernblot experiments (Fig. 3-2).

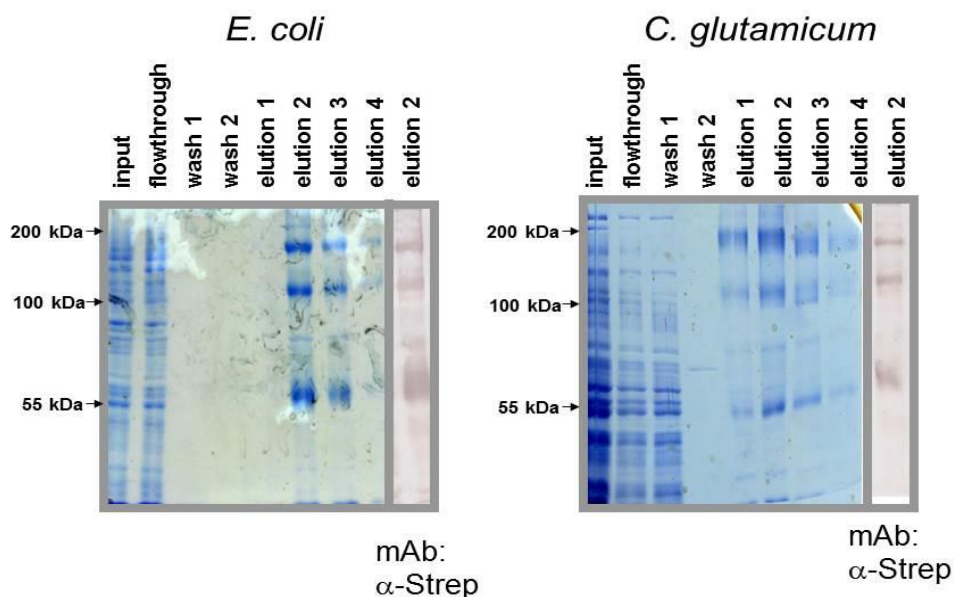


Fig. 3-2: SDS-PAGE/western blot analysis of Strep-Tactin purifications of fusion BetP expressed in *E. coli* DH5a (left) and *C. glutamicum* DHPF (right). Trimeric fusion BetP protein visible in the upper band at the expected apparent molecular weight of 200 kDa. Monomeric and dimeric degradation products visible at 60 kDa and 120 kDa respectively.

Although the protein appeared to be stable in the *C. glutamicum* membrane, severe degradation was observed upon purification of this protein from *C. glutamicum*. Furthermore no uptake activity could be reconstituted from preparations containing the fusion-BetP-protein (data not shown). For a further analysis of the contribution of the different subunits to the transport activity *in vivo*, the effect of inactivation of different

subunits was tested. Introduction of the inactivating W141A mutation (Gärtner et al., 2011) to different protomers revealed strong position effects.

Inactivation of the third and second subunit in the fusion-trimer led to a reduction of the maximal activity of about 50% compared to the fusion protein with three intact subunits, whereas the inactivation of the first subunits abolished the uptake activity nearly completely. The amount of heterologously expressed fusion protein appeared to be equal for all of the variants tested, as judged by western blot analysis of the membrane protein fraction of those strains (Fig. 3-3).

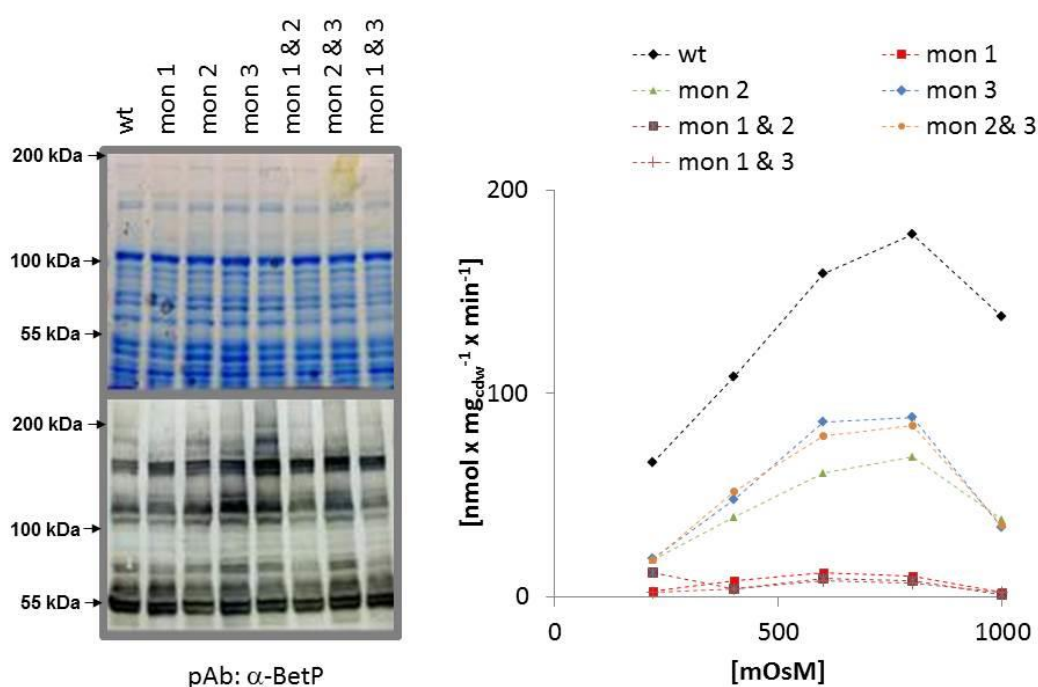


Fig. 3-3: SDS-PAGE/western blot analysis of *E. coli* MKH13 cells that expressed different genetically fused BetP trimers (left). The indicated protomers in each fusion-BetP construct were inactivated by the introduction of the W141A mutation. *In vivo* uptake activity conferred by the respective constructs in *E. coli* MKH13 cells (right). Trimeric fusion BetP protein visible in the upper band at the expected apparent molecular weight of 200 kDa. Monomeric and dimeric degradation products visible at 60 kDa and 120 kDa respectively.

These findings suggested that only the first subunit took part in the transport reaction. The lowered activity in the mutants that carried the W141A mutation in the second and third subunit was most likely due to interference of the mutated subunits with the membrane integration of the first protomer, as most of the observed activity was obviously due to the

first monomer. The fact that the W141A mutation in the third or in the second as well as in both of those subunits had exactly the same phenotype supported this interpretation. First of all it was aimed to avoid the observed proteolysis in *E. coli*. The distinct bands of the proteolysis products visible in SDS-PAGE of the respective *E. coli* membrane fractions indicated proteolytic cleavage most likely to occur at either the terminal sequences of the fused protomers or the artificial linker sequences.

3.1.2 Fusion BetP: b. pFel

The hypothetical cleavage in the linker sequences was addressed by fusion BetP from the pFel vector series. Those vectors allowed the systematic elongation of the linker sequence by either hydrophobic poly-alanine sequences or hydrophylic, repetitive SSG motifs. The linker encoding sequences in those vectors were introduced in the DNA sequence inbetween the Age1/BamH1 (first linker sequence) and the Kpn1/Kpn21 (second linker sequence) restriction sites.

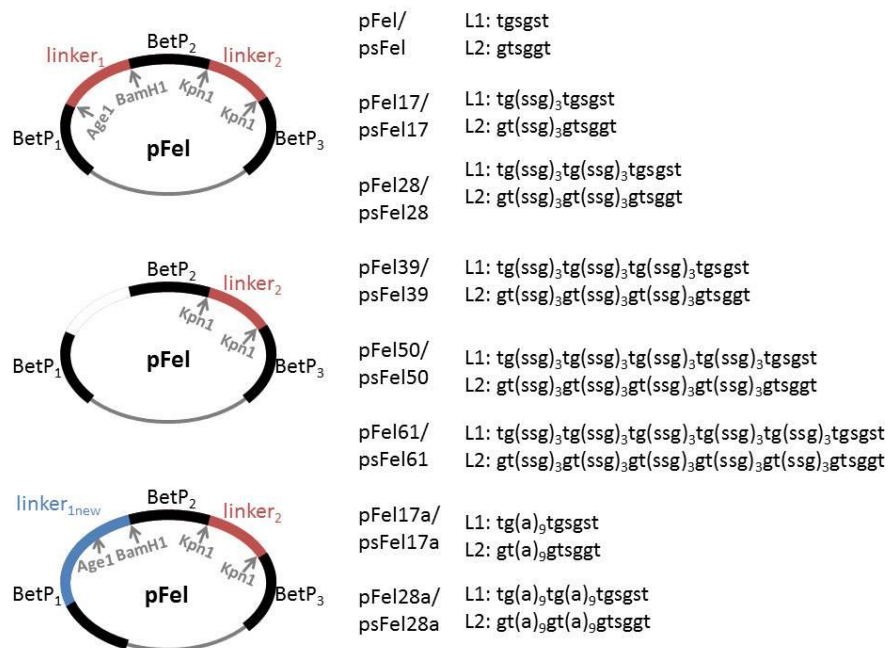


Fig. 3-4: Schematic representation of the pFel vectors with the restriction sites relevant for cloning. The cloning strategy for the elongation of the first linker by introduction of synthetic oligonucleotide sequences in the first linker sequence (left). Amino acid linker sequences of the first (L1) and second (L2) linker sequence encoded by the indicated pFel/psFel vector (right). The number in the plasmid name corresponds to the length of the amino acid linker sequence (SSG-linker or poly-A linker indicated by a).

For the elongation of the linker sequences appropriate synthetic oligonucleotides were ligated with the Age1/BamH1 or Kpn1/Kpn21 cut pFel vector. The oligonucleotides were designed in a way that the insertion of the oligonucleotide sequence disrupted the original Age1 or Kpn21 site respectively. The oligosequence itself contained the Age1 or Kpn21 recognition sequence itself, followed by a 9 amino acid coding sequence of the desired linker sequence. Therefore the linkers could be stepwise elongated by repetitive linker sequence insertion (Fig. 3-4). The length of the linker sequence tested as well as its composition did neither affect transport activity nor the regulation of the expressed fusion protein *in vivo* in *E. coli* (Fig. 3-5). All fusion proteins tested exhibited a maximal uptake activity of 50 to 90 $\text{nmol mg}_{\text{cdw}}^{-1} \times \text{min}^{-1}$ at external osmolalities of 600 to 800 mOsM corresponding to a biochemical activation of 4-10 fold above the non-stimulated activity. None of the SSG-linker sequences lead to the stable expression of the corresponding fusion-BetP-protein in *E. coli*.

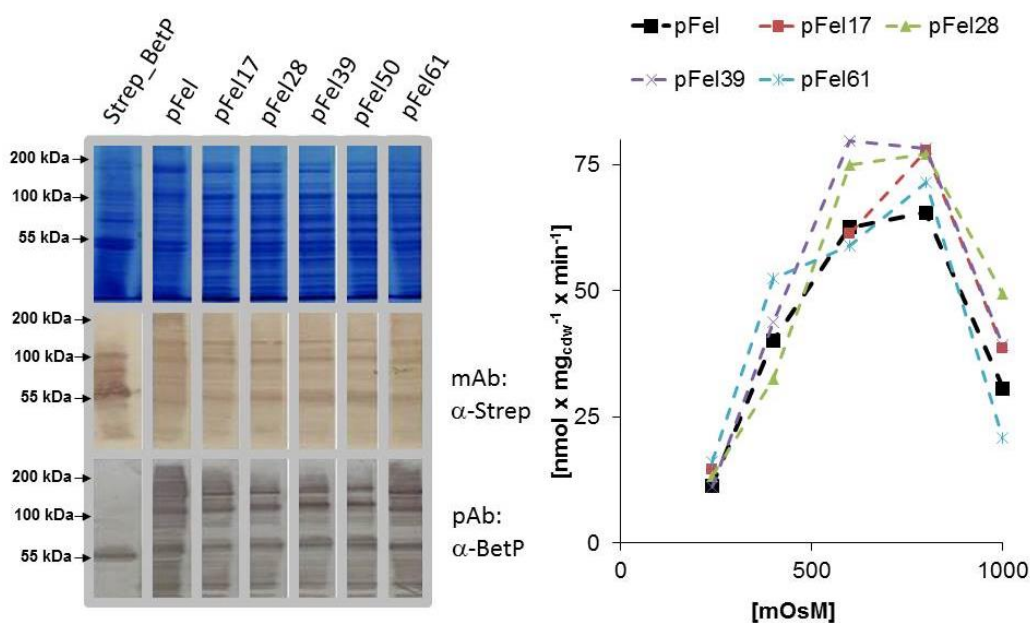


Fig. 3-5: SDS-PAGE/western blot analysis of *E. coli* MKH13 cells that had expressed different genetically fused BetP trimers by the respective pFel vectors (left). In vivo betaine uptake activity of *E. coli* MKH13 cells upon expression of the indicated pFel encoded fusion BetP proteins in dependence of the external osmolality (right). Trimeric fusion BetP protein visible in the upper band at the expected apparent molecular weight of 200 kDa. Monomeric and dimeric degradation products visible at 60 kDa and 120 kDa respectively. Linker elongations for the pFel50 and pFel61 vector were cloned by Manaf Hassan (Hassan 2012).

The same held true for the hydrophobic poly-alanine linkers (pFel17a and 28a) tested (Data not shown). As the linker sequences weren't likely to be the target of proteolytic degradation in *E. coli*, those target sequences were assumed to be located within the BetP protomers. To address terminal protein domains as being the target for proteolysis, fusion BetP proteins composed out of truncated variants of BetP protomers were designed. To retain the osmoregulatory properties of the protomers a truncation of the last 12 c-terminal amino acids from each protomer was introduced, as this truncation was already shown to affect the osmoregulation only partially (Schiller & Morbach 2004; Burkovski et al. 1998). The fusion protein composed of BetP_DC12 monomers exhibited indeed only very few degradation suggesting that the proteolytic target must have been located within the last 12 c-terminal amino acids of each BetP protomer. Expression analysis of fusion-BetP composed of c-terminally truncated BetP_DC12 monomers indeed led to an enhanced physical stability of the protein in the *E. coli* membrane. Only minor degradation bands were visible in western blots whereas the most prominent BetP band migrated at an apparent molecular weight of 200 kDa corresponding to the size of the intact fusion protein (Fig. 3-6).

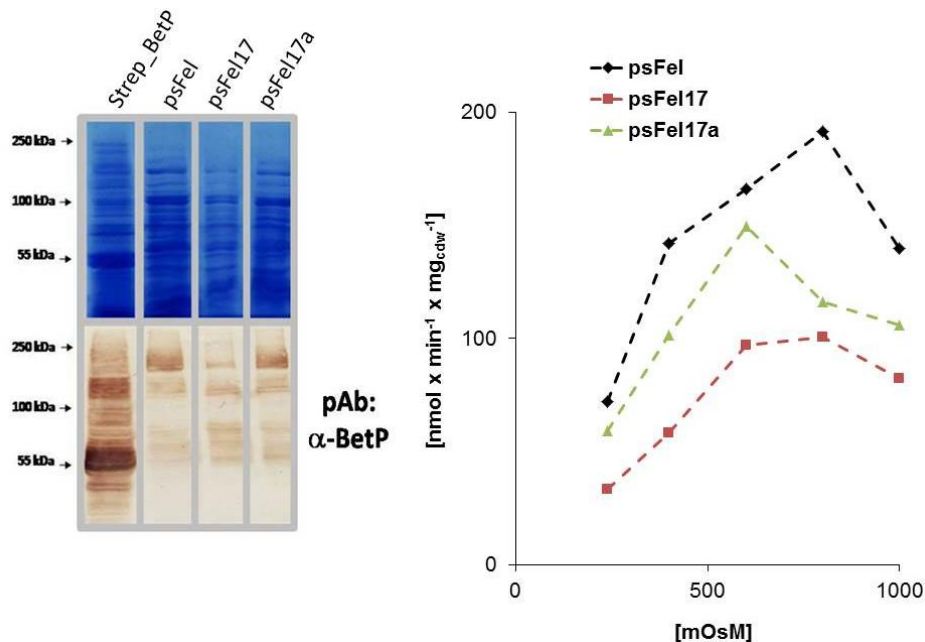


Fig. 3-6: SDS-PAGE/western blot analysis of *E. coli* MKH13 cells that had expressed different genetically fused BetP_ΔC12 trimers by the respective psFel vectors (left). *In vivo* betaine uptake activity of of *E. coli* MKH13 cells upon expression of the indicated pFel encoded fusion BetP proteins in dependence of the external osmolality (right). Trimeric fusion BetP protein visible in the band at the expected apparent molecular weight of 200 kDa.

As observed for fusion BetP constructs composed of full-length protomers, the fusion variants composed of the truncated variants exhibited exactly the same regulation and activity as the respective non-fused variants.

Again only a minor effect of the linker sequence and composition on activity and regulation of the fusion protein could be confirmed (Fig. 3-6). In contrast to the situation in *E. coli* all fusion BetP proteins tested appeared to be stable in the *C. glutamicum* membrane regardless of linker length and composition (Fig. 3-7). The protomers of the fusion protein in *C. glutamicum* appeared to be functional inequivalent albeit the chemical stability of the linker sequences.

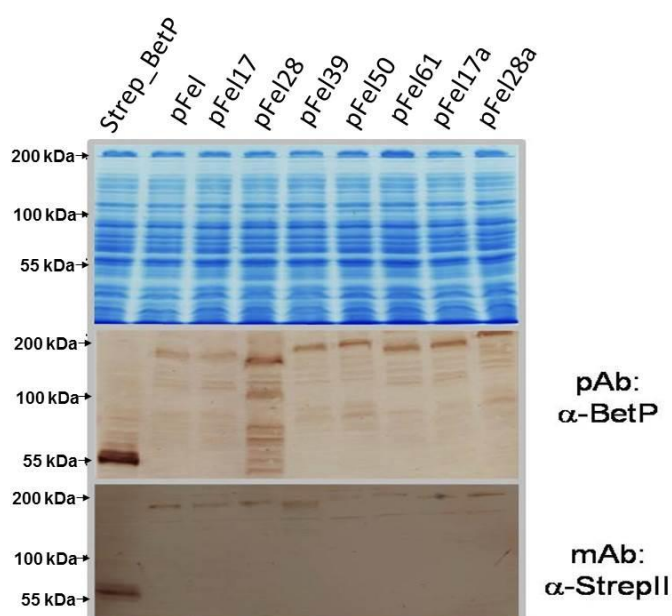


Fig. 3-7: SDS-PAGE/western blot analysis of membrane fractions of *C. glutamicum* DHPF cells that had expressed different genetically fused BetP trimers by the respective pFel vectors. Trimeric fusion BetP protein visible in the band at the expected apparent molecular weight of 200 kDa. Linker length and composition as described (Fig. 3-4). SDS-PAGE and western blot done by Manaf Hassan (Hassan 2012)

As observed for pFus encoded fusion BetP in *E. coli* (3.1.1), the inactivation of the different subunits in the pXMJ19_Fel encoded fusion protein by the W141A mutation exhibited position specific effects (Fig. 3-8). These effects were however less pronounced in *C. glutamicum* than in *E. coli* (Fig. 3-3).

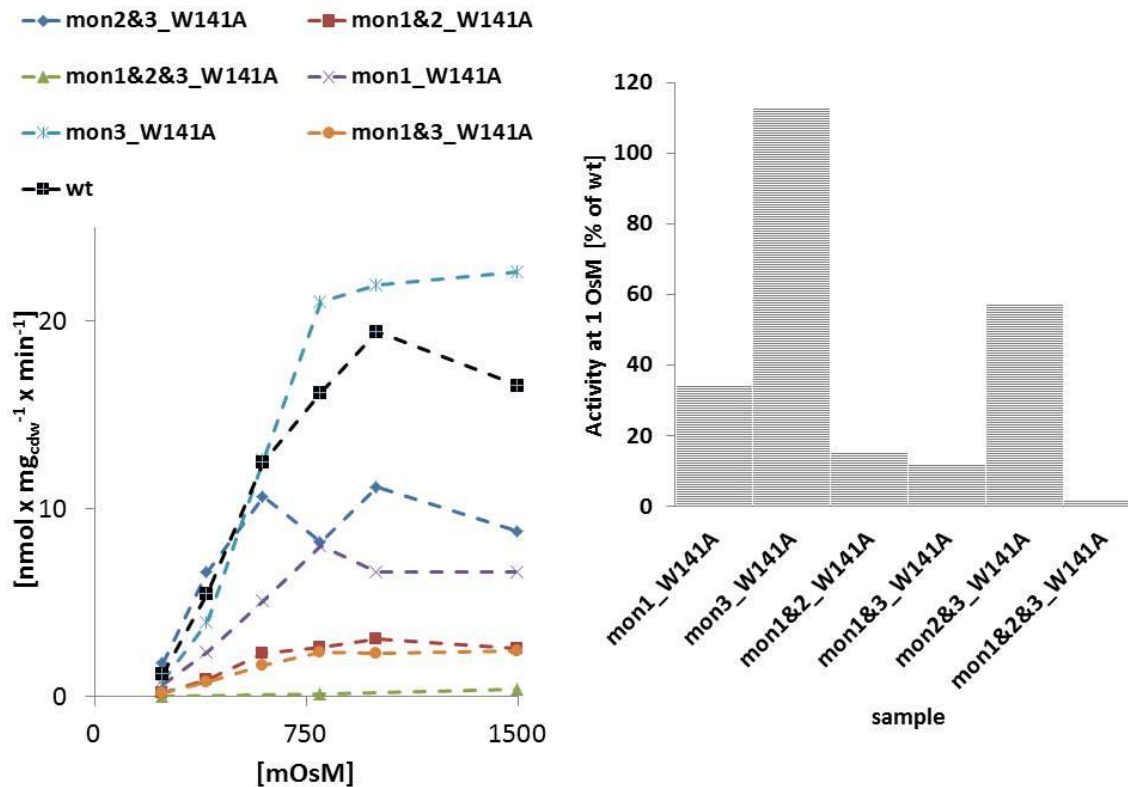


Fig. 3-8: Betaine uptake activity of *C. glutamicum* DHPF cells that expressed pXMJ19_Fel encoded fusion BetP variants with the inactivating W141A mutation in the indicated subunits (left). Comparison of the betaine transport activity of the different strains at an external osmolality of 1 OsM with the activity in the respective construct with three active subunits (right).

The activity of the fusion BetP variant with the inactivating W141A mutation in the first subunit remained at about 30% in *C. glutamicum* whereas it was shown to be nearly completely abolished in *E. coli* (Fig. 3-3). The observed functional inequivalency of the subunits *in vivo* with an obviously low contribution of the second and third subunit to the transport activity suggested the formation of functional BetP trimers composed mainly of the first subunits of the fusion-trimers encoded by the pFus and pFel vectors. As expected the fusion BetP proteins expressed in *C. glutamicum* which were not prone to proteolytic degradation appeared to form high molecular weight aggregates which were interpretable as trimers of trimeric fusion-proteins as judged by BN-PAGE western blots. The fusion BetP proteins in *E. coli*, that were cleaved in their terminal sequences in contrast migrated mostly at the same apparent molecular weight as wildtype BetP (Fig. 3-9).

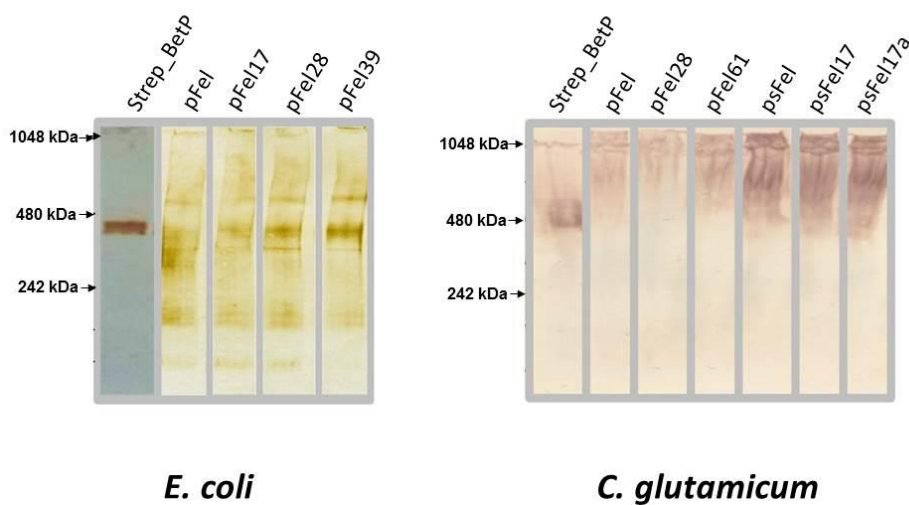


Fig. 3-9: Blue-native-PAGE/western-blot analysis of membrane fractions of *E. coli* MKH13 and *C. glutamicum* DHPF strains that expressed the indicated fusion BetP. Aggregated fusion BetP visible in the at apparent molecular weights of 500-1000 kDa (*C. glutamicum*) and 400 kDa (*E. coli*)

The aggregation of the fusion proteins could in contrast to proteolysis not be avoided by alterations in the amino acid linker sequence of the fusion proteins. These constructs were therefore not used for further cross-talk analysis.

3.2 Individually tagged BetP

3.2.1 N-terminal affinity tags

The second strategy to obtain hetero-trimeric BetP proteins involved the co-expression of BetP monomers with different affinity purification tags. Those proteins would ideally assemble randomly to trimeric BetP proteins. Sequential affinity purification against three different affinity purification tags would then have led to a preparation with a defined homogenous protomer composition of each BetP trimer. Specific mutations impairing either catalytic activity or regulation of a defined number of subunits per trimer would have enabled the examination of catalytic and regulative cross-talk *in vitro*. The purification of BetP-trimers was established more than ten years ago by use of a Strep-tag fused to the n-terminus of BetP. C-terminal tags were reported to interfere with BetP expression and cell viability (Rübenhagen et al., 2001). Therefore it was decided to fuse all affinity tags of interest to the N-terminus of BetP.

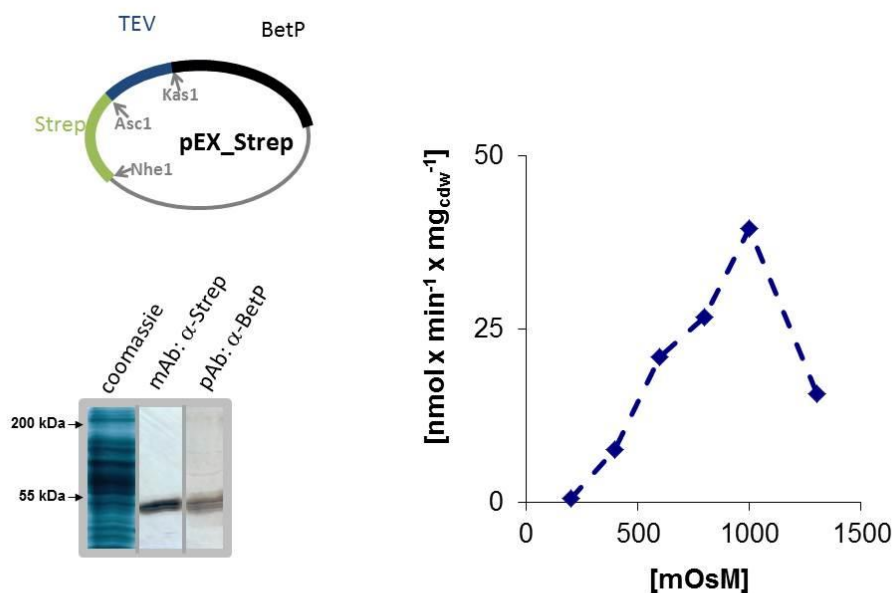


Fig. 3-10: Schematic representation of the pEX_Strep vector with the restriction sites relevant for cloning of different tag and linker sequences (upper left). SDS-PAGE/ western-blot analysis of the membrane fraction of *E. coli* MKH13 cells that had expressed Strep tagged BetP from the pEX_Strep vector. BetP band visible at the expected molecular weight of approx. 60kDa (lower left). *In vivo* betaine uptake activity of Strep_BetP expressed from pEX_Strep in *E. coli* MKH13 cells (right).

The pEX vector was designed to allow subcloning of various tag sequences between the Nhe1/Asc1 restriction enzyme recognition sites. To avoid tag specific alterations of activity and regulation, the amino acid linker between tag and BetP coding sequences contained the recognition sequence for the TEV protease (NH₂-ENLYFQG-COOH). pEX_Strep_BetP encoded BetP exhibited a maximal activity of 40 nmol x mg_{cdw}⁻¹ x min⁻¹ in *E.coli* MKH13 cells. The uptake activity was regulated in the dependence of the external osmolality in the same manner than that of the pASK-IBA5_Strep_BetP protein (Fig. 3-10).

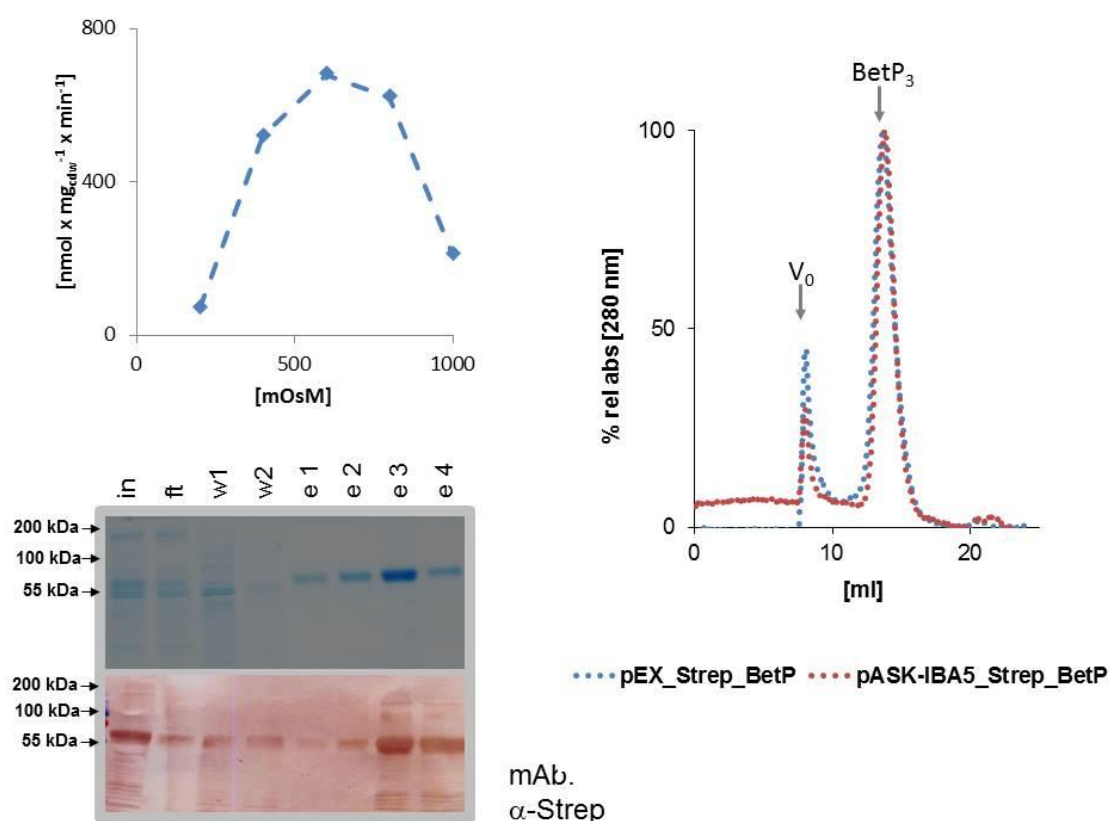


Fig. 3-11: Betaine uptake activity of reconstituted Strep tagged BetP expressed from the pEX_Strep_BetP vector (upper left). SDS-PAGE /western blot analysis of the purification of this protein from the *E.coli* membrane protein fraction. BetP band visible at the expected molecular weight of aprox. 60kDa (lower left). SEC analysis of the purified protein in comparison to the purified pASK-IBA_Strep_BetP encoded protein (arrows indicating the exclusion volume of the SEC column (V_0) as well as the elution volume of trimeric BetP ($BetP_3$)).

Expression of homo-trimeric BetP protein from the pEX_Strep_BetP resulted in purifyable protein that exhibited osmoregulated betaine uptake activity upon reconstitution in proteoliposomes. The recombinant protein exhibited the same few aggregation as the protein purified from expression of the original pASK-IBA5 encoded Strep_BetP protein as

judged by SEC (Fig. 3-11). Several recognition sites for site specific proteases were introduced in the linker sequence spacing the tag from the BetP sequence in the pEX vectors. Cleavage of the tag sequence via TEV protease worked well whereas the trombin and FactorXa protaeses appeared to be not applicable in cleaving of the tag sequence from Strep-tagged BetP in crude *E. coli* membrane extracts (Fig. 3-12).

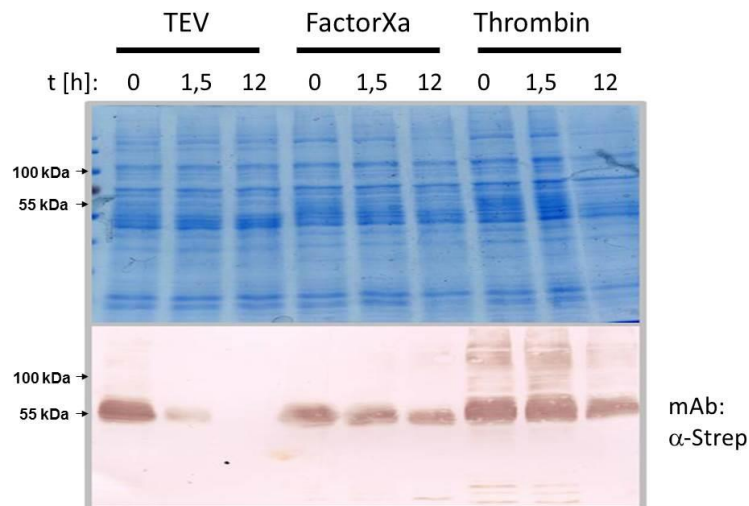


Fig. 3-12: SDS-PAGE western blot analysis of Strep_tag removal by different site specific proteases. Crude solubilisates of membrane fractions of *E. coli* cells that had expressed Strep_BetP variants with the different recognition elements in the linker sequences were treated for the indicated times with the appropriate protease.

Therefore the pEX vector encoding for BetP with a TEV cleavable linker sequence was chosen to test different affinity tags for their applicability in BetP expression and purification. Active His-tagged BetP encoded by pEX_His_BetP was purifyable. The activity of the protein *in vitro* appeared to be regulated by the external osmolality in the same way than the original Strep_BetP but the overall activity was reduced to $250 \text{ nmol} \times \text{mg}^{-1} \times \text{min}^{-1}$ corresponding to roughly 25% of that of the reference protein. Purified His-BetP exhibited severe aggregation in SEC experiments in agreement with the low activity (Fig. 3-13). The induction of the His_BetP expression led furthermore to complete growth arrest of *E. coli* and a co-expression of this variant together with the Strep-BetP was not possible (Data not shown).

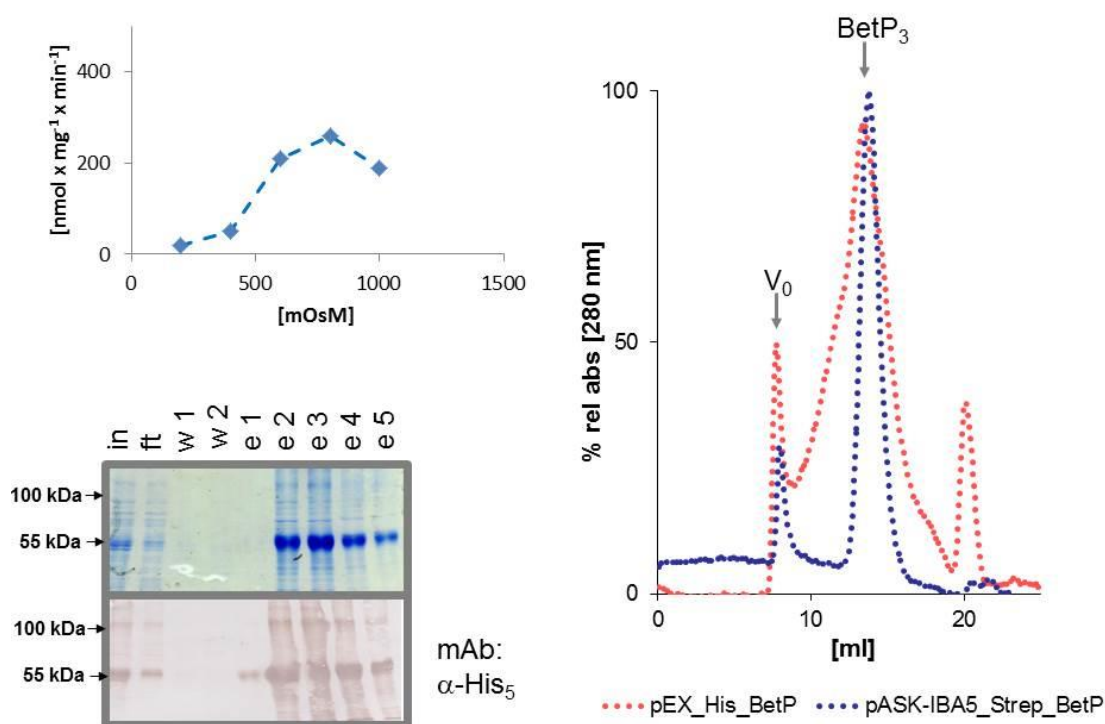


Fig. 3-13: Betaine uptake activity of reconstituted His tagged BetP expressed from the pEX_His_BetP vector (upper left). SDS-PAGE /western bolt analysis of the IMAC-purification of this protein from the *E.coli* membrane protein fraction. BetP band visible at the expected molecular weight of aprox. 60kDa (lower left). SEC analysis of the purified protein in comparison to the purified pASK-IBA5_Strep_BetP encoded protein (arrows indicating the exclusion volume of the SEC column (V_0) as well as the elution volume of trimeric BetP (BetP₃))(right).

Different affinity tags suitable for IMAC based protein purifications were tested for their applicability. Expression of pEX encoded BetP with a N-terminal HAT-tag and HQ-tag had the same dramatic consequences for *E. coli* as the His-tag. Consequently no uptake could be measured in *E. coli* MKH13 cells that expressed those constructs. The detrimental effects of BetP expression with a n-terminal His-tag could be overcome by spacing the His-tag further apart by either an octadecanoyl SSG linker sequence or a fluorescent mVenus protein. With these linker elongations it was possible to measure specific and regulated betaine uptake activity in the corresponding *E. coli* MKH13 cells. The uptake activity reached about $100 \text{ nmol} \times \text{mg}_{\text{cdw}}^{-1} \times \text{min}^{-1}$ and was further just as regulated as that of the Strep_BetP reference (Fig. 3-14).

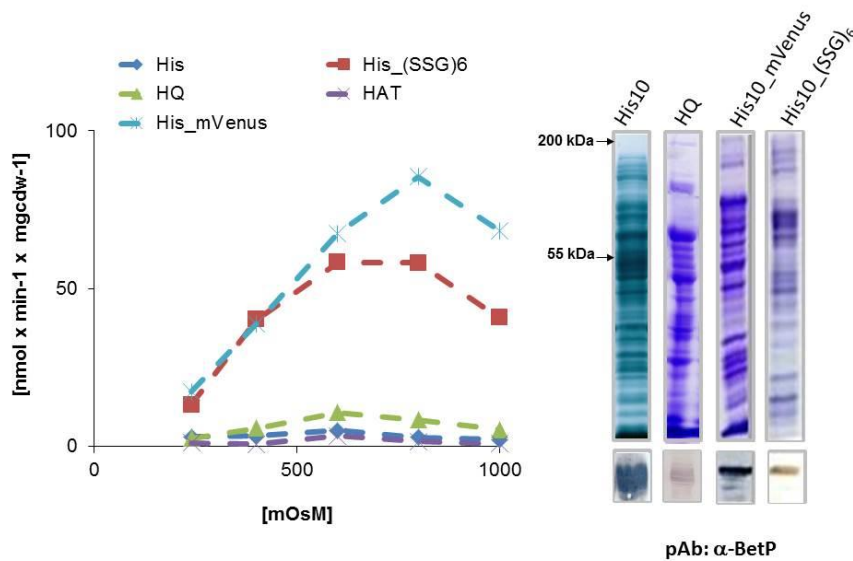


Fig. 3-14: SDS-PAGE/western blot analysis of *E. coli* MKH13 cells that had expressed pEX encoded BetP proteins with different N-terminal affinity tags suitable for IMAC purifications (right). *In vivo* betaine uptake activity of *E. coli* MKH13 cells upon expression of the indicated differently tagged BetP variants in dependence of the external osmolality (left).

The purification of the pEX_His_SSG6_BetP and pEX_His_mVenus_BetP encoded proteins did however not lead to preparations with reconstitutable betaine uptake activity. Instead the same kind of stability problems of the solubilised proteins, as observed for the decahistidine tagged BetP were recognised (Data not shown). A variety of 19 different amino acid tags fused to the N-terminus of BetP was tested in total for their usability in the design of heterotrimeric BetP. Uptake measurements of the respective constructs expressed in *E. coli* suggested no correlation of expression and activity with the size of the tags. The n-terminal fusion of the 27 kDa Glutathione-S-Transferase protein to the N-terminus of BetP resulted in an extremely high maximal uptake activity of about $200 \text{ nmol} \times \text{mg}_{\text{cdw}}^{-1} \times \text{min}^{-1}$ whereas the N-terminal fusion of the 30 kDa Maltose binding protein led to a maximal uptake activity of only $30 \text{ nmol} \times \text{mg}_{\text{cdw}}^{-1} \times \text{min}^{-1}$. The net charge of the amino acid tag did as well not affect the activity of the fused BetP protein *in vivo*. The highly surface charged variants of the green fluorescent protein (Lawrence et al., 2007) pos36_GfP and neg30_GfP led to exactly the same activity and regulation when fused to the N-terminus of BetP (Fig. 3-15). In summary it was observed that all tags except the IMAC

tags and the Chitin-binding domain (CBD) tag fused to the N-terminus of BetP led to expression of an active and osmoregulated BetP protein in *E. coli* MKH13.

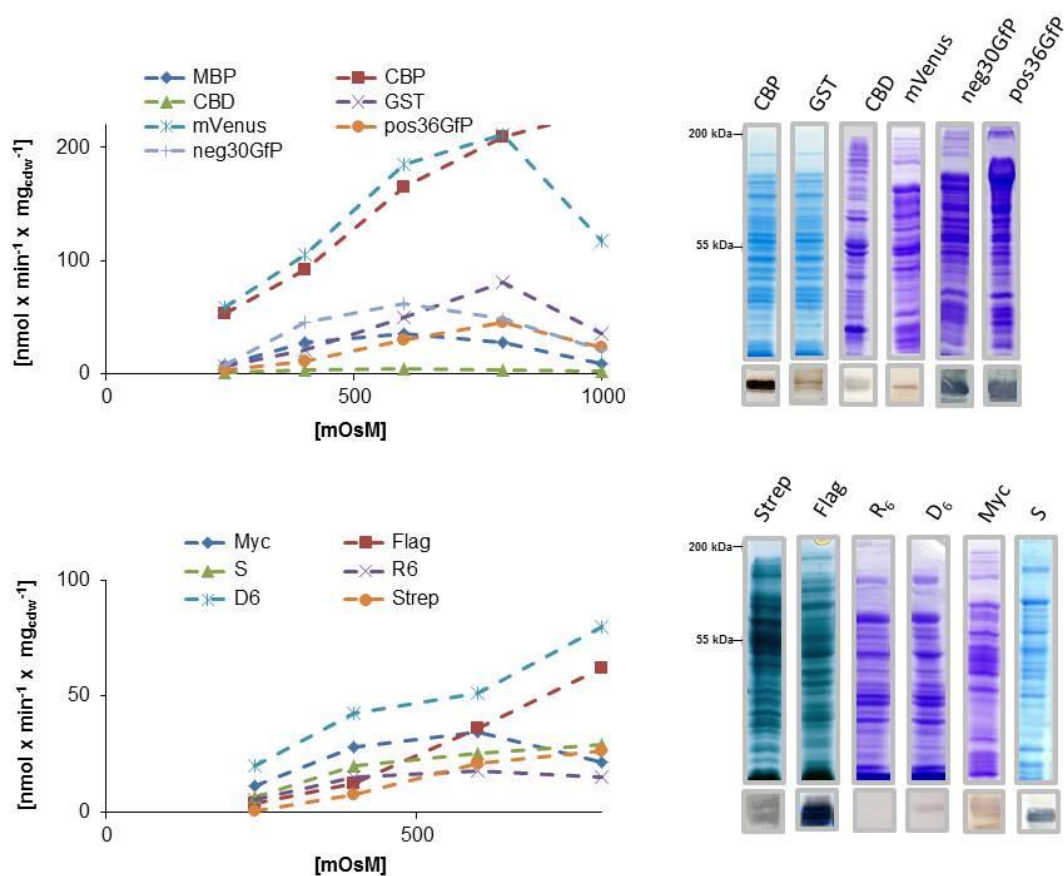


Fig. 3-15: SDS-PAGE/western blot analysis of *E. coli* MKH13 cells that had expressed pEX encoded BetP proteins with different N-terminal affinity tags (right). *In vivo* betaine uptake activity of *E. coli* MKH13 cells upon expression of the indicated differently tagged BetP variants in dependence of the external osmolality (left). The tags comprised either whole protein sequences (upper panels) or small epitope tags (lower panels).

Surprisingly no tag sequence except for the Strep-tag led to the purification of active protein via the respective affinity resin. GST, Flag and S tag lead to aggregation of the protein on the respective affinity resin, whereas the Calmodulin sepharose did not bind Calmodulin-Binding-Peptide (CBP) -tagged BetP (Fig. 3-16).

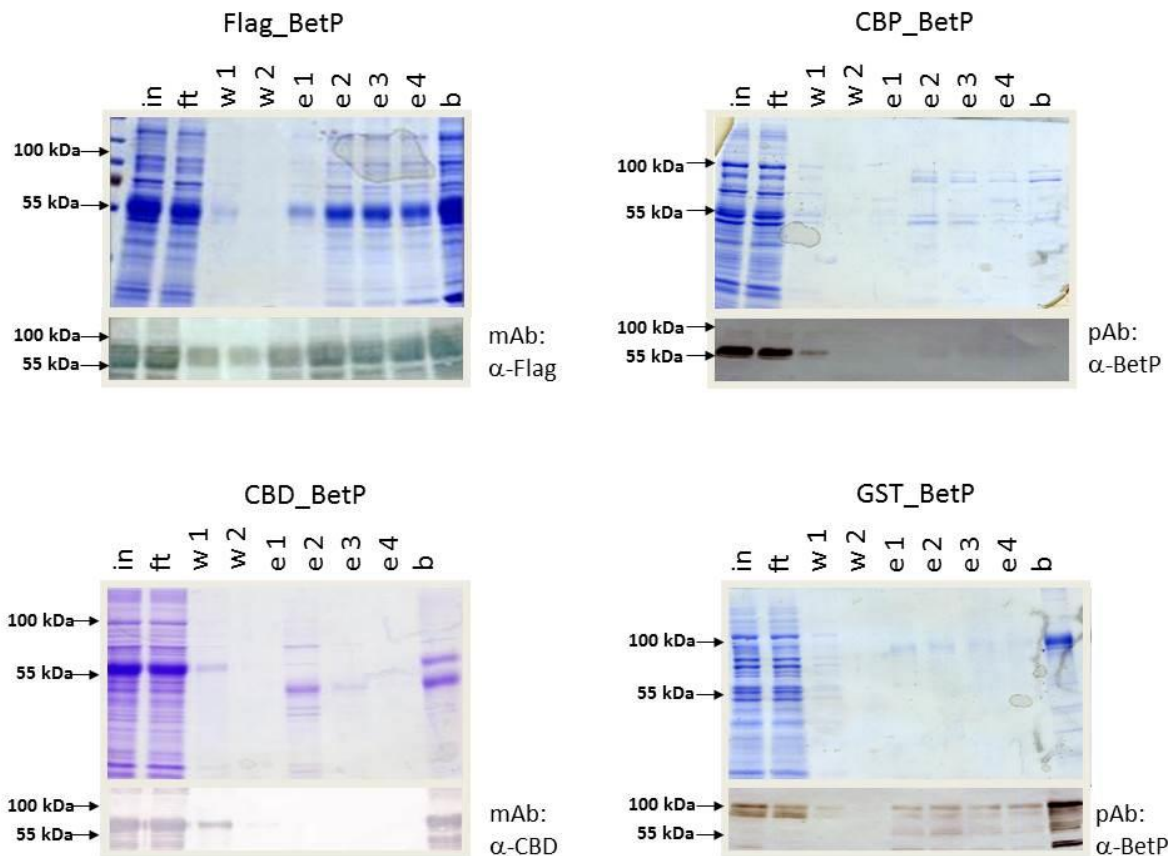


Fig. 3-16: SDS-PAGE/western blot analysis of purifications of BetP variants with the indicated N-terminal tag sequence via the respective affinity resin. Solubilisation and binding of the protein to the affinity resin was carried out in all cases according to the Strep_Tactin protocol except for the addition of 2 mM CaCl₂ in case of the CBP tagged BetP. Elution was carried out by addition of Flag-Peptide 0,2 mg/ml (Flag-BetP); 5 mM EGTA (CBP-BetP); Promega TEV protease (CBD_BetP) and 30mM GSSH (GST_BetP).

Although no active BetP protein could be purified by any other than the Strep-tag so far, different tags were addressed for their applicability in co-purifications together with Strep_BetP. Such a preparation would have enabled studies on negative dominance. The co-purification of inactivated Strep_BetP together with active BetP comprising another tag, would have led to a Strep-Tactin purified preparation in which every active subunit would have been neighboured by at least one inactivated one. The Flag_BetP protein expressed from the pD_Flag_BetP/Strep_BetP vector (for vector construction see 3.5) could be co-purified by purification of the Strep-tagged protein via Strep-Tactin. No betaine uptake activity could be reconstituted from those preparations. The purified protein exhibited

severe aggregation in SEC experiments although a reasonable fraction of Flag_BetP appeared to be assembled in trimers with the Strep_BetP as judged by SEC (Fig. 3-17).

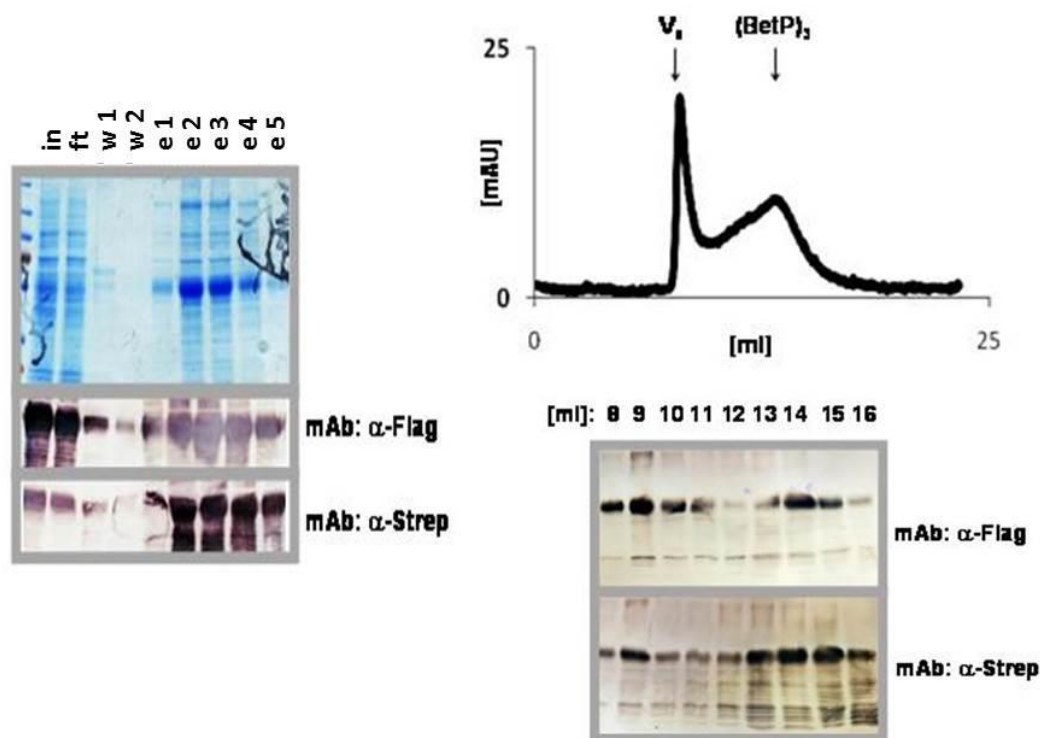


Fig. 3-17: SDS-PAGE/western blot analysis of purifications of co-expressed Strep_BetP and Flag_BetP variants via Strep_Tactin (left). SEC analysis of the purified protein (arrows indicating the exclusion volume of the SEC column (V_0) as well as the elution volume of trimeric BetP (BetP_3)) (upper right). Identification of the co-purified SEC separated proteins via SDS-PAGE/western blot analysis of the SEC fractions (lower right).

The aggregation tendency was observed also for Gfp_BetP in GPC experiments from crude membrane extracts (Data not shown). No explanation could be found why the Strep-tag sequence was the only tag that did not interfere with the stability of the protein in detergent solution. As none of the different tags tested led to successful purifications, no further affinity tags were tested in this position.

3.3 Stability of BetP trimers

The oligomeric state of BetP was assumed to be a stable trimer, suggested by the crystallisation of the protein in 2D and 3D crystals as well as analytical ultracentrifugation (Ziegler et al. 2004; Ressler et al. 2009). None of the methods would have revealed fast protomer exchanges between trimers in the membrane. Therefore such a protomer exchange was addressed as protomer exchange would have been highly critical for the examination of protomer cross-talk. Although none of the N-terminal tags other than the Strep-tag led to the purification of BetP trimers, that could have been reconstituted in an active way in proteoliposomes, most of those tags led to expression of active BetP protein in *E. coli* (3.2.1). As a co-purification of Strep_BetP and Flag_BetP appeared to be possible those two variants were chosen for this protomer exchange. *E. coli* membranes containing Strep_BetP or Flag_BetP were pooled and fused via freeze thawing and extrusion. After incubation of the fused membranes at room temperature the proteins were solubilised and subjected to Strep-Tactin purification. No Flag_BetP was co-purified together with the Strep_BetP finally proving the absence of protomer exchange between BetP trimers in the membrane.

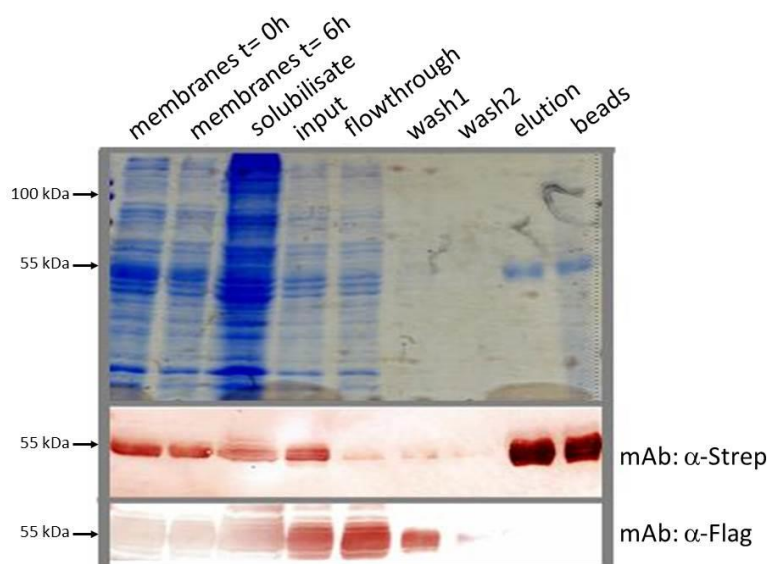


Fig. 3-18: SDS-PAGE/western blot analysis of Strep-Tactin pulldown of Flag_BetP via Strep_BetP upon fusion of *E. coli* membranes containing each one of those proteins.

3.4 C-terminal affinity tags

None of the N-terminally fused affinity tags led to proper BetP preparations except for the N-terminal Strep-tag. The primary structure of BetP comprises no large hydrophylic loop sequence that would allow the insertion of an affinity tag as used for the purification of LacY or several GPCR proteins. It was found in earlier studies, that an affinity-tag at the C-terminus of BetP has dramatic physiological effects on the *E. coli* cells expressing such a construct (Rübenhagen et al., 2001). Nevertheless we addressed the C-terminus again for the attachment of an amino acid tag sequence because of the lack of any different option. At first the introduction of a His-tag coding sequence to the C-terminus of the full length protein was tested. Because of the assumed detrimental effects of a C-terminal tag sequence the tag was immediately combined with different linker sequences between the His-tag and the BetP protein.

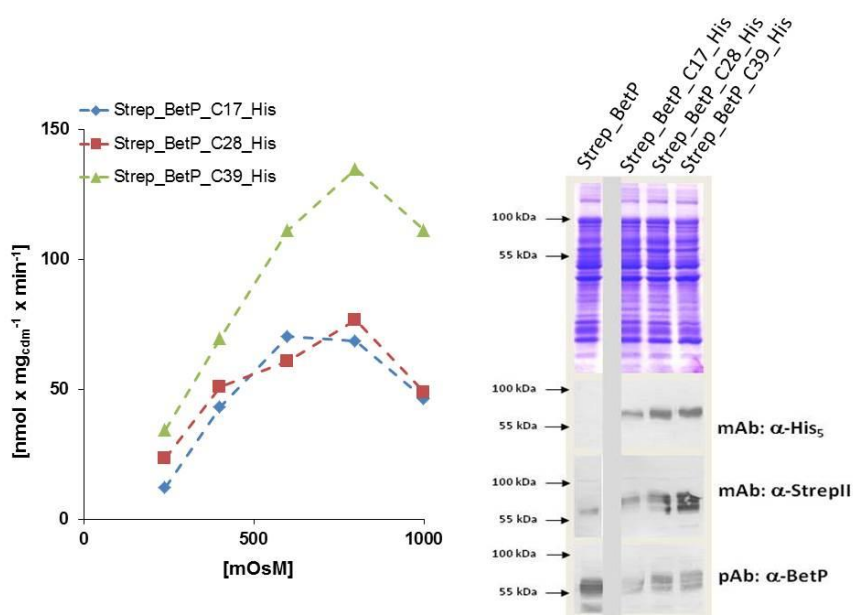


Fig. 3-19: SDS-PAGE/western blot analysis of *E. coli* MKH13 cells that had expressed different BetP proteins with C-terminal His-tags. A linker sequence of the indicated length was inserted inbetween the BetP and the His-tag coding sequence. (right). *In vivo* betaine uptake activity of *E. coli* MKH13 cells upon expression of the indicated BetP variants in dependence of the external osmolality (left).

The C-terminal His-tag did not interfere with expression, activity or regulation of the resultant BetP construct. The overall activity observed for the C-terminally His-tagged BetP

was highest with the longest 39-mer linker inbetween His-tag and BetP. SDS-PAGE/western blot analysis of membranes containing those constructs immediately revealed severe stability problems of the C-terminal tag. Immunoblotting against the C-terminal His-tag suggested the expression of the heterologous protein without any degradation. The additional band visible in blots against the whole protein and the N-terminal Strep-tag sequence in comparison to the immuno-blot-signal of the His-tag sequence showed hereagainst that approximately only 50% of the Strep_BetP_His proteins contained the desired His-tag (Fig. 3-19). The observed proteolysis at the C-terminus was consistent with the results obtained in expression of the fusion BetP variants (Fig. 3-5, Fig. 3-6). For this reason the stability of C-terminal tags at the C-terminally truncated BetP_DC12 variant was addressed. Homotrimeric BetP composed of Strep_BetP_DC12_His protomers appeared to be stable. The same held true for the Strep_BetP_DC12_Flag variant. Both proteins conferred osmotically activatable betaine uptake activity to *E. coli* MKH13 cells.

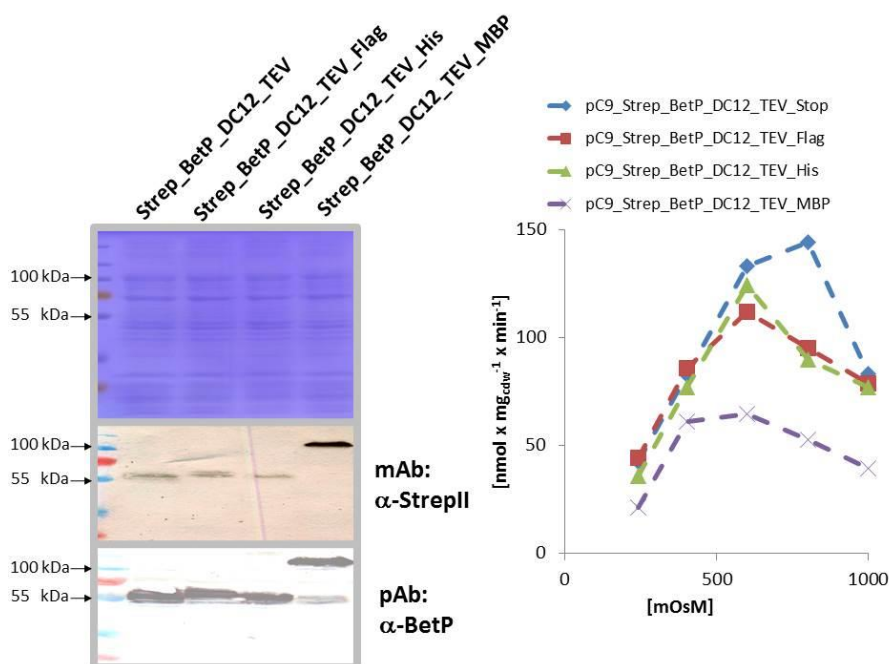


Fig. 3-20 : SDS-PAGE/western blot analysis of *E. coli* MKH13 cells that had expressed different Strep_BetP_DC12 proteins with the indicated C-terminal affinity purification tags. (left). *In vivo* betaine uptake activity of *E. coli* MKH13 cells upon expression of the indicated BetP variants in dependence of the external osmolality (left).

The His- and the Flag-tag fused to the C-terminus of BetP_DC12 caused alterations in neither activity nor regulation of this protein. The maltose-binding protein at the same position led to a reduced activity but without effects on regulation. Minor tag cleavage was observed for the MBP-tagged BetP_DC12 whereas no tag cleavage was observed for the C-terminal His- and Flag-tag (Fig. 3-20).

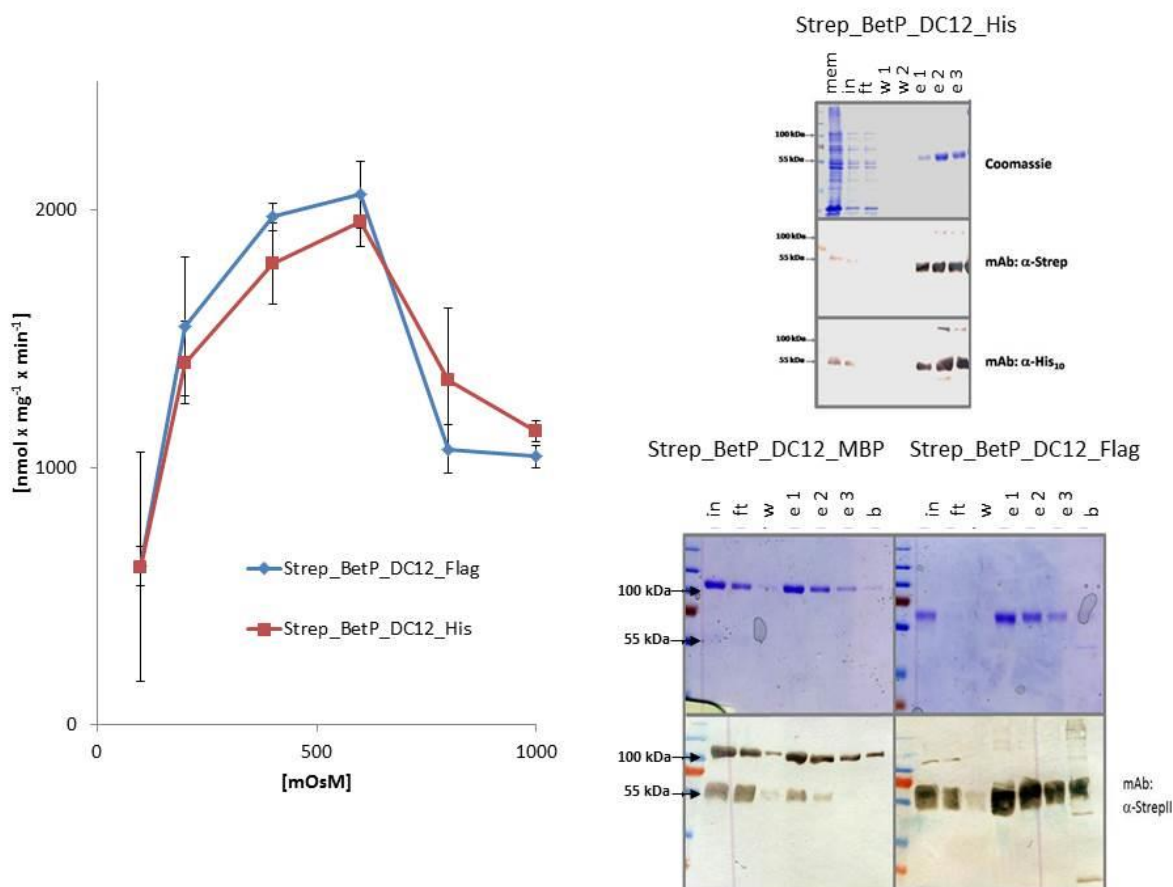


Fig. 3-21: SDS-PAGE/western blot analysis of affinity purifications of differently C-terminal tagged BetP_DC12 proteins (right). Indicated variants were purified from crude membrane extracts (Strep_BetP_DC12_His; upper panel) or Strep_Tactin pre-purified (Strep_BetP_DC12_MBP, Strep_BetP_DC12_Flag; lower panel). *In vitro* betaine uptake activity of reconstituted protein in dependence of the external osmolality (left).

Both proteins could be purified to homogeneity and retained their osmoregulated betaine transport activity upon reconstitution. His- and Flag-tagged BetP_DC12 could be quantitatively purified whereas a huge amount of Strep_BetP_DC12_MBP was lost in purification attempts on amylose resin. The expression efficiency of the two proteins was low compared to the full length variant of BetP in *E. coli* (approximately 10%).

3.5 Co-expression and purification of BetP heteromers

As both Strep_BetP_DC12_His and Strep_BetP_DC12_Flag could be purified and reconstituted in an active and regulated state those were the first constructs allowing a sequential affinity purification via IMAC and subsequent Flag epitope purification. It could be shown that both affinity resins did not lead to unspecific purification of BetP (Data not shown). Therefore preparations purified via His-tag and Flag-tag must have comprised both protomers in each trimer. For the co-expression it was decided not to make use of the commercial Duett vector system for two reasons: (i) Expression of BetP from this T7 based vector system resulted in loss of expression in earlier studies. (ii) The T7 expression system requires *E. coli* strains carrying the γ -prophage for efficient expression. The latter would have led to constructs for which *in vivo* activity studies in *E. coli* MKH13 would have been impossible. Therefore the pD vectors were cloned.

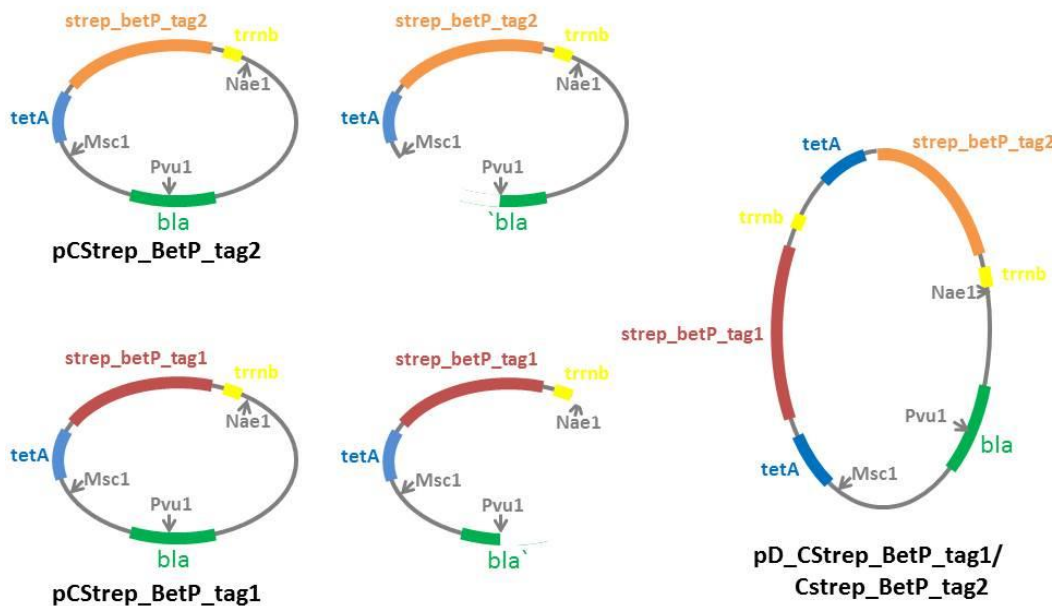


Fig. 3-22: Schematic representation of the construction of the pD vectors, used for the co-expression of different BetP variants. Restriction sites relevant for cloning are shown in grey, β -Lactamase coding sequence in green, tetA promoter sequence in blue and terminator sequence of the *rrnB* gene in yellow.

The construction of those vectors allowed the successive introduction of a principally non-limited number of genes all expressed under control of the TET-promotor as single mRNAs with each containing its own translation initiation and termination sites (Fig. 3-22). Those vectors appeared to be a robust system for the co-expression of different BetP protomers in *E. coli*. Co-expressed Strep_BetP_DC12_His and Strep_BetP_DC12_Flag retained its regulatory and catalytic properties upon reconstitution after sequential affinity purification on IMAC and Flag affinity resin. The introduction of a third C-terminal tag resulted in several complications. The maltose binding protein as well as the Glutathione-S-transferase were tested for this purpose. None of the two tags led to purification of satisfying yields (Fig. 3-21). The decoration of the C-terminus of the third subunit via plasmid encoded affinity tags was not further addressed for another obvious reason.

The typical yield of expression of Strep_BetP_DC12_His and Strep_BetP_DC12_Flag was about 10% of that of full-length Strep_BetP. The expression of three C-terminal tagged BetP protomers would therefore have led to very low amounts of purifiable hetero-trimeric protein. Another option for the purification of hetero-trimeric protein would have been the omission of the Strep-tag coding sequence in the N-termini of the two BetP_DC12_tag protomers. By this approach the sequential affinity purification against the two C-terminal tags of the BetP_DC12 monomers followed by a Strep-Tactin purification of trimers containing full-length Strep-BetP the stoichiometry of the purified protein would have been clearly defined. The omission of the Strep-tag coding sequence at the N-terminus of BetP_DC12_His led to severe stability problems that resulted in the co-purification of a huge amount of contaminating proteins in IMAC purifications. With this preparation no protein could be purified on Strep-Tactin affinity resin after Flag-M2 purification (Fig. 3-23).

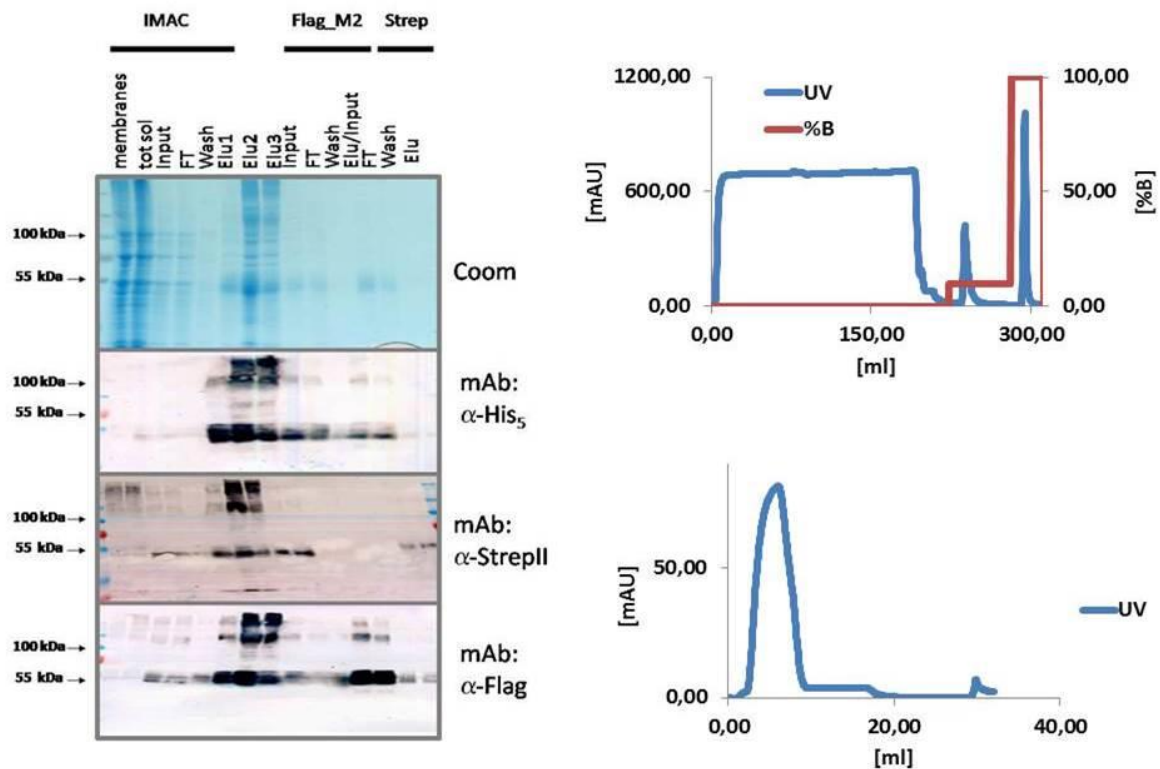


Fig. 3-23: SDS-PAGE/western blot analysis of the sequential affinity purifications of co-expressed BetP_DC12_His/BetP_DC12:Flag/Strep_BetP via IMAC, Flag-M2 and subsequent Strep-Tactin purification (left). UV chromatograms of the IMAC and Strep-Tactin purification (right).

Therefore those purification attempts were not followed. As omission of the n-terminal Strep-tag sequence was obviously not useful for the separation of heteromers, chemical modification of the C-terminus of the third subunit was addressed *in vitro*. Such an alternative to amino acid tags would have led to the possibility of hetero-trimer preparation from co-expressed Strep_BetP_DC12_His; Strep_BetP_DC12_Flag and a full-length protomer with a covalently attached chemical modification. The Strep_BetP_E577C and Strep_BetP_G511C mutants were chosen as third protomers to be expressed in combination with Strep_BetP_DC12_His and Strep_BetP_DC12_Flag for this purpose because those single cysteines were shown not to interfere with the activity and regulation of the protein. Furthermore those residues were shown to be highly accessible for the sulfhydryl reactive Bodipy_FL-iodoacetamide dye. HDPD-Biotin was chosen as label (2.4.4.2) and introduced during the IMAC purification. IMAC and Flag tag pre-purified and Biotin

labeled protein was then subjected to purification of biotinoylated protein via Strep-Tactin. Heteromeric BetP trimers containing the E577C or G511C mutation were not purified in amounts sufficient for reconstitution and functional analysis (data not shown). Purification of those heteromers via thiol activated sepharose yielded also to amounts of protein too low for further analysis although it was possible to purify Strep-Tactin purified, homo-trimeric Strep_BetP_E577C via thiol activated sepharose (data not shown).

3.6 Cross-talk in BetP heteromers

3.6.1 Catalytical cross-talk in BetP

None of our attempts led to the purification of hetero-trimeric BetP with a protomer stoichiometry, defined by a three step affinity purification. With the established protocol (3.5) it was only possible to guarantee that a single full-length protomer would have been neighbored by one Strep_BetP_DC12_His and a Strep_BetP_DC12_Flag monomer. Although preparations obtained this way did not necessarily comprise a defined monomer stoichiometry, they allowed the examination of catalytic cross-talk in a way that dominant effects of inactivation of the BetP_DC12 subunits would have clearly led to a completely inactive preparation even in presence of an active Strep_BetP monomer in the trimer. For the inactivation of the two truncated monomers binding of both substrates was abolished by single site mutations. To abolish betaine binding the mutations Y197L and W377L were introduced disrupting the cage like betaine binding site (Ott 2008).

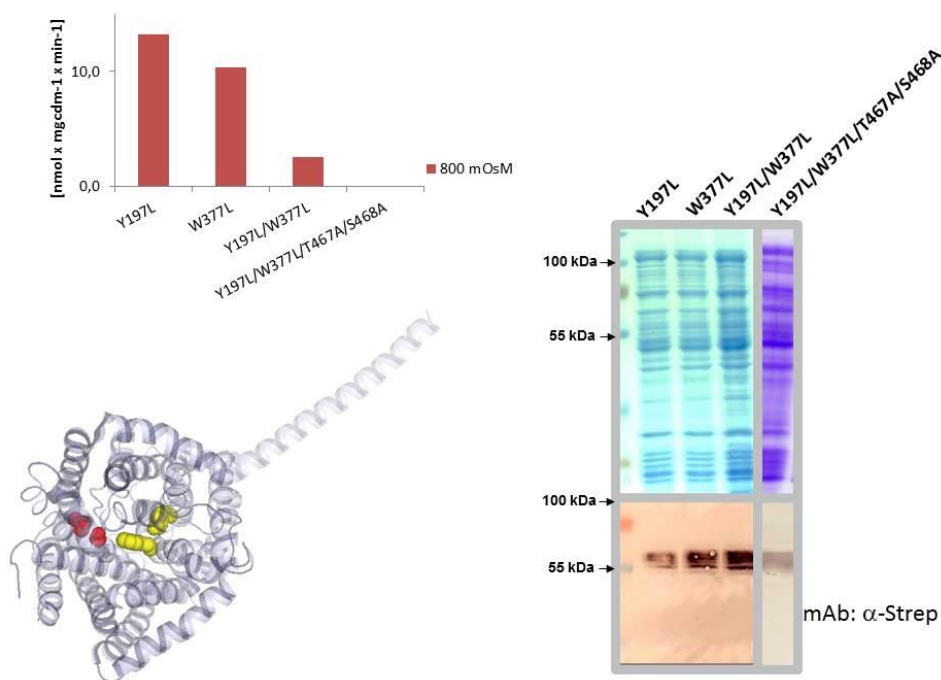


Fig. 3-24: SDS-PAGE/western blot analysis of *E. coli* MKH13 cells that had expressed different Strep_BetP proteins with the indicated single site mutations (right). *In vivo* betaine uptake activity of *E. coli* MKH13 cells upon expression of the indicated BetP variants at an external osmolality of 800 mOsM (upper left). Schematic representation of the single site mutations in the structural BetP model (PDBentry: 2WIT) (lower left).

To further abolish sodium binding, the Na² binding site was disrupted by introduction of the T467A and S468A mutation (Khafizov et al., 2012). To address negative dominance on effects in the transport reaction, full-length Strep_BetP was co-expressed together with catalytically inactive Strep_BetP_DC12_His and Strep_BetP_DC12_Flag. The resultant construct was confirmed to exhibit no residual betaine uptake activity. The co-expression of the two inactivated Strep_BetP_Y197L/W377L/T467A/S468A_DC12_His and Strep_BetP_Y197L/W377L/T467A/S468A_DC12_Flag monomers together with the full length Strep_BetP led to a preparation in which wildtype like regulated betaine uptake activity was measurable.

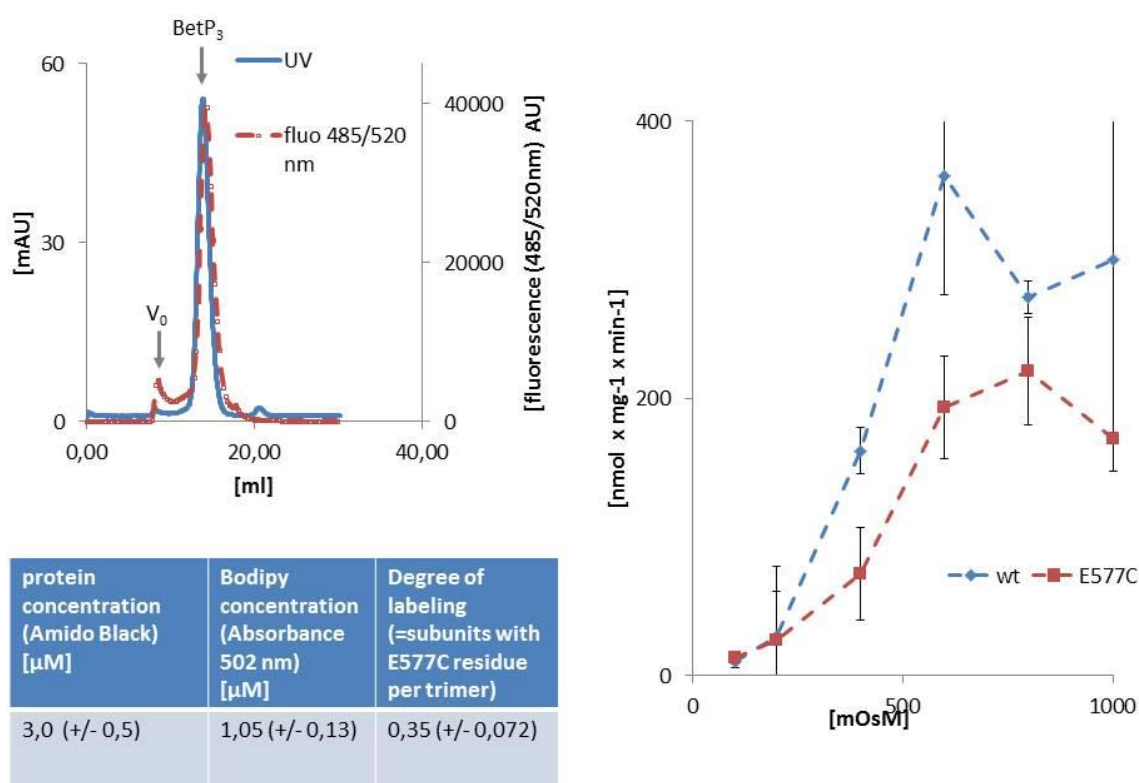


Fig. 3-25: *In vitro* activity of reconstituted, heterotrimeric BetP proteins composed of Strep_BetP_Y197L/W377L/T467A/S468A_DC12_His and Strep_BetP_Y197L/W377L/T467A/S468A_DC12_Flag together with Strep_BetP (wt) or Strep_BetP_E577C (E577C) purified against the His- and Flag-tag of the inactivated subunits (right). FSEC chromatogramm of heterotrimeric Strep_BetP_Y197L/W377L/T467A/S468A_DC12_His/Strep_BetP_Y197L/W377L/T467A/S468A_DC12_Flag/Strep_betP_E577C labeled with Bodipy. Exclusion volume of the superose column and elution volume of trimeric BetP indicated by arrows (upper left). Estimation of degree of labeling via amido and dye absorbance (lower left).

The activity observed reached about $400 \text{ nmol} \times \text{mg}^{-1} \times \text{min}^{-1}$ resembling about 30% of that of homo-trimeric Strep_BetP *in vitro* suggesting the complete absence of any kind of catalytical cross-talk. Because of the unknown macroscopic stoichiometry of full-length BetP and the inactivated monomers we aimed to elucidate that stoichiometry to further convince the absence of any kind of catalytic cross-talk. Herefore the inactivated Strep_BetP_Y197L/W377L/T467A/S468A_DC12_His and Strep_BetP_Y197L/W377L/T467A/S468A_DC12_Flag monomers were co-expressed together with the single cysteine variant Strep_BetP_E577C. The E577C mutation was shown to have no influence on the activity and regulation of homo-trimeric BetP (3.8). After co-expression and sequential affinity-purification the preparation was labeled at the cysteine 577 with the sulfhydryl reactive dye Bodipy_FI_IA. The reconstituted protein again exhibited wildtype like regulation and about 30% of activity of homo-trimeric Strep_BetP upon reconstitution *in vitro*. Fluorescence-size-exclusion-chromatography experiments with this preparation and dye concentration measurements showed that the fluorescently labeled full-length protein was present at about one third of the total protein amount and that the labeled protein was in the correct oligomeric state (Fig. 3-25). Therefore the absence of any kind of catalytic cross-talk between BetP protomers could be proven.

3.6.2 Regulatory cross-talk in BetP

The proof of absence of catalytic cross-talk in BetP enabled the examination of regulatory cross-talk. As the catalytic inactivation of two monomers in the trimeric transport protein had no influence on the activity of the third one, it was now possible to study the impact of an impaired regulatory function in the catalytically inactivated monomers on the third subunit. To impair the regulatory function of the inactivated monomers the A564P mutation was introduced to those. This mutation in the C-domain was shown to render homo-trimeric BetP into a highly active but completely deregulated betaine transport protein *in vitro* (Fig. 3-26).

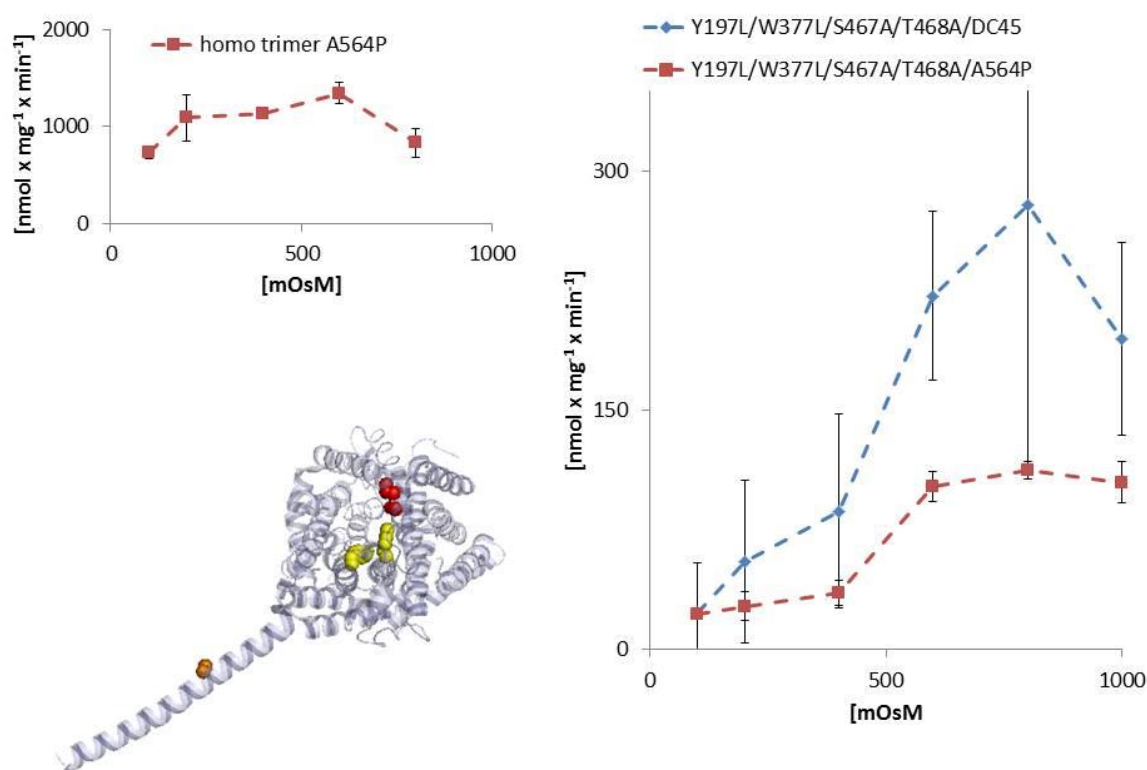


Fig. 3-26: *In vitro* activity of reconstituted Strep_BetP co-expressed with inactivated Strep_BetP_DC12_His and Flag which were either truncated to DC45 or mutated to A564P to impair the regulation of those (right). Activity of reconstituted homo-trimeric Strep_BetP_A564P (upper left). Schematic representation of the inactivating (yellow and red) and deregulating A564P (brown) single site mutations in the structural BetP model (PDBentry: 2WIT)(lower left).

Co-purification of Strep_BetP_Y197L/W377L/T467A/S468A/A564P_DC12_His and Strep_BetP_Y197L/W377L/T467A/S468A/A564P_DC12_Flag together with the full-length Strep-BetP led to a preparation in which completely normal regulation of the betaine uptake activity could be confirmed. The absolute uptake activity was lower than the one observed for the full-length protein surrounded by only catalytically inactivated monomers. The normal regulation of the full-length monomer in this context suggested the absence of any kind of regulatory action of the C-domain of a neighbouring subunit. To further confirm this result the inactivated protomers were truncated by 45 amino acids. This truncation had been known for a long time to abolish the regulatory properties, and led to a severely reduced overall activity of homo-trimeric BetP (Schiller & Morbach 2004). The truncation of the last 45 amino acids in the inactivated monomers did not impair the regulation of the third Strep_BetP protomer (Fig. 3-26).

Therefore the absence of any regulatory function of the C-domain on the neighbouring subunits was proven. Although the C-terminus itself had obviously no regulatory function on the neighbouring subunit regulatory cross-talk still remained possible. It was further addressed if the binding sites for the C-domain, build by the neighbouring protomers, are involved in the regulation. To disrupt possible interactions between the C-domain of the active, full-length protomer and the neighbouring subunits the complete loop2 of the two neighbouring, inactivated subunits was mutated to an inert sequence as this loop harbours the proposed interaction site between the C-terminus and the protein body of the neighbouring subunit (Ressl et al., 2009). Herefore the R129A/I130A/D131S/E132G/A133G/P134A/ΔE135 (loop2) mutations were introduced into the inactivated and deregulated protomers that carried the c-terminal affinity tags.

Co-purification of Strep_BetP_R129A/I130A/D131S/E132G/A133G/P134A/ΔE135/Y197L/W377L/T467A/S468A/A564P_DC45_His and Strep_BetP_R129A/I130A/D131S/E132G/A133G/P134A/ΔE135/Y197L/W377L/T467A/S468A/A564P_DC45_Flag together with the full length Strep-BetP led to a preparation in which wildtype like activity and regulation of the co-purified Strep_BetP protomer could be confirmed (Fig.3-27).

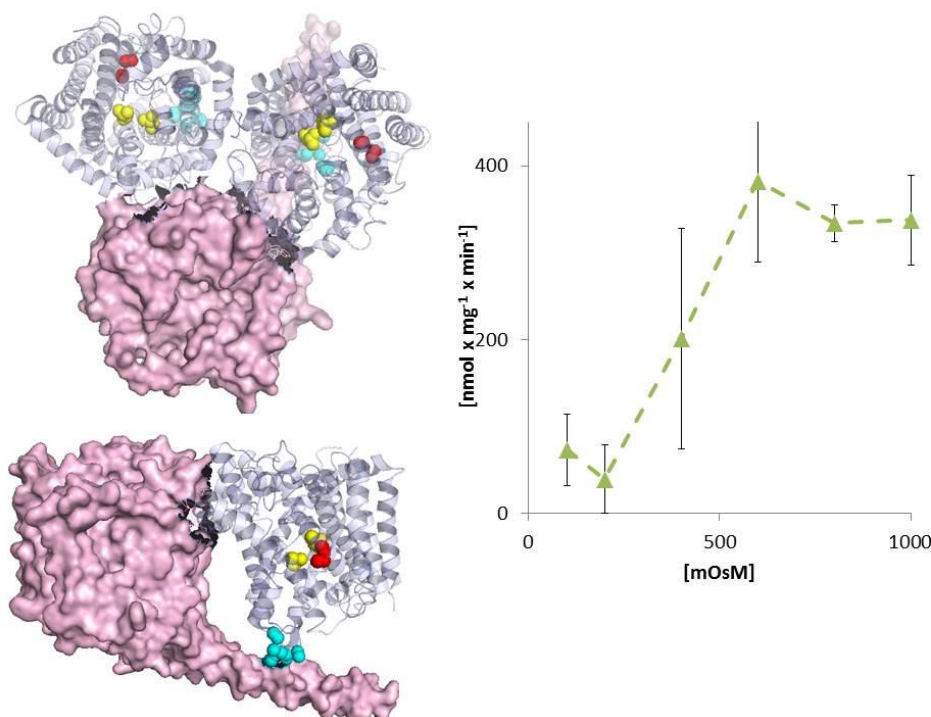


Fig. 3-27: *In vitro* activity of reconstituted Strep_BetP coexpressed with inactivated Strep_BetP_DC12_His and Flag that were additionally truncated to DC45 and mutated in the complete loop2 sequence (right). Schematic representation of the inactivating (yellow and red) single site mutations and the mutated loop2 (cyan) in the structural BetP model (PDBentry: 2WIT)(lower left).

Thereby it was clearly proven that conformational communication (cross-talk) is not necessary for both activity and regulation of BetP.

3.7 Re-analysis of monomeric BetP

No protomer cross-talk is required for transport and regulation of BetP. This result was in striking contrast to the interpretations of the relevant regulatory cross-talk concluded from results obtained by monomeric BetP (Perez et al. 2011). In this study it was shown that the mutation of the residues T351 in helix 7 and W101 in transmembrane helix 2 to alanine was sufficient to completely disrupt the protomer interaction, leaving monomeric BetP in the *E. coli* membrane. These monomeric BetP was interpreted to be not regulated by the external osmolality *in vivo*. Consistent with this finding it was published that the regulation of this mutant is severely impaired *in vitro*. The conclusion drawn in this publication was in

stark contrast to the observations made during cross-talk analysis via hetero-trimeric BetP (3.6.1,3.6.2). Therefore we aimed to re-address the behaviour of monomeric BetP with the published monomeric variants. The monomeric mutants Strep_BetP_W101A/T351A and Strep_BetP_W101A/F345A/T351A exhibited strictly osmoregulated betaine uptake activity upon expression in *C. glutamicum*. Upon expression in *E. coli* the Strep_BetP_W101A/F345A/T351A variant was not activatable by osmotic stress whereas the Strep_BetP_W101A/T351A variant was clearly activated under hyperosmotic conditions. The activation maximum of the W101A/T351A mutant reflected exactly that of wildtype BetP in *C. glutamicum* cells whereas it was shifted to higher osmolalities in *E. coli* (Fig.3-28). Comparison of the data with the published behaviour (Perez et al. 2011) of the two proteins expressed in *E. coli* showed that this result was in agreement with the published data. Both mutants expressed in *C. glutamicum* appeared to be completely monomeric in native PAGE experiments. This finding was of course in perfect agreement with the absence of cross-talk proven for the hetero-trimeric, *E. coli* expressed protein (3.6.2).

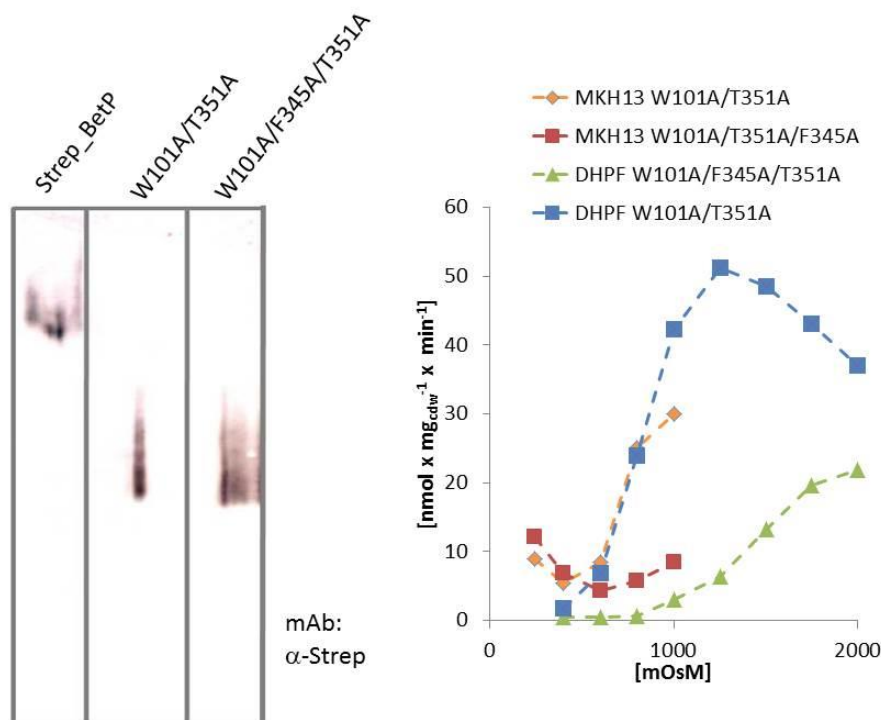


Fig. 3-28: *In vivo* activity of Strep_BetP_W101A/T351A and Strep_BetP_W101A/F345A/T351A measured in *E. coli* MKH13 and *C. glutamicum* DHPF cells (right). BN-PAGE/western blot analysis of membrane fraction of *C. glutamicum* DHPF cells that had expressed the indicated BetP variants (left). Strep BetP band visible at approx. 400 kDa.

Although this finding could have been taken as extremely convincing proof for the absence of cross talk, the oligomeric state of the mutant forms expressed in *C. glutamicum* was further investigated *in vivo*.

In the previous study it had been shown that BetP protomers carrying single cysteine mutations S328C in the amphiphatic helix 7 and D97C in TM2 (+c) were quantitatively crosslinkable in detergent solubilised state via homobifunctional sulfhydryl crosslinkers (Perez et al. 2011). Strep_BetP carrying these mutations appeared to be crosslinkable *in vivo* as well. Surprisingly a reasonable amount of the W101A/T351A (double) mutant appeared to be crosslinkable in the *E. coli* membrane whereas hardly any of the W101A/F345A/T351A protein could be crosslinked under these conditions. A possible osmolality dependent oligomerisation could clearly be ruled out as the crosslink efficiency appeared to be independent of the external osmolality (Fig. 3-29).

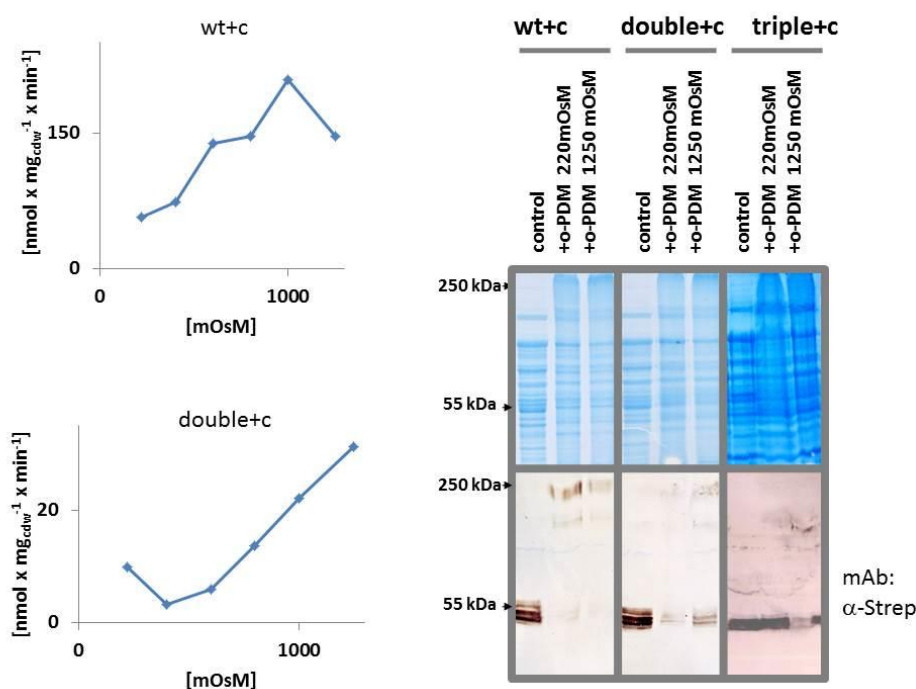


Fig. 3-29: Activity of Strep_BetP (wt+c) and the monomer mutant Strep_BetP_W101A/T351A (double+c) carrying additionally the S328C/D97C single cysteine mutations *in vivo* in *E. coli* MKH13 cells (left). SDS-PAGE analysis of membrane fractions of the corresponding strains after *in vivo* crosslinking with ortho-phenylbismaleimid at iso- (220 mOsM) and hyperosmotic (1250 mOsM) external osmolality. Cross-linked BetP band visible at the expected molecular weight of aprox. 200 kDa. Non-cross-linked BetP band visible at the expected molecular weight of aprox. 60kDa (right).

The regulation of the W101A/T351A variant together with its obvious osmo-regulation *in vivo* showed that it was not possible to draw a conclusion about regulatory cross-talk with

this mutant variant as its oligomeric state was not defined. The absent crosslinkability of the triple W101A/F345A/T351A mutant was in line with the interpretation of regulatory cross-talk. Interestingly, both mutants were regulated in *C. glutamicum* cells and appeared to be trimeric at least to reasonable amounts in *in vivo* crosslink experiments. Thereby no decision could be made about the necessity of regulatory cross-talk in BetP. The crosslink efficiency of both monomer mutants in *C. glutamicum* showed clearly that the published contact sites in the BetP trimer involve more regions of the protein and are surely not limited to the contact sites published (Fig. 3-30).

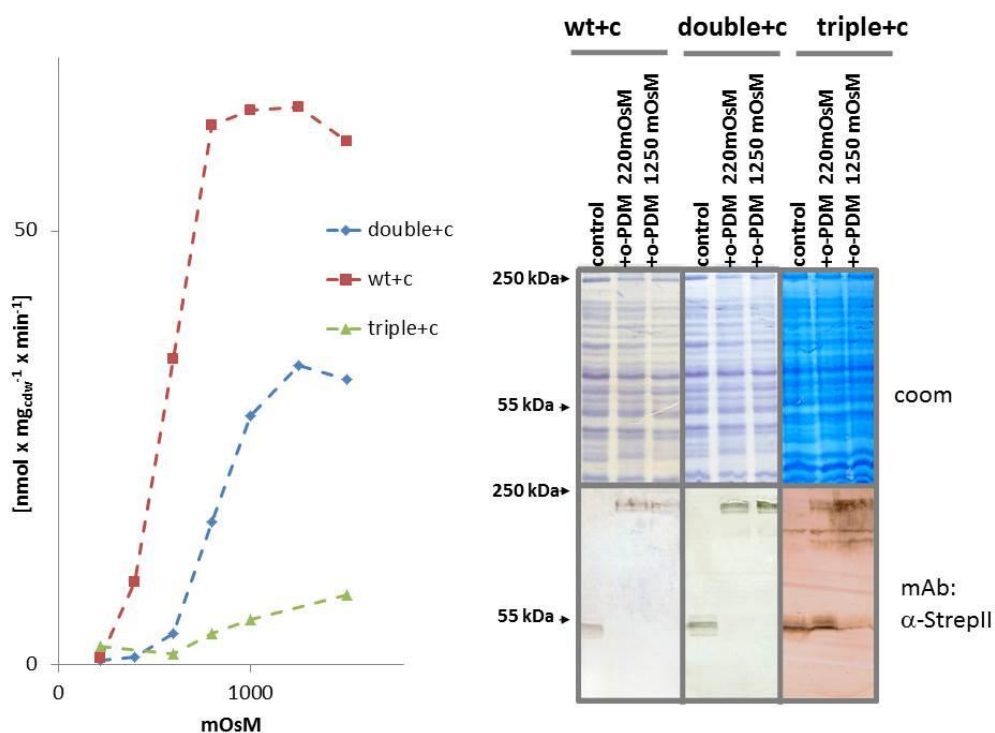


Fig. 3-30: Activity of Strep_BetP (wt+c), the monomer mutant Strep_BetP_W101A/T351A (double+c) and the the monomer mutant Strep_BetP_W101A/F345A/T351A (triple+c), all carrying additionally the S328C/D97C single cysteine mutations *in vivo* in *C. glutamicum* DHPF cells (left). SDS-PAGE analysis of membrane fractions of the corresponding strains after *in vivo* crosslinking with ortho-phenylbismaleimid at iso- and hyperosmotic external osmolality (right).

As it was suggested from the 3D-structure that the C-terminal domain of the protein is involved in protomer contacts the contribution of this domain to the oligomerisation was addressed *in vivo* in *C. glutamicum*. The combination of the W101A/T351A double mutation together with the truncation of the C-terminus by 45 amino acids led indeed to complete

monomerisation of the protein *in vivo* in *C. glutamicum* as judged by *in vivo* crosslinks of the respective S328C/D97C mutant. Hereby the severe contribution of the C-terminus to the oligomerisation of BetP was shown in striking contrast to the state of the art model of trimer formation. Of course this variant was not regulated, too. The missing regulation was indeed also observed for the respective trimeric DC45 mutant (Fig. 3-31).

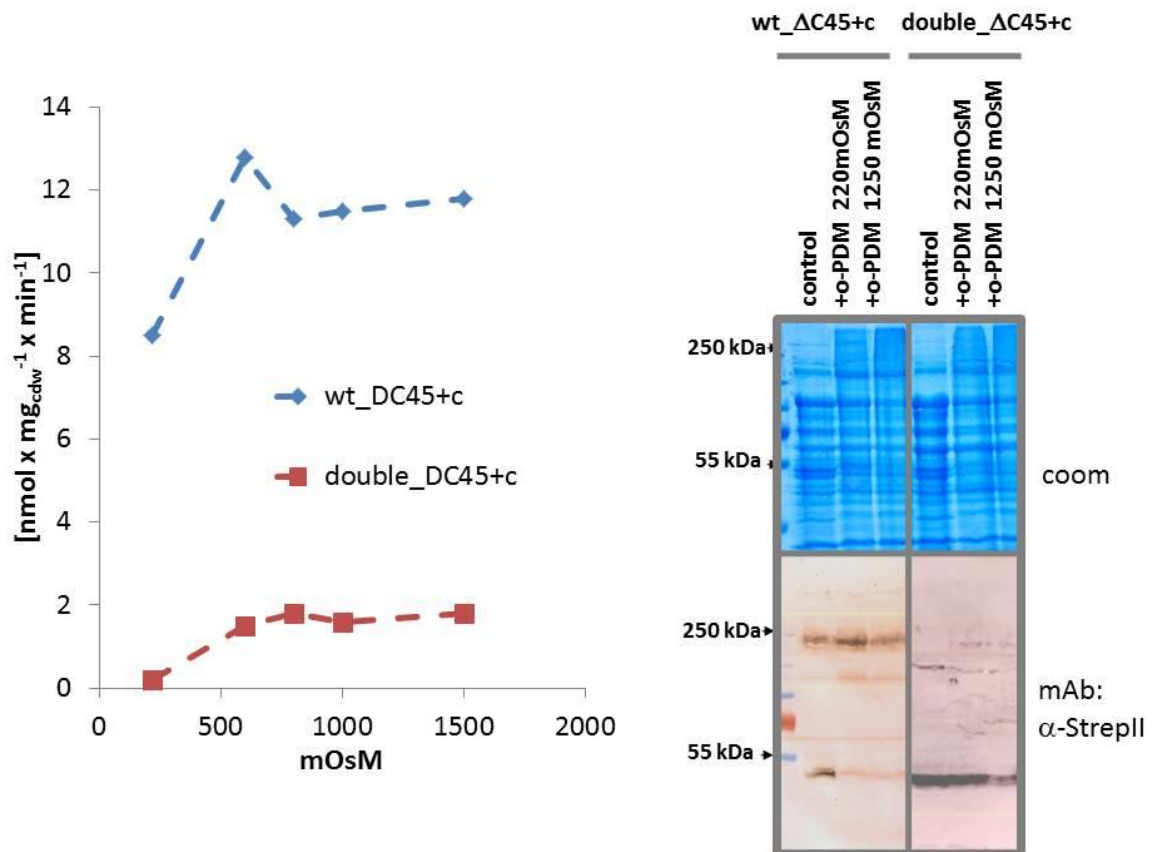


Fig. 3-31: Activity of Strep_BetP_DC45 (wt+c), the monomer mutant Strep_BetP_W101A/T351A_DC45 carrying additionally the S328C/D97C single cysteine mutations *in vivo* in *C. glutamicum* DHPF cells (left). SDS-PAGE analysis of membrane fractions of the corresponding strains after *in vivo* crosslinking with ortho-phenylbismaleimid at iso- (220 mOsM) and hyperosmotic (1250 mOsM) external osmolality (right).

Therefore no conclusion about cross-talk could be drawn from the results obtained with the monomeric BetP variant. The only conclusion that seemed to be obvious from these results was that C-terminal interactions were sufficient to led to BetP trimerisation in the *C. glutamicum* membrane.

3.8 BetP dynamics via single molecule fluorescence

As all structural information available for BetP was obtained from static crystal structures we aimed to decipher the conformational dynamics via single molecule fluorescence studies on appropriately labeled BetP proteins. In first studies the C-terminal flexibility was addressed in either Bodipy labeled Strep_BetP_E577C and the respective non-regulated Strep_BetP_A564P/E577C variant in detergent micelles, or in microsomes of *C. glutamicum* that had Strep_BetP expressed with a C-terminal attached eGFP molecule.

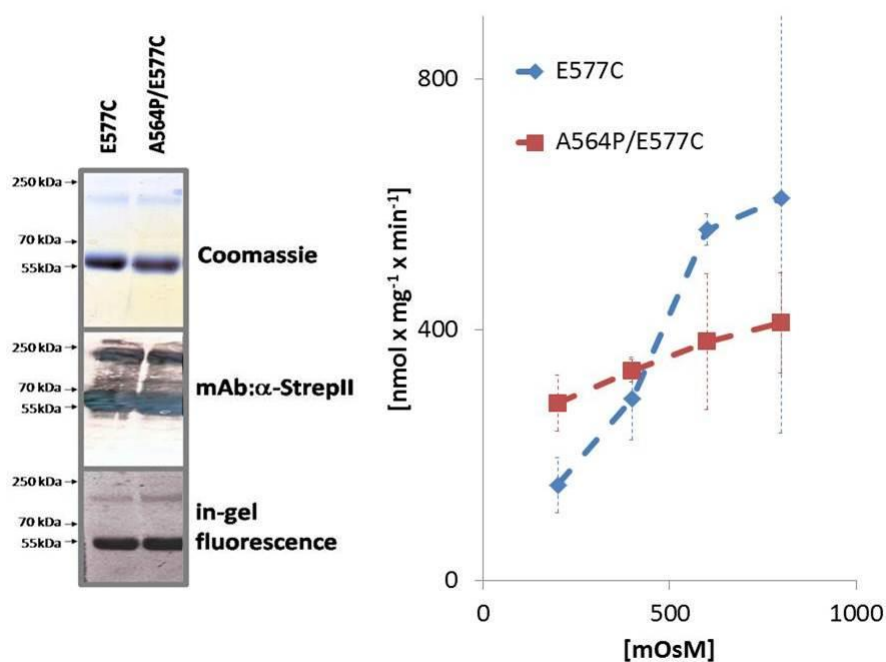


Fig. 3-32: SDS-PAGE/western-blot and in-gel-fluorescence analysis of Strep_BetP_E577C and Strep_BetP_A564P/E577C purified via Strep-Tactin and labeled with Bodipy_FI_IA dye (left). Activity of the respective labeled protein upon reconstitution in liposomes (right).

In those studies the homo-FRET/fluorescence anisotropy was tested as readout for the flexibility of the C-terminal domain. The modifications of the C-domain via attachment of a Bodipy label to the C577 residue or even a complete eGFP protein to the C-terminus did neither impair function nor regulation of the resultant protein. None of those constructs led to reproducible results. All single molecule fluorescence measurements were carried out by

Jakub Kubiak in the group of Claus Seidel (Heinrich Heine Universität, Düsseldorf). Therefore fluorescence studies with homo-trimeric BetP variants were not continued.

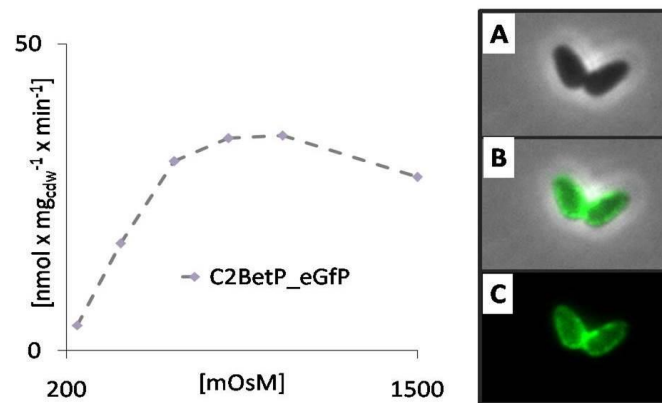


Fig. 3-33: *In vivo* activity of Strep_BetP with C-terminal attached eGFP in *C. glutamicum* DHPF cells in dependence of the external osmolality (left). Fluorescence microscopic analysis of these cells (A: phase contrast; B: eGFP fluorescence; C: overlay) (right).

As the purification of functional and regulatory active heteromeric BetP was established to an extent where the trimeric context of one special subunit was clearly defined, the first prerequisite for the analysis of BetP dynamics via FRET studies was achieved. To address BetP dynamics in a single monomer via single molecule FRET experiments, a series of different residues was mutated to cysteine in order to find appropriate label positions. The positions were selected on the basis of fret distance calculations that were carried out by Hugo Sanabaria (AK Seidel). Residues that exhibited an appropriate distance change in *in silico* fret distance predictions were further tested *in silico* for the interference of a cysteine side chain with the proteins conformational flexibility in these positions by Christine Ziegler (Universität Regensburg). To address the movements of the four helix bundle in comparison to the scaffold of the protein the periplasmic residues G510, G511, E512, and N513 all located in the periplasmic loop preceding TM12 in the scaffold domain were mutated to cysteine. As FRET partner positions, the residues E175, H176 and N177 preceding TM4 in the four helix bundle domain and positions Q447 and M451 preceding TM10 in the scaffold domain were chosen. Fortunately all mutants tested resembled activity and regulation of the respective non-cysteine variant. Although weak accessibility of

the E175C mutant for the sulfhydryl reactive Bodipy_FI_IA dye was confirmed in in-gel-fluorescence experiments (Fig. 3-34) this mutant was chosen for fret experiments in heterotrimeric BetP.

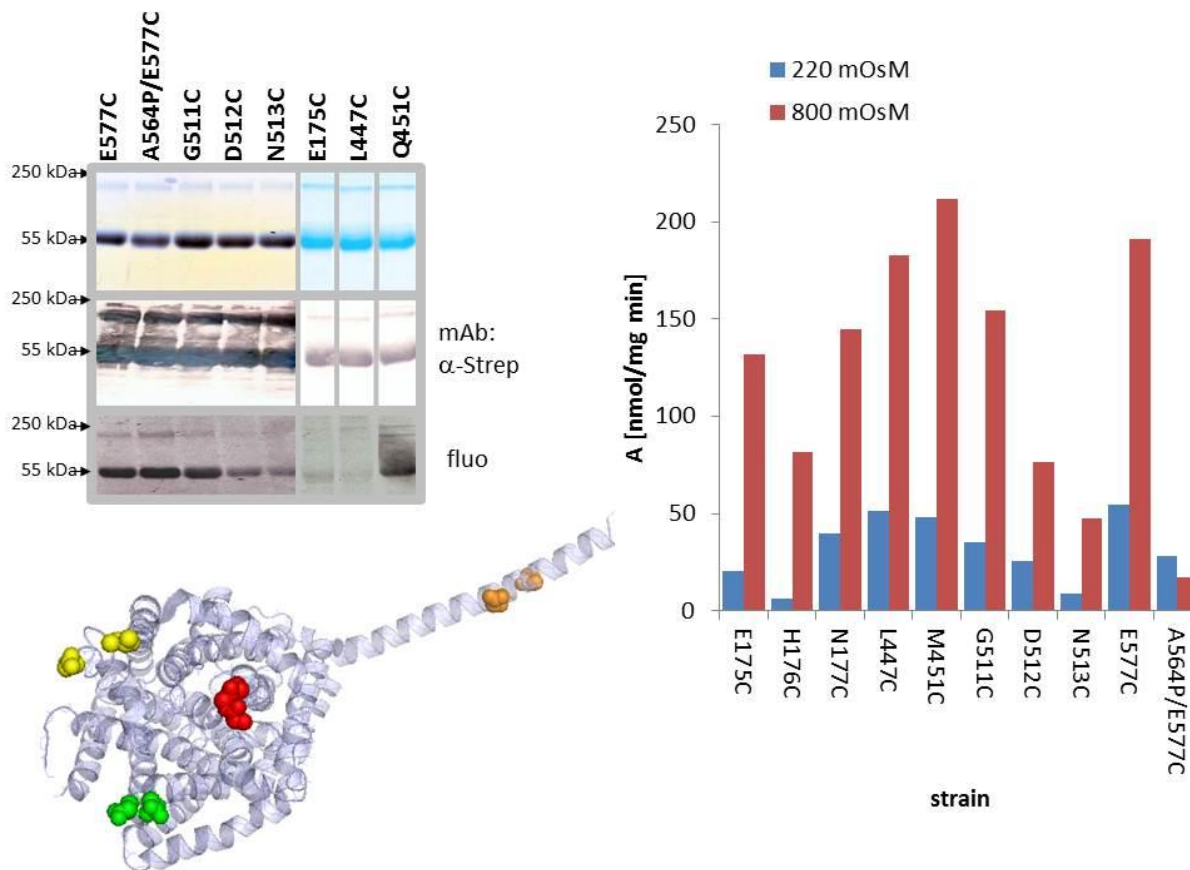


Fig. 3-34: SDS-PAGE/western-blot and in-gel-fluorescence analysis of the indicated homo-trimeric BetP mutants purified via Strep-Tactin and labeled with Bodipy_FI_IA dye (upper left). Schematic representation of the single cysteine mutations introduced for fluorescence labeling. Positions G510/G511/D512/N513 shown in red; E175/H176/N177 shown in green; L447/M451 shown in yellow and E572/E577 shown in brown in the structural BetP model (PDBentry: 2WIT)(lower left). *In vivo* betaine uptake activity of the respective mutants in *E. coli* MKH13 cells at external osmolalities of 220 and 800 mOsM (right)

Herefore this mutation was combined with the G510C mutation on a single protomer, which was then co-expressed with inactive cystless Strep_BetP_DC12_His and Strep_BetP_DC12_Flag. Recent results obtained in the collaborating group of Claus Seidel suggest that the different conformational states in this hetero-trimeric BetP with FRET-pair label at G510C/E175C in a single protomer are measurable upon activation in response to the activation of the protein (personal communication Claus Seidel).

3.9 Analysis of the osmo-transportome of *C. glutamicum*

The redundancy of osmotransporters in *C. glutamicum* is interesting as many questions arose from the fact that there are 4 different osmoregulated uptake systems. BetP is the only member of this group for which the osmosensing function has finally been proven *in vitro* in the proteoliposomal system. It is highly dangerous to draw physiologic conclusions about osmolyte import only from the behaviour of BetP as important aspects might be overlooked just because a lack of knowledge about the other osmolyte import systems. For a proper analysis of other osmoregulated transport systems it is necessary to investigate their function *in vitro* the proteoliposomal system ensures the analysis of transporter regulation avoiding the action of any unknown cellular factor taking part in the regulation. Most attempts to characterise different osmoregulated transporters of *C. glutamicum* were formerly been concentrated on the ectoine transport system EctP. This was mainly caused by the fact that this system had shown to be the transporter with the highest transport capability for osmolytes except for BetP in *C. glutamicum* (Peter et al. 1998). Consistent with earlier studies, the expression of EctP led to cell death in *E.coli*. Furthermore none of the osmotransporters of *C. glutamicum* could be expressed in *Saccharomyces cerevisiae* (data not shown). The osmoregulated transport permeases of *C. glutamicum*, ProP and LcoP, were expressed in *E.coli* and inserted to the membrane. LcoP exhibited betaine uptake activity upon expression in *E. coli* with the same apparent affinity of roughly 150 μ M, and regulation as published for this protein in *C. glutamicum* (Fig. 3-35) (Steger et al., 2004).

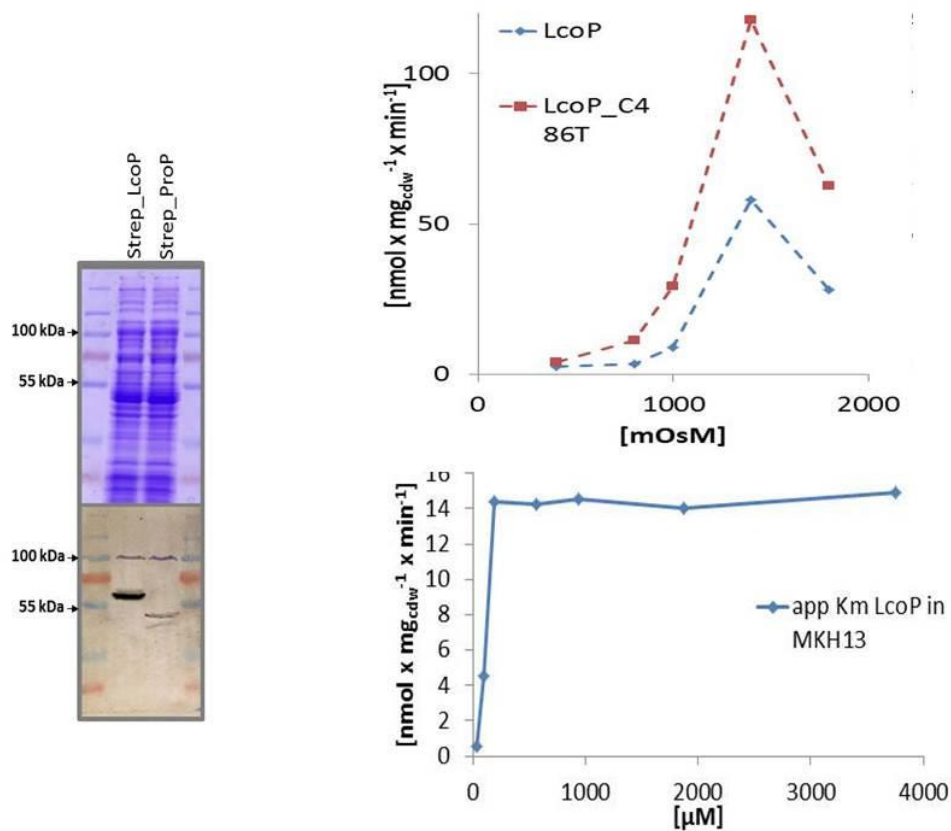


Fig. 3-35: SDS-PAGE/western blot analysis of membrane fractions of *E. coli* MKH13 cells that had expressed Strep_ProP and Strep_LcoP respectively (left). *In vivo* betaine uptake activity of Strep_LcoP and the cysless Strep_LcoP_C483T variant in dependence of the external osmolality in *E. coli* MKH13 cells (upper right). Betaine uptake activity in *E. coli* MKH13 cells that had expressed Strep_LcoP at an external osmolality of 1250 mOsM in dependence of the external betaine concentration (lower right).

The cysless variant of this protein exhibited furthermore the same characteristics which would enable any kind of studies reliant on common thiol chemistry methods. ProP exhibited stability problems upon solubilisation (data not shown), whereas LcoP appeared to be stable in a variety of detergents including LDAO, TritonX100 and DDM. LDAO was chosen for the Strep-Tactin purification of Strep_LcoP.

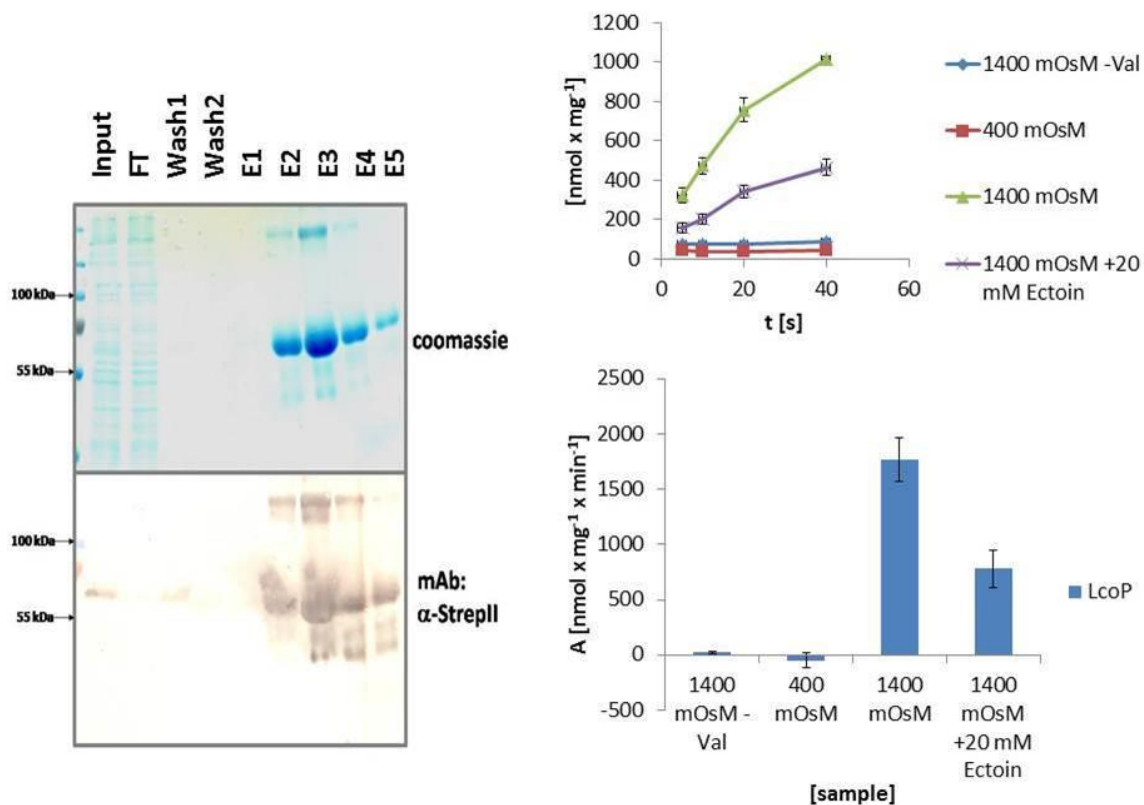


Fig. 3-36: SDS-PAGE western blot analysis of the Strep_Tactin purification of Strep_LcoP from LDAO solubilised membrane fractions of the respective *E. coli* DH5 α cells (left). Uptake kinetics of the reconstituted protein in proteoliposomes in dependence of the external osmolality and competing ectoine (upper right). Uptake rates calculated from these kinetics (lower right).

The protein retained its osmoregulated betaine uptake activity which could be competed by ectoine consistent with the published characteristics of LcoP in *C. glutamicum* (Steger et al., 2004). The LcoP protein is as BetP a member of the BCC-transporter family. As BetP it is built by (predicted) 12 transmembrane helices and hydrophylic N- and C-terminal domains. The C-terminal domain of LcoP is about 100 aa in length and mainly negatively charged in contrast to the 45 amino acid C-terminal domain of BetP that is mainly positively charged. As the osmoregulation was then ultimately shown to be an intrinsic protein function in the proteoliposomal system the function of the terminal domains in this transporter in the osmoregulation was addressed *in vivo*. Truncation of the last 70 C-terminal amino acids as well as truncation of the first 40 N-terminal amino acids resulted in a complete loss of osmoregulation of LcoP activity *in vivo* in *E. coli*. The osmoregulation of the protein was also

strongly impaired although not completely abolished in truncation mutants where the N-domain was truncated by only 20 amino acids or the C-domain by only 40 amino acids (Fig. 3-37).

BetP:

VKDLSDVVIY LEYREQQRFN ARLA**RERRVH**NEHRKRELA**A**KRRRERKASGAGKRR

LcoP:

KDLSTDPAAIR**QR**YAKAAISNAVVRGL**EEHGDDF**ELSI**EP**A**EEGR**GAGATFDSTADHITD**WYQRT**DEEGNDVDYDFTTGKWADGWTP**EST**EEGEVDA**KKD**

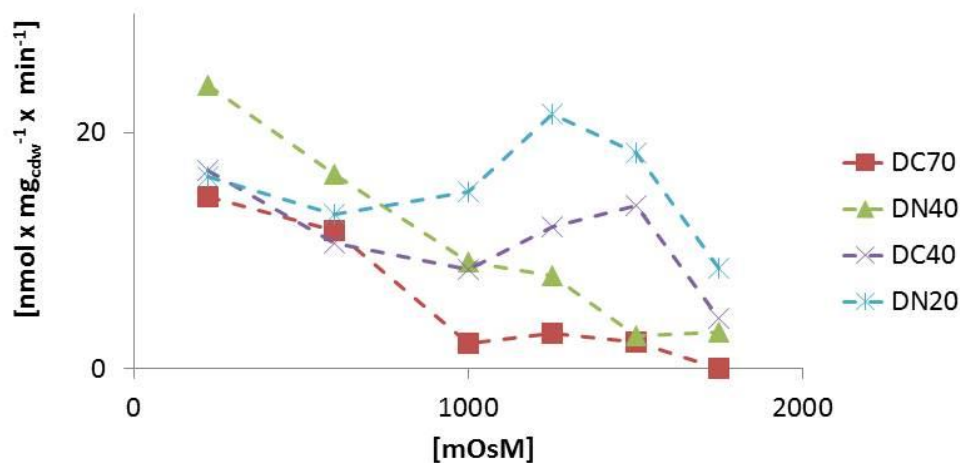


Fig. 3-37: Primary structure of the C-terminal hydrophilic domains of BetP and LcoP. Amino acids with negatively charged side chains coloured in blue positively charged side chains shown in red. Grey bars indicate α -helical regions observed in the crystal structure for BetP and predicted by Ramachandran plots for LcoP (upper panel). *In vivo* uptake activity of C- and N-terminal truncation variants of LcoP in *E. coli* MKH13 cells in dependence of the external osmolality.

The stability of the protein suggested LcoP to be a promising target for structural analysis via crystallisation. The protein proved to be in a completely monodisperse oligomeric state after purification to homogeneity in LDAO and DDM (Fig. 3-38, Fig. 3-36). The molecular weight of the protein appeared to be similar to that of BetP as judged by size exclusion chromatography (Fig. 3-38). Consistent with the assumed smaller micellar size of the mixed protein/Lipid/detergent micelles the apparent molecular weight of the DDM purified protein appeared to be slightly higher than that of the LDAO purified protein.

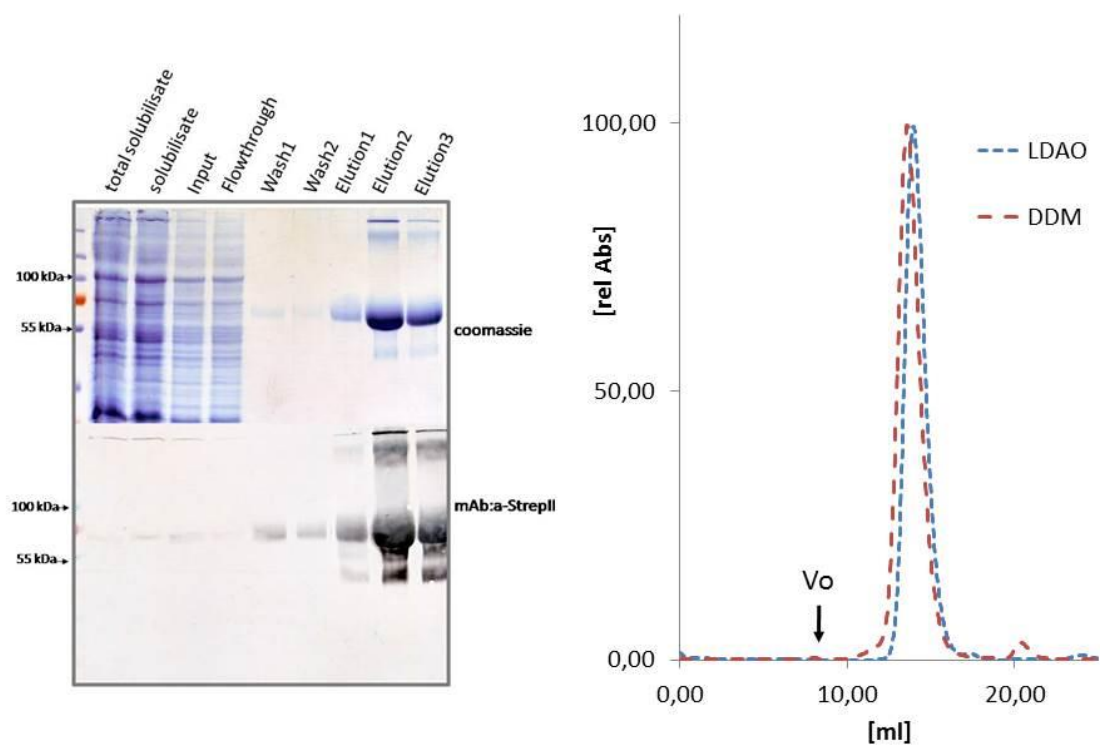


Fig. 3-38: SDS-PAGE western blot analysis of the Strep_Tactin purification of Strep_LcoP from DDM solubilised membrane fractions of the respective *E. coli* DH5 α cells (left). SEC- chromatograms of Strep_LcoP on a 24 ml Superose6 column (right).

LDAO purified LcoP yielded crystals in first screens that diffracted to a resolution of roughly 1,5 nm (personal communication Rebecca Gaertner). The crystallisation was carried out by Rebecca Gaertner (Johann-Wolfgang-Goethe Universität, Frankfurt).

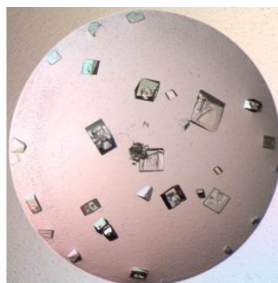


Fig. 3-39: Crystals of Strep_Lcop purified in LDAO. Protein crystallised by Rebecca Gaertner (Johann-Wolfgang-Goethe Universität, Frankfurt).

4 Discussion

4.1 LcoP is an osmo-sensor

With the proof of osmo-regulation of LcoP *in vitro* we were able to add a new member to the list of secondary active transport proteins that are shown to be regulated by osmolality *in vitro* without the need of any cellular factor. It will be of major importance to extend the number of proteins for which this function is proven, as *in vitro* studies of osmo-regulation in osmolyte transport proteins are limited to BetP (from *C. glutamicum*); OpuA (from *L. lactis*) and ProP (from *E. coli*) so far. Those three proteins exhibit remarkable differences in their osmo-sensing properties. ProP seems to be activated by changes in the hydration state of the protein as it can be activated *in vitro* by a variety of different stimuli including ions, non-charged osmolytes and molecular crowding induced by high concentrations of polyethyleneglycol (Racher et al., 2001). Although implications have been found for an important function of the C-terminal soluble dimerisation domain in the regulation of this transporter (Hillar et al., 2005), no domain could be detected to date in which mutations lead to a complete loss of regulation without loss of function. Furthermore it was shown that the regulation of ProP is modulated *in vivo* by the soluble protein ProQ (Kunte et al. 1999; Smith et al. 2004). Therefore only for BetP and the ABC transporter OpuA the protein domains necessary for regulation could be clearly elucidated (Peter et al. 1998; Schiller & Morbach 2004; Biemans-Oldehinkel et al. 2006). As OpuA is an ABC transporter no reference protein for the BCC-transporter BetP could be subjected to *in vitro* analysis so far. In the present work we were able to prove the osmoregulatory function for LcoP *in vitro* (Fig. 3-36). LcoP, being a BCC-transport protein like BetP, comprises significant sequence homology to BetP as well as remarkable differences. The regulation of this protein is obviously not or only to a minor extent affected by the surrounding lipids reflected in comparable activation of LcoP in *C. glutamicum* (Steger et al., 2004) and *E. coli* (Fig. 3-36, Fig. 3-35), albeit the completely different membrane composition of *C. glutamicum* (Özcan et al., 2007). Furthermore the function of the terminal, hydrophilic domains becomes obvious by the missing regulation of C- and N-terminal truncation variants *in vivo* (Fig. 3-37). The crucial role of the terminal domains in the regulation of this protein is similar to the situation in BetP (Peter et al. 1998; Schiller & Morbach 2004; Ressler et al. 2009). The

C-terminal hydrophylic domain of LcoP is about 2 times as large as the one of BetP and comprises mainly negatively charged residues (Fig. 3-37). It is therefore obvious that the regulatory action must comprise some differences. Herefore it will be interesting to check whether the same specific stimulus, namely potassium, is responsible for the regulation of LcoP or not. The phenomenologic description of a stimulus is of course not sufficient for understanding the relevant molecular mechanism.

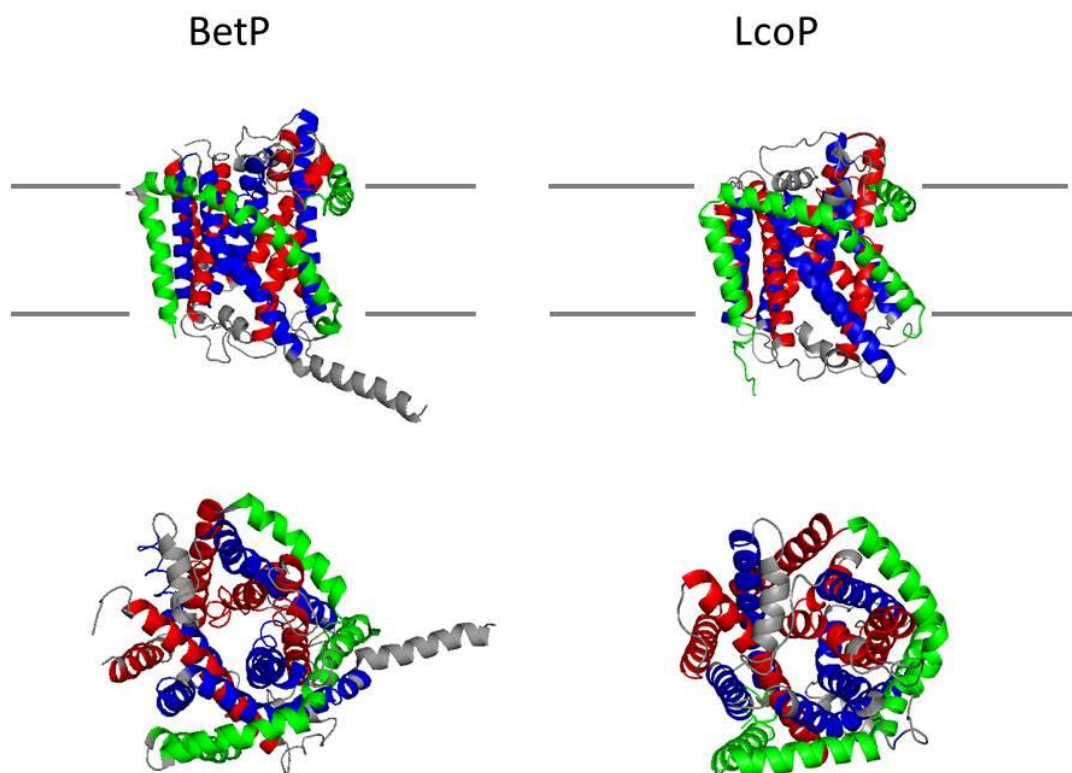


Fig. 4-1: Structure comparison of the experimentally established BetP structure (Ressl et al., 2009) and a structural model of the membraneous part of the LcoP protein (without the soluble, terminal extensions) derived by modelling LcoP on the established CaiT structure (Schulze 2010) with the structure prediction program 3D-PSSM (Kelley et al., 2000). The structure of only one protomer is shown in side view (upper panel) and top view (lower panel) with grey bars indicating the membrane plane. TM1,2 and the periplanar helix7 are shown in green whereas the helices of the first repeat (TM3-7) are shown in red and those of the second repeat (TM8-12) are shown in blue.

Therefore the three-dimensional structure of this protein is currently addressed. LcoP appears to be a promising candidate for crystallisation studies for two reasons. First of all it could be shown to be stable in a variety of detergents including harsh detergents like LDAO (Fig. 3-38) which is a hint for extraordinary protein stability that enhances the possibility of

successful crystallisation (Sonoda et al., 2011). LcoP exhibits furthermore significant sequence homology to the BCC-transporters BetP and CaiT (Fig. 4-1) for which 3D structures are established (Ressl et al. 2009; Schulze et al. 2010). This homology would allow simple molecular replacement for phasing of a given diffraction pattern. The structure of the BetP protein could only be elucidated in a mutant variant that is not regulated by osmolality in the expression host at all (Ressl et al., 2009). Therefore the conclusions drawn from structural informations for the regulation of BetP remain highly speculative. If the structure determination of a regulated LcoP variant will be possible it will provide insight into the regulating mechanism. The relatively narrow opening of the substrate exit at the cytoplasmic face of the translocation pathway has been speculated to be a consequence of regulative inter-protomer cross-talk (Gärtner et al., 2011) as well as being responsible for the high substrate selectivity of BetP (Perez et al., 2012).

Betaine is the exclusive substrate for BetP. In contrast to BetP, LcoP exhibits a rather low substrate selectivity. Ectoine is transported by LcoP with a K_M value of twice of that observed for the main substrate betaine (Steger et al., 2004) (Fig. 3-36). It will be interesting to test the proposed correlation of width of the transport conduit and substrate selectivity via elucidation of the LcoP structure.

Like the BetP protein LcoP appeared to be in a trimeric state in detergent solution (Fig. 3-38). Therefore it will be interesting to test if the conclusions about cross-talk for the betaine permease BetP drawn from the current work will also hold true for the LcoP protein.

4.2 Monomeric BetP ?

During the current work the role of trimerisation of BetP was investigated by the collaborating group of Christine Ziegler (Perez et al. 2011). The absent trimerisation due to minimal modifications in the periplasmic interfaces of the protein allowed a proof of functionality of a single subunit in agreement with the absence of negative dominance proven in the current work (Fig. 3-25, Fig. 3-26, Fig. 3-27). However it could be shown that the trimerisation of the protein is much more complex and does obviously not only include amino acid side chain interactions but most likely also lipid mediated interactions (Fig.

3-31). Careful interpretation of the published characteristics of the monomer BetP variants showed in agreement with the measurements carried out in the current work, that the published monomer mutant variant still exhibits osmo-regulation (Perez et al. 2011) (Fig. 3-28). This interpretation is in striking contrast to the original one. A BetP mutant variant which is monomeric and still regulated by the osmolality would be a final proof that the trimeric assembly is not crucial for both activity and regulation of BetP.

Unfortunately we could show that all variants that exhibited at least partial osmo-regulation also formed trimers at least to some extent *in vivo*. Crosslinkability in the used S328C/D97C double cysteine variants with the short homo-bifunctional cross-linker o-PDM is a very convincing measure for trimerisation as the length of this cross-linker is roughly 0,6 nm and thus only allows for cross-linking in an wildtype like, trimeric arrangement (Ressl et al., 2009) (Fig. 4-2).

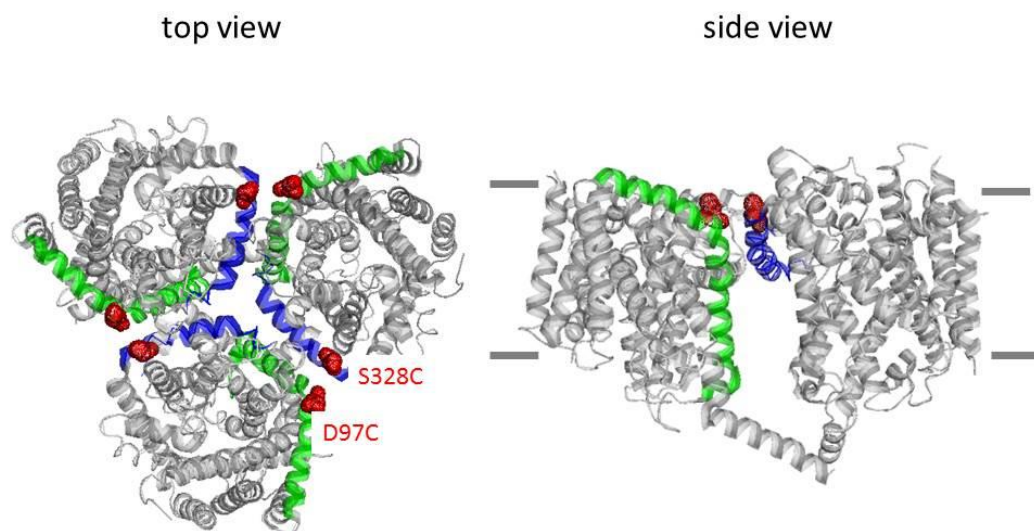


Fig. 4-2: Top view (left) and side view (right) of the structural arrangement of the sites used for trimerisation analysis via crosslink. TM2 represented in green , h7 represented in blue. S328C/D97C sites highlighted in red. Membrane indicated by gray bars and chainA omitted for clarity in the side view representation. (Modified according to PDBentry:2WIT (Ressl et al., 2009))

The only protein variants that were not crosslinkable were the W101A/F345A/T351A triple mutant variant in *E. coli* and the W101A/T351A_DC45 mutant variant in *C. glutamicum* (Fig. 3-31, Fig. 3-28). The necessity of C-terminal truncation for monomerisation of the protein in the *C. glutamicum* host membrane strikingly demonstrates the important role of the C-domain in trimerisation. C-terminal contacts are indeed sufficient to assemble the trimer correctly in the lipid surrounding of *C. glutamicum*. The different trimerisation

characteristics of the W101A/T351A variant in dependence of the membrane lipid composition (Fig. 3-29, Fig. 3-31) is in agreement with the observed dependence of the regulatory characteristics of the membrane lipid head groups (Schiller et al., 2006). Obviously the assembly mechanism of the BetP trimer is more complex as proposed in the previous study (Perez et al., 2011b). Any conformational signal to be transmitted via the C-domain to the adjacent protomer could thereby rely on the lipid environment.

The question remains what conclusion about cross-talk can be drawn from the properties of BetP which is impaired in trimerisation. The re-analysis of the mutant variants impaired in trimerisation has not provided further insight into cross-talk on the level of activity and regulation.

In any case one major obstacle can't be overcome by any BetP mutant impaired in trimerisation. The absence of interacting protomers will principally never allow for the examination of conformational inter-protomer communication. Furthermore it had been shown that the BetP protomers in the trimeric arrangement have to be tilted to about 15 degree relative to the membrane plane in comparison to the flat protomer arrangement observed in the crystal structure (Ressl et al. 2009; Nicklisch et al. 2012; Tsai et al. 2011). This finding clearly puts characteristics of monomerised mutant variants in question. The physical link between the protomers might be necessary for the correct function. The necessity of the trimeric contacts for wildtype like regulatory properties of BetP does not necessarily include inter protomer signal transduction that could be interpreted as cross-talk. Only hetero-trimeric BetP allows for the investigation of the inter-protomer transduction of conformational information and its functional relevance.

4.3 Genetic fusion of BetP trimers

Because of the extreme attractiveness of a fusion BetP construct it was extensively tried to establish such a system. The expression of fused BetP trimers would have led to a system which would have allowed for the analysis of cross-talk *in vivo*. The only example of a trimeric transport protein for which this approach was successfully applied is the AcrB multi-drug efflux pump (Takatsuka and Nikaido, 2009).

The stability problems observed in *E. coli* for trimers composed of full-length BetP protomers suggests the accessibility of the last 12 C-terminal amino acids for proteases (Fig.

3-5, Fig. 3-6). The observed stability of the same construct in *C. glutamicum* might either be due to a lack of the responsible protease in that organism, or to interactions of the very end of the C-domain with the negatively charged *C. glutamicum* membrane. Such an interaction could prevent the C-domain from degradation as it would render this part of the protomer sequence inaccessible for proteases. This interpretation is supported by the fact that 6 positively charged residues and only one negatively charged residue are located in that region. However this can't be the only explanation as the full-length C-domain of wildtype BetP is stable in *E. coli*. Although there is no direct evidence for this stability it can convincingly be concluded as the regulation patterns of Strep_BetP_DC12 and Strep_BetP expressed in *E. coli* significantly differ from each other (Schiller & Morbach 2004)(Fig. 3-21). The fusion proteins could be expressed in a stable and active state in both organisms but it was not possible to address cross-talk in any of those constructs for a simple reason. Obviously the proteins formed higher oligomeric structures that we interpret as being mostly trimers of trimeric fusion protein (Fig. 3-9). Besides the enlarged apparent molecular weight of the fusion BetP proteins compared to the wildtype, most of the observed activity in the fusion BetP was originated from the first protomer (Fig. 3-8, Fig. 3-3). The formation of trimers composed of first subunits of fusion BetP would explain both the position effects and the aggregation.

Another possible explanation for the major contribution of the first subunit to the observed activity that has to be kept in mind is that the first subunit is the only one in the fused trimer that comprises a free N-domain which is not sterically restricted by covalent attachment to the C-terminus of the neighbouring subunit. The formation of nonameric fusion BetP aggregates would be a logic consequence if the steric restriction of the N-domains of the second and third subunits prevents the oligomerisation. So far the mechanism of membrane integration and oligomer formation of BetP is completely unknown. BetP comprises no N-terminal signal sequence for membrane integration via chaperones like the SEC/YIDC system (Dalbey et al., 2011). Therefore even the order of the two events namely oligomer formation and membrane integration is completely unknown. Two principal events might lead to the formation of trimers composed of first subunits only (Fig. 4-3):

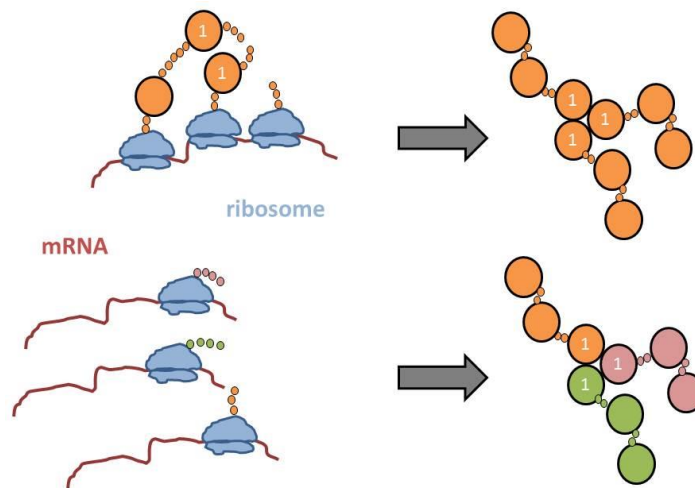


Fig. 4-3: Schematic representation of two different possibilities for fusion-BetP to assemble to nonameric aggregates via trimerisation of first subunits originated from the same (upper panel) or different mRNA molecules (lower panel). Ribosomes are represented in blue, mRNA in red and nascent BetP proteins as well as the nonameric aggregates brown, green and pink colour. The first subunit of each trimeric polypeptide chain is numbered.

- (i) The first subunits that assemble might originate from different ribosomes translating fusion BetP from the same mRNA .
- (ii) The first subunits that assemble might originated from ribosomes translating the fusion proteins from different mRNA`s.

Both scenarios would necessitate completely different strategies to overcome the aggregation problems. Mutations in the ribosome binding site could prevent aggregation in (i), whereas a lower concentration of mRNA could prevent aggregation in (ii).

If the oligomer formation is realised during the early state of translation it would be easy to rationalise that the simultaneous translation of several fusion BetP proteins from a single mRNA leads to the formation of trimers composed of first subunits mainly (scenario (i)). It was possible to obtain hetero-trimeric BetP protein originating from different mRNAs in the hetero-trimer approach where different BetP variants had been co-expressed (3.5). For this reason scenario (i) seems to be unlikely. Therefore we assume that trimers are most likely formed by first subunits of fusion BetP from different mRNA molecules (scenario (ii)), albeit we can not exclude aggregation described in (i) to a minor extent (Fig. 4-3). The remarkable stability and strength of the trimeric quaternary structure of BetP is reflected by the fact

that obviously the attachment of the second and third subunit did not impair the activity and regulation of the trimer composed of first subunits of the fusion-trimer.

If the formation of higher aggregates would have rendered the fusion proteins inactive it would have been possible to select random linker sequences cloned by the insertion of random linker libraries. Only linkers leading to the formation of correct fusion trimer would then have conferred betaine mediated osmo-tolerance to *E. coli* MKH13. Thereby it would have been possible to select for appropriate linker sequences. There might still be possibilities to obtain active and trimeric fusion BetP.

Because of the osmo-regulated betaine transport activity of higher aggregates *in vivo*, that precluded the linker optimisation by any unbiased approach, the fusion-BetP approach was not further followed.

It might have been possible to reduce the formation of higher oligomers by reducing the translation efficiency by mutations in the ribosome binding site of the heterologously transcribed mRNA to circumvent aggregation of fusion BetP molecules originated from a single mRNA (scenario i (Fig. 4-3)). Furthermore the transcription efficiency could have been varied by a change to a tunable plasmid/host system to circumvent aggregation of fusion BetP originated from different mRNA molecules (scenario ii (Fig. 4-3)). Altered translation rates would have again necessitated the test of a vast number of different linkers without any bias of the linker length. The necessity of many genetic manipulations of *E. coli* MKH13 to express fusion BetP in a tunable fashion in those cells led to the decision not to test this option.

Furthermore it becomes obvious, especially after the BN-PAGE experiments carried out with the BetP variants impaired in trimerisation (Fig. 3-28), that the apparent molecular mass of BetP in detergent is not an accurate measure for the oligomerisation in the membrane. This principal experimental limitation led us to discard the fusion BetP approaches.

To overcome the problem of higher oligomer formation it appeared to be crucial to co-express different BetP protomers not physically connected by amino acid linkers.

4.4 The N-terminal domain is sensitive to alterations

It has been shown in several studies that the N-terminal soluble domain of BetP is involved in the osmoregulation of this protein (Peter et al. 1998; Ott et al. 2008). As the attachment of affinity tags to the C-terminus of BetP has been reported to result in severe growth defects of the expressing *E. coli* cells we addressed the N-terminus first for the applicability of different affinity tags (Rübenhagen et al., 2001). The newly established TEV cleavable linker appeared to be applicable for the usage of the N-terminal Strep tag (Fig. 3-11) but however not for any other tag tested (Fig. 3-16). The reason remains completely unclear. It is widely accepted that any tag might alter physical properties of the tagged protein (Bucher et al., 2002). Indeed several tag structures were published to enhance solubility of heterologously expressed proteins (Davis et al., 1999) or even to promote membrane insertion of covalently linked membrane proteins (Kefala et al., 2007). No correlation for the observed instability of the differently N-terminal tagged BetP variants with the physical properties of the tag itself could be found (Fig. 3-21). The instability was, except for the Strep-tag, observed for all different tags regardless of size, charge and hydrophobicity of the tag structure. This problem has most likely been due to the linker sequence in all cases. Most of the amino-terminal tags lead to the expression of active and regulated BetP *in vivo* albeit the instability of the respective variants *in vitro* (Fig. 3-15). The *in vivo* activity of the individually N-terminally tagged BetP led to a similar problem as already observed for the fusion BetP approach. This activity prevented any unbiased linker optimisation because of the lack of an appropriate selection system.

Even more surprising than the instability of all N-terminally tagged BetP variants other than Strep_BetP was the observation that the absence of the Strep-tag in the hetero-oligomeric BetP variants obviously leads to similar stability problems (Fig. 3-23). It seems as if the Strep-tag in that position is not only applicable in this position but even necessary for the proteins stability in detergent.

4.5 State of art in the hetero-trimeric BetP production: applications in single molecule approaches and limitations

Surprisingly it was possible to decorate the C-terminus of BetP with a variety of different tags (Fig. 3-20). The observed sensitivity to proteolysis of the tag structure as observed for C-terminally His-tagged full-length BetP (Fig. 3-19) leads to two severe drawbacks. First of all such an instability would lead to unacceptable loss of protein especially in trials where three of those tags would be used to sequentially purify hetero-trimers. Second, and even more important, it would never be possible to examine the effect of the C-terminal tag in a homo-trimeric preparation as there would always be the possibility that any observed characteristics in both activity and regulation might be due to C-terminal proteolysis. The observed instability of tags attached to the C-terminus of full-length BetP is consistent with results obtained in the fusion-BetP approach (Fig. 3-3, Fig. 3-5). Consequently the fusion of tags to C-terminal truncated BetP_DC12 proteins leads to the stabilisation of the tag structure (Fig. 3-21). The truncation of the last 12 C-terminal amino acids has an impact on the regulation of the protein as the activation threshold is, in agreement with earlier studies (Peter et al. 1998; Schiller & Morbach 2004), shifted to lower osmolalities both *in vivo* and *in vitro* (Fig. 3-21). Although the resultant proteins don't exhibit exactly the same properties as the full-length protein it is obvious that the osmoregulation in these protomers would, in a hetero-trimeric context, still allow for any kind of cross-talk that is necessary for the observed activity and regulation of the BetP_DC12 variant. We never succeeded in the purification of homogenous-hetero-trimeric preparations because of the yield limitations. The purification of co-expressed Strep_BetP_DC12_His/Strep_BetP_DC12_Flag/Strep_BetP via IMAC and anti-Flag is already sufficient to generate trimeric BetP with which molecular dynamics can be addressed via single-molecule-FRET (sm-FRET) experiments. The available crystal structures of BetP led to the assignment of a possible transport mechanism (Perez et al., 2012). But all structural information obtained by crystallisation harbours the severe drawback that the protein is solubilised in detergent prior to crystallisation which might lead to various artefacts. The regulatory properties of the protein strictly depend on the lipid environment preventing any conclusion about conformational changes in the activation of the protein drawn from the crystal structure. Therefore it is obvious that the observed conformations and proposed conformational dynamics need to be tested in the

membrane environment. Sm-FRET experiments have successfully contributed to the understanding of substrate induced conformational changes in different transporters (Majumdar et al., 2007; Zhao et al., 2010). The two transport proteins, LacY and LeuT, examined for their molecular dynamics in the mentioned studies are monomeric. The sm-FRET approach relies on the labeling of exactly two residues per transport protein. Only hetero-trimeric BetP can fulfill this requirement for the sm-FRET analysis. Therefore the first major obstacle in the sm-FRET analysis of BetP has been overcome. It will be highly interesting not only to test the proposed transport mechanism but to establish the molecular dynamics involved in activation of BetP. With heterotrimeric BetP obtained by the established procedure it was recently possible to measure distances between the fluorescently labeled residues C510/C175 (Fig. 3-34) both in detergent and proteoliposomal membrane (Jakub Kubiak, personal communication).

4.6 The nature of cross-talk in BetP

Oligomerisation of any protein might be caused by different levels of protomer interaction. The most trivial reason for a membrane protein to oligomerise might be the spatial restriction of the protein in this organelle (Grasberger et al., 1986). The BetP oligomerisation is in contrast highly specific and stable, even in detergent solution (Ziegler et al. 2004). During the current work several studies had been published suggesting possible protomer cross-talk in BetP. The crystal structure of this protein suggested only few residues contributing to the trimer formation (Ressl et al., 2009). The contact interface at the periplasmic face of the protein is solely constituted by residues from TM2 and the amphiphatic helix 7. Both helices are not part of the inverted repeat arrangement in which the conformational changes are suggested to occur during transport (Fig. 4-1), (Forrest et al., 2011). Similar contact sites have been observed in the trimeric LeuT-type transporter CaiT from *Escherichia coli*. As for BetP the protomer contacts in CaiT are mainly mediated by the amphiphatic helix 7 running perpendicular around the protomer at the contact interface of the protomers (Schulze et al. 2010). The occurrence of intramembraneous salt bridges in the protomer contact sites of CaiT is believed to cause an even more rigid trimerisation as observed for BetP. The functional relevance of trimerisation in CaiT has so far not been

addressed. For the trimeric LeuT-type transporter Glt_{PH} (GltT) from *Pyrococcus horikoshi* it was shown that the artificial rigidity at the protomer interfaces introduced by cysteine cross-linking did not interfere with the transport function (Groeneveld and Slotboom, 2007). Being a member of the EAAT-transporter family Glt_{PH} comprises a completely different architecture compared to BetP. The inverted repeat motif of Glt_{PH} includes two V-shaped helices that form the protomer contact sites. Furthermore the transport mechanism of this protein differs significantly from the one proposed for BetP (Perez et al., 2012; Reyes et al., 2009)

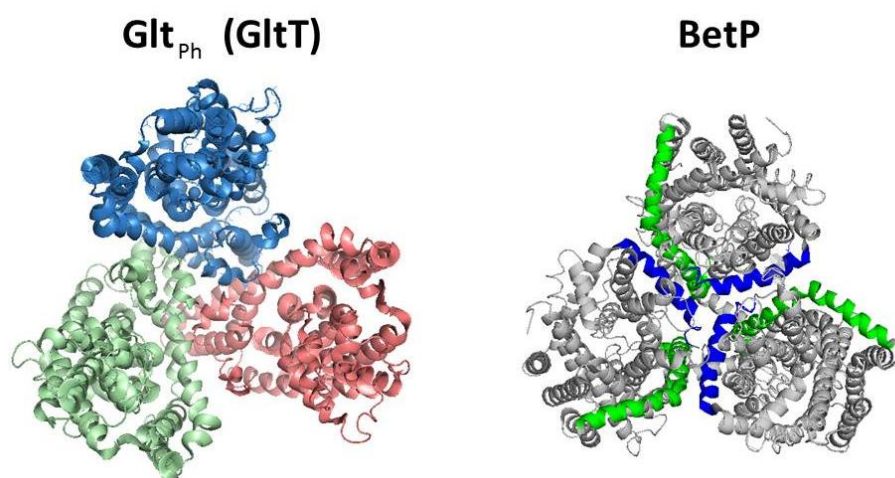


Fig. 4-4: Top view of the structural arrangement of Glt_{PH} and BetP. Single protomers of Glt_{PH} represented in light blue, light green and light red color. Single protomers of BetP represented in gray color with TM2 and h7 highlighted in green and blue color respectively. (Structures modified from PDBentries: 2WIT (BetP) (Ressl et al., 2009) and 2NWX (Glt_{PH}) (Boudker et al., 2007)

The only example of a trimeric transporter in which a signal domain of one protomer trans-activates an adjacent protomer is the ammonium transporter Amt1.1 from *Arabidopsis thaliana*. In this transporter the C-terminal soluble domain is believed to regulate the activity of the adjacent protomer in dependence of the phosphorylation state of a specific threonine in the C-domain. (Lanquar and Frommer, 2010; Lanquar et al., 2009; Loqué et al., 2007). Activation of BetP protomers via the C-domain of an adjacent protomer would comprise an elegant explanation for the trimer formation.

The potassium specific activation pattern of BetP exhibits strong sigmoidicity suggesting a cooperative potassium binding mechanism (Rübenhagen et al. 2001; Peter et al. 1996) (Stanislav Maximov, personal communication). The cooperativity is currently believed to reflect several activating potassium binding sites as observed in structures of rubidium

soaked BetP crystals. The Hill coefficient of about 4-5 of the activation together with the number of presumably activating potassium (rubidium) binding sites found, correlates well with cooperative potassium binding in one single subunit but not with cooperativity of potassium binding between different C-domains (Stanislav Maximov, Camillo Perez, personal communication). Several observations have been published during the current work suggesting different mechanisms of functional inter-protomer cross-talk in BetP. The regulatory behaviour of the monomeric BetP variants led to the assumption of a regulatory relevant inter-protomer cross-talk (Perez et al., 2011).

Especially the interaction of the C-domain with loop2 of the adjacent protomer was suggested to be crucial for the regulation of BetP. The plasticity of this interaction was suggested to be transmitted via TM3 to the periplasmic side of the protein, where it would be involved in the gating of the periplasmic substrate conduit. (Gärtner et al., 2011; Perez et al., 2012). The actual model for the molecular mechanism of BetP activation therefore clearly includes cross-talk between the different protomers. The regulatory relevant binding sites for potassium would thereby be established by residues of the C-domain of one protomer and residues of loop2 of the adjacent protomer (Ressl et al., 2009) (Camilo Perez, personal communication).

In agreement with the conclusion drawn from the monomeric BetP (Perez et al., 2011) we could confirm wildtype like activity of a single BetP protomer being in a trimer with two inactivated monomers (Fig. 3-25).

Surprisingly the regulation of a single BetP protomer was neither affected by the introduction of the deregulating A564P mutation nor by the complete deletion of the C-domain in the two adjacent monomers (Fig. 3-26). This finding convincingly suggests the absence of a functionally relevant action of the C-domain on the adjacent protomer.

We could show that the regulation of a single BetP protomer is not affected even if the adjacent protomers are not only catalytically inactive and do not harbour a C-domain but also lack interaction sites in the loop2 sequence for the C-domain of the active protomer (Fig. 3-27). Thereby any signal transmission via this contact site can clearly be excluded.

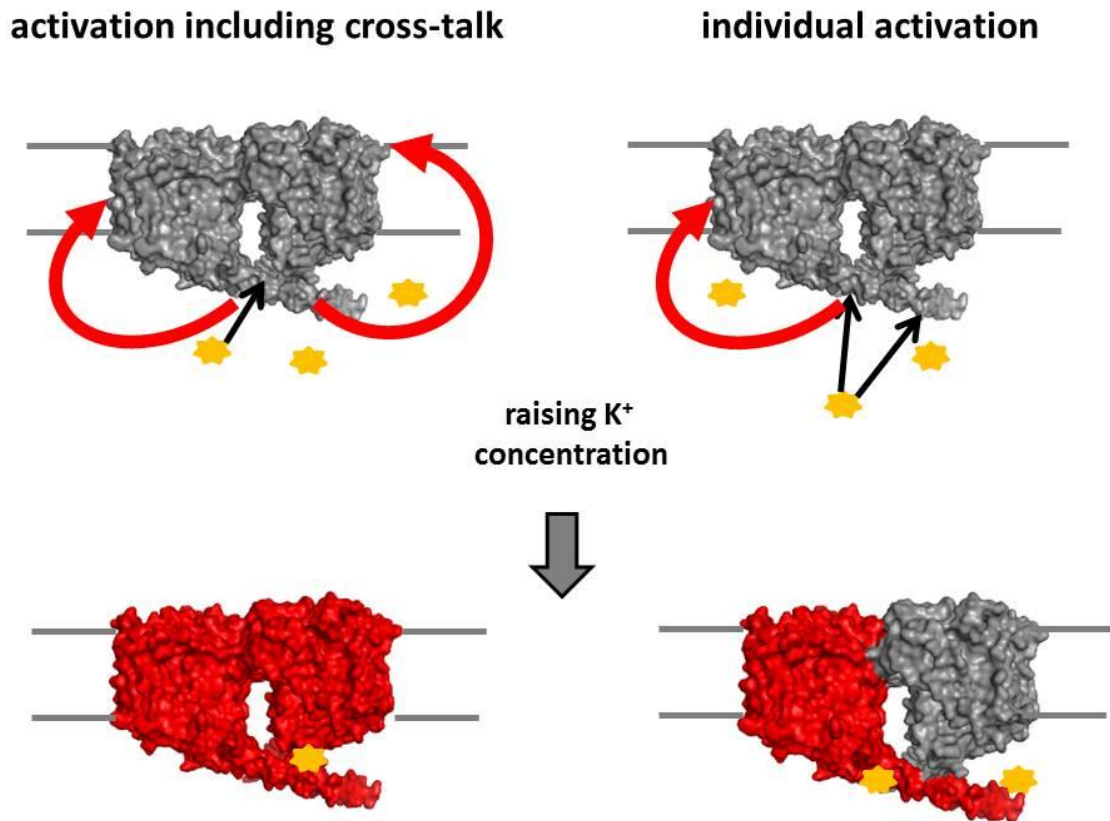


Fig. 4-5: Different models of activation of BetP due to raising potassium concentrations. The suggested cross-talk including model in which potassium (yellow stars) binding between C-domain and loop2 of the adjacent protomer lead to activation (red color) of both monomers is shown on the left panel. The actual model in which binding of potassium to not further specified binding sites in the C-domain leads to the activation of the protomer harbouring this c-domain only is shown on the right panel. BetP structures taken from PDBentry 2WIT, (Ressl et al., 2009) chain B omitted for clarity.

The data presented in the current study suggest the complete absence of any functionally relevant cross-talk between protomers of BetP. This finding is in striking contrast to the current models of protomer interaction of this transporter. The activation of each monomer relies only on the presence of the intact regulatory C-domain of this monomer providing evidence for the original interpretation of this domain being the activator for the own protomer to which it is connected (Fig. 4-5) (Schiller et al 2004).

In future studies the acceptor domain for the C-domain could be investigated with the hetero-trimers. Single cysteines introduced to the C-domain would then be decorated with hetero-bifunctional cross-linkers. The covalent attachment of the second reactive group of these cross-linkers to the domain interacting with the C-domain would lead to a stable,

covalent connection of C-domain and acceptor domain. This chemical bond would allow for the identification of the acceptor domain in peptide mass-fingerprint experiments.

The central question now remains:

What is the reason for the stable trimeric quaternary structure of BetP?

Most likely the trimerisation of the protein provides stability in the host membrane. This interpretation would be in good agreement with the low absolute activity observed for monomeric BetP (Perez et al., 2011). The advantage of the trimeric assembly might simply be that several additional structural elements necessary for the stabilisation of the monomeric transporter are not needed for the trimeric one. The trimerisation might thereby simply reflect evolutionary minimisation of a transport system for osmoregulated-betaine uptake.

The absence of any kind of functional cross-talk is also surprising as the protein was shown to exhibit conformational asymmetry between the protomers in several studies (Perez et al., 2012; Tsai et al., 2011; Ziegler et al., 2004). Beside the trivial explanation of crystallisation artefacts this observation clearly suggested cross-talk. BetP being a symporter might comprise a low activation energy for the global conformational change between the inward-facing and outward-facing state in the absence of substrates. If this is the case then the absence of substrate in two protomers would allow this conformational change to be driven in two substrate free protomers by one active protomer. An extremely low activation energy for this conformational change in the two inactive, cargo free protomers would thereby not alter the transport rate of the active protomer. The absence of negative dominance effects (Fig. 3-25) does therefore not exclude a conformational coupling between the protomers. Even if such a coupling would be present, we can clearly exclude its functional relevance. To address functional irrelevant coupling intra-protomer crosslink studies could be carried out. If the conformational transition from the outward to the inward facing conformation in the inactivated protomers would be prevented by crosslinking of bundle and hash domain it might lead to a loss of transport activity in the active, non-crosslinked protomer.

In summary it can be concluded that the protomers in the trimeric Betaine permease BetP function completely independent from each other.

5 Abstract

The secondary active glycine-betaine transporter BetP of the gram-positive soil bacterium *Corynebacterium glutamicum* has become a paradigm for osmo-regulated transport systems. BetP is the only transport protein regulated by osmolality for which the sensing domain is clearly established and for which structural information at the level of atomic resolution is available. Biochemical studies have shown that the transporter is activated by raising potassium concentrations both *in vivo* and *in vitro* which are sensed by the C-terminal, hydrophilic domain, located in the cytoplasm. The C-terminal sensor domain was shown to be involved in inter-protomer contacts in the homo-trimeric quaternary structure of the transporter. It was furthermore shown that mutations impairing the trimerisation of the transporter severely affect the regulatory function. Furthermore several structural studies reported conformational asymmetry of single protomers to occur in BetP. These findings suggested the occurrence of a regulatory relevant cross-talk between the protomers of the homo-trimeric BetP. The interaction of the C-terminal domain with the cytoplasmic loop2 of the adjacent protomer was speculated to be crucial for the osmosensing function. To test the relevance of conformational cross-talk between BetP protomers, artificial hetero-trimeric BetP was established in the current work. With this system it was possible to clearly exclude any functionally relevant cross-talk in the activation of BetP. The established hetero-trimers were shown to be a useful tool for the analysis of the molecular dynamics of the transporter via spectroscopic methods. Beside BetP only two different transport proteins have been proven to be regulated by the external osmolality. Purification and reconstitution of the osmoregulated betaine transporter LcoP from *C. glutamicum* proved the osmosensing function of this carrier as well. For LcoP the osmosensing domains in this transporter could be identified in the C- and N-terminal hydrophilic domains. Furthermore it could be shown that this protein is a promising candidate for structural analysis. It may therefore be used as test system for conclusions that were drawn for the whole family of Betaine-Carnithine-Choline-Transporters based on data obtained from the the betaine permease BetP.

6 Zusammenfassung

Der sekundär aktive Glycinbetain Transporter BetP des Bodenbakteriums *Corynebacterium glutamicum* ist mittlerweile ein Paradigma für Transportproteine deren Aktivität durch die Osmolalität reguliert wird. BetP ist das einzige osmotisch regulierte Transportprotein für das die Sensordomäne bekannt und gleichzeitig strukturelle Information auf atomarer Ebene verfügbar ist. In verschiedenen Studien wurde gezeigt, dass BetP durch Erhöhung der internen Kaliumkonzentration sowohl *in vivo*, als auch *in vitro* aktiviert wird. Die Kaliumkonzentration wird durch die C-terminale hydrophile Domäne sensiert. Die Sensordomäne befindet sich auf der zytoplasmatischen Seite der Membran. Diese Domäne ist auch an der Ausbildung von Kontakten zwischen den einzelnen Protomeren des homotrimeren Transportproteins beteiligt. Es war weiterhin bekannt, dass Mutationen die mit der Assemblierung des Homotrimers interferieren, auch einen starken Einfluss auf die Regulation des Proteins zeigen. Weiterhin wurde in verschiedenen Studien eine konformationelle Asymmetrie zwischen verschiedenen Protomeren beobachtet. Aufgrund dieser Ergebnisse wurde eine funktionell relevante konformationelle Kopplung zwischen den Protomeren eines BetP Trimers vermutet. Für die Aktivierung des Proteins wurde weiterhin die Interaktion zwischen der C-terminalen Sensordomäne eines Protomers und Loop2 des Nachbarprotomers als unerlässlich betrachtet. Um die funktionelle Relevanz einer möglichen konformationellen Kopplung zwischen den Protomeren eines BetP Trimers zu testen wurden in der vorliegenden Arbeit artifizielle BetP Heterotrimere etabliert. Mithilfe dieser war es möglich jede Form der vorgeschlagenen Signaltransduktion zwischen den Protomeren auszuschliessen. Es konnte weiterhin gezeigt werden, dass diese Heterotrimere die Untersuchung der molekularen Dynamik von BetP mittels fluoreszenzspektroskopischer Methoden erlauben. Die osmotische Regulation *in vitro* ist bisher nur für drei Transportproteine bewiesen. In der vorliegenden Arbeit konnte diese Funktion auch für das Transportprotein LcoP von *C. glutamicum* nachgewiesen werden. Die Sensordomänen dieses Proteins konnten durch Mutagenesestudien aufgefunden werden. Es wurde gezeigt, dass LcoP ein vielversprechender Kandidat für strukturelle Studien ist und somit ein attraktives Testsystem für die Hypothesen darstellen könnte, die derzeit alle auf der Basis von BetP für die gesamte Betain-Carnithin-Cholin-Transporter Familie aufgestellt werden.

7 References

- Abramson, J. and Wright, E. M.** (2009). Structure and function of Na(+)-symporters with inverted repeats. *Current opinion in structural biology* **19**, 425–32.
- Biemans-Oldehinkel, E., Mahmood, N. A. B. N. and Poolman, B.** (2006). A sensor for intracellular ionic strength. *Proceedings of the National Academy of Sciences of the United States of America* **103**, 16–21.
- Boudker, O., Ryan, R. M., Yernool, D., Shimamoto, K. and Gouaux, E.** (2007). Coupling substrate and ion binding to extracellular gate of a sodium-dependent aspartate transporter. *Nature* **445**, 387–93.
- Bucher, M. H., Evdokimov, A. G. and Waugh, D. S.** (2002). Differential effects of short affinity tags on the crystallization of Pyrococcus furiosus maltodextrin-binding protein. *Acta Crystallographica Section D Biological Crystallography* **58**, 392–397.
- Casagrande, F., Ratera, M., Schenk, A. D., Chami, M., Valencia, E., Lopez, J. M., Torrents, D., Engel, A., Palacin, M. and Fotiadis, D.** (2008). Projection structure of a member of the amino acid/polyamine/organocation transporter superfamily. *The Journal of biological chemistry* **283**, 33240–8.
- Chung, C. T., Niemela, S. L. and Miller, R. H.** (1989). One-step preparation of competent Escherichia coli: transformation and storage of bacterial cells in the same solution. *Proceedings of the National Academy of Sciences of the United States of America* **86**, 2172–5.
- Culham, D. E., Henderson, J., Crane, R. A. and Wood, J. M.** (2003). Osmosensor ProP of Escherichia coli Responds to the Concentration, Chemistry, and Molecular Size of Osmolytes in the Proteoliposome Lumen. *Biochemistry* **42**, 410–420.
- Dalbey, R. E., Wang, P. and Kuhn, A.** (2011). Assembly of bacterial inner membrane proteins. *Annual review of biochemistry* **80**, 161–87.
- Davis, G. D., Elisee, C., Newham, D. M. and Harrison, R. G.** (1999). New Fusion Protein Systems Designed to Give Soluble Expression in Escherichia coli. *Biotechnology and Bioengineering* **65**, 382–388.
- Farwick, M., Siewe, R. M. and Krämer, R.** (1995). Glycine betaine uptake after hyperosmotic shift in Corynebacterium glutamicum. *Journal of bacteriology* **177**, 4690–5.

- Forrest, L. R.** (2013). (Pseudo-)symmetrical transport. *Science* **339**, 399–401.
- Forrest, L. R. and Rudnick, G.** (2009). The rocking bundle: a mechanism for ion-coupled solute flux by symmetrical transporters. *Physiology* **24**, 377–86.
- Forrest, L. R., Zhang, Y.-W., Jacobs, M. T., Gesmonde, J., Xie, L., Honig, B. H. and Rudnick, G.** (2008). Mechanism for alternating access in neurotransmitter transporters. *Proceedings of the National Academy of Sciences of the United States of America* **105**, 10338–43.
- Forrest, L. R., Krämer, R. and Ziegler, C.** (2011). The structural basis of secondary active transport mechanisms. *Biochimica et biophysica acta* **1807**, 167–88.
- Gao, X., Lu, F., Zhou, L., Dang, S., Sun, L., Li, X., Wang, J. and Shi, Y.** (2009). Structure and mechanism of an amino acid antiporter. *Science* **324**, 1565–8.
- Gärtner, R. M., Perez, C., Koshy, C. and Ziegler, C.** (2011). Role of bundle helices in a regulatory crosstalk in the trimeric betaine transporter BetP. *Journal of molecular biology* **414**, 327–36.
- Ge, L., Perez, C., Waclawska, I., Ziegler, C. and Muller, D. J.** (2011). Locating an extracellular K⁺-dependent interaction site that modulates betaine-binding of the Na⁺-coupled betaine symporter BetP. *Proceedings of the National Academy of Sciences of the United States of America* **108**, E890–8.
- Grant, S. G., Jessee, J., Bloom, F. R. and Hanahan, D.** (1990). Differential plasmid rescue from transgenic mouse DNAs into *Escherichia coli* methylation-restriction mutants. *Proceedings of the National Academy of Sciences of the United States of America* **87**, 4645–9.
- Grasberger, B., Minton, a P., DeLisi, C. and Metzger, H.** (1986). Interaction between proteins localized in membranes. *Proceedings of the National Academy of Sciences of the United States of America* **83**, 6258–62.
- Groeneveld, M. and Slotboom, D.-J.** (2007). Rigidity of the subunit interfaces of the trimeric glutamate transporter GltT during translocation. *Journal of molecular biology* **372**, 565–70.
- Haardt, M., Kempf, B., Faatz, E. and Bremer, E.** (1995). The osmoprotectant proline betaine is a major substrate for the binding-protein-dependent transport system ProU of *Escherichia coli* K-12. *Molecular & general genetics* **246**, 783–6.

- Hillar, A., Culham, D. E., Vernikovska, Y. I., Wood, J. M. and Boggs, J. M.** (2005). Formation of an Antiparallel , Intermolecular Coiled Coil Is Associated with in Vivo Dimerization of Osmosensor and Osmoprotectant Transporter ProP in Escherichia coli. *Biochemistry* **44**, 10170–10180.
- Inoue, H., Nojima, H. and Okayama, H.** (1990). High efficiency transformation of Escherichia coli with plasmids. *Gene* **96**, 23–28.
- Jardetzky, O.** (1966). A simple allosteric model for membrane pumps. *Nature* **221**, 996-970
- Kefala, G., Kwiatkowski, W., Esquivies, L., Maslennikov, I. and Choe, S.** (2007). Application of Mystic to improving the expression and membrane integration of histidine kinase receptors from Escherichia coli. *Journal of structural and functional genomics* **8**, 167–72.
- Kelley, L. A., MacCallum, R. M. and Sternberg, M. J.** (2000). Enhanced genome annotation using structural profiles in the program 3D-PSSM. *Journal of molecular biology* **299**, 499–520.
- Khafizov, K., Perez, C., Koshy, C., Quick, M., Fendler, K., Ziegler, C. and Forrest, L. R.** (2012). Investigation of the sodium-binding sites in the sodium-coupled betaine transporter BetP. *Proceedings of the National Academy of Sciences of the United States of America* **109**, E3035–44.
- Koch, A. L.** (2000). The Bacterium 's Way for Safe Enlargement and Division †. *Applied and Environmental Microbiology* **66**, 3657–3663.
- Krämer, R. and Morbach, S.** (2004). BetP of Corynebacterium glutamicum, a transporter with three different functions: betaine transport, osmosensing, and osmoregulation. *Biochimica et biophysica acta* **1658**, 31–6.
- Krishnamurthy, H. and Gouaux, E.** (2012). X-ray structures of LeuT in substrate-free outward-open and apo inward-open states. *Nature* **481**, 469–74.
- Krishnamurthy, H., Piscitelli, C. L. and Gouaux, E.** (2009). Unlocking the molecular secrets of sodium-coupled transporters. *Nature* **459**, 347–55.
- Kunte, H. J., Crane, R. A., Culham, D. E., Richmond, D., Wood, J. M. and Kunte, R. G.** (1999). Protein ProQ Influences Osmotic Activation of Compatible Solute Transporter ProP in Escherichia coli K-12. *Journal of bacteriology* **181**, 1537–1543.

- Kyhse-Andersen, J.** (1984). Electroblotting of multiple gels: a simple apparatus without buffer tank for rapid transfer of proteins from polyacrylamide to nitrocellulose. *Journal of biochemical and biophysical methods* **10**, 203–9.
- Lanquar, V. and Frommer, W. B.** (2010). Adjusting ammonium uptake via phosphorylation. *Plant Signaling & Behaviour* **5**, 736–738.
- Lanquar, V., Loqué, D., Hörmann, F., Yuan, L., Bohner, A., Engelsberger, W. R., Lalonde, S., Schulze, W. X., Von Wirén, N. and Frommer, W. B.** (2009). Feedback inhibition of ammonium uptake by a phospho-dependent allosteric mechanism in Arabidopsis. *The Plant cell* **21**, 3610–22.
- Lawrence, M. S., Phillips, K. J. and Liu, D. R.** (2007). Supercharging proteins can impart unusual resilience. *Journal of the American Chemical Society* **129**, 10110–2.
- Loqué, D., Lalonde, S., Looger, L. L. and Wire, N. Von** (2007). A cytosolic trans-activation domain essential for ammonium uptake. *Nature* **446**, 195–198.
- Mahmood, N. A. B. N., Biemans-Oldenhinkel, E. and Poolman, B.** (2009). Engineering of ion sensing by the cystathionine beta-synthase module of the ABC transporter OpuA. *The Journal of biological chemistry* **284**, 14368–76.
- Majumdar, D. S., Smirnova, I., Kasho, V., Nir, E., Kong, X., Weiss, S. and Kaback, H. R.** (2007). Single-molecule FRET reveals sugar-induced conformational dynamics in LacY. *Proceedings of the National Academy of Sciences of the United States of America* **104**, 12640–5.
- Möker, N., Brocker, M., Schaffer, S., Krämer, R., Morbach, S. and Bott, M.** (2004). Deletion of the genes encoding the MtrA-MtrB two-component system of *Corynebacterium glutamicum* has a strong influence on cell morphology, antibiotics susceptibility and expression of genes involved in osmoprotection. *Molecular microbiology* **54**, 420–38.
- Nicklisch, S. C. T., Wunnicke, D., Borovykh, I. V, Morbach, S., Klare, J. P., Steinhoff, H.-J. and Krämer, R.** (2012). Conformational changes of the betaine transporter BetP from *Corynebacterium glutamicum* studied by pulse EPR spectroscopy. *Biochimica et biophysica acta* **1818**, 359–66.
- Ott, V. M.** (2008). Der Regulationsmechanismus des Osmosensors BetP aus *Corynebacterium glutamicum*.

- Ott, V., Koch, J., Späte, K., Morbach, S. and Krämer, R.** (2008). Regulatory properties and interaction of the C- and N-terminal domains of BetP, an osmoregulated betaine transporter from *Corynebacterium glutamicum*. *Biochemistry* **47**, 12208–18.
- Özcan, N., Krämer, R., Morbach, S. and Kra, R.** (2005). Chill Activation of Compatible Solute Transporters in *Corynebacterium glutamicum* at the Level of Transport Activity. *Journal of bacteriology* **187**, 4752–4759.
- Özcan, N., Ejsing, C. S., Shevchenko, A., Lipski, A., Morbach, S. and Krämer, R.** (2007). Osmolality, temperature, and membrane lipid composition modulate the activity of betaine transporter BetP in *Corynebacterium glutamicum*. *Journal of bacteriology* **189**, 7485–96.
- Perez, C., Koshy, C., Ressler, S., Nicklisch, S., Krämer, R. and Ziegler, C.** (2011). Substrate specificity and ion coupling in the Na⁺/betaine symporter BetP. *The EMBO journal* **30**, 1221–9.
- Perez, C., Khafizov, K., Forrest, L. R., Krämer, R. and Ziegler, C.** (2011). The role of trimerization in the osmoregulated betaine transporter BetP. *EMBO reports* **12**, 804–10.
- Perez, C., Koshy, C., Yildiz, O. and Ziegler, C.** (2012). Alternating-access mechanism in conformationally asymmetric trimers of the betaine transporter BetP. *Nature* **490**, 126–30.
- Peter, H., Burkovski, A. and Krämer, R.** (1996). Isolation, characterization, and expression of the *Corynebacterium glutamicum* betP gene, encoding the transport system for the compatible solute glycine betaine. *Journal of bacteriology* **178**, 5229–34.
- Peter, H., Burkovski, a and Krämer, R.** (1998). Osmo-sensing by N- and C-terminal extensions of the glycine betaine uptake system BetP of *Corynebacterium glutamicum*. *The Journal of biological chemistry* **273**, 2567–74.
- Peter, H., Weil, B., Burkovski, a, Krämer, R. and Morbach, S.** (1998). *Corynebacterium glutamicum* is equipped with four secondary carriers for compatible solutes: identification, sequencing, and characterization of the proline/ectoine uptake system, ProP, and the ectoine/proline/glycine betaine carrier, EctP. *Journal of bacteriology* **180**, 6005–12.

- Piscitelli, C. L., Krishnamurthy, H. and Gouaux, E.** (2010). Neurotransmitter/sodium symporter orthologue LeuT has a single high-affinity substrate site. *Nature* **468**, 1129–32.
- Porath, J., Carlsson, J., Olsson, I. and Belfrage, G.** (1975). Metal chelate affinity chromatography, a new approach to protein fractionation. *Nature* **258**, 598–9.
- Quick, M., Shi, L., Zehnpfennig, B., Weinstein, H. and Javitch, J. A.** (2012). Experimental conditions can obscure the second high-affinity site in LeuT. *Nature structural & molecular biology* **19**, 207–11.
- Racher, K. I., Culham, D. E. and Wood, J. M.** (2001). Requirements for Osmosensing and Osmotic Activation of Transporter ProP from Escherichia coli. *Biochemistry* **40**, 7324–7333.
- Ressl, S., Terwisscha van Scheltinga, A. C., Vorrhein, C., Ott, V. and Ziegler, C.** (2009). Molecular basis of transport and regulation in the Na(+)/betaine symporter BetP. *Nature* **458**, 47–52.
- Reyes, N., Ginter, C. and Boudker, O.** (2009). Transport mechanism of a bacterial homologue of glutamate transporters. *Nature* **462**, 880–5.
- Rigaud, J.-L. and Lévy, D.** (2003). Reconstitution of membrane proteins into liposomes. *Methods in enzymology* **372**, 65–86.
- Romantsov, T., Stalker, L., Culham, D. E. and Wood, J. M.** (2008). Cardiolipin controls the osmotic stress response and the subcellular location of transporter ProP in Escherichia coli. *The Journal of biological chemistry* **283**, 12314–23.
- Romantsov, T., Battle, A. R., Hendel, J. L., Martinac, B. and Wood, J. M.** (2010). Protein localization in Escherichia coli cells: comparison of the cytoplasmic membrane proteins ProP, LacY, ProW, AqpZ, MscS, and MscL. *Journal of bacteriology* **192**, 912–24.
- Rösgen, J., Pettitt, B. M. and Bolen, D. W.** (2005). Protein folding, stability, and solvation structure in osmolyte solutions. *Biophysical journal* **89**, 2988–97.
- Rübenhagen, R., Rönsch, H., Jung, H., Krämer, R. and Morbach, S.** (2000). Osmosensor and osmoregulator properties of the betaine carrier BetP from Corynebacterium glutamicum in proteoliposomes. *The Journal of biological chemistry* **275**, 735–41.
- Rübenhagen, R., Morbach, S. and Krämer, R.** (2001). The osmoreactive betaine carrier BetP from Corynebacterium glutamicum is a sensor for cytoplasmic K⁺. *The EMBO journal* **20**, 5412–20.

- Saier, M. H.** (2000). Families of transmembrane transporters selective for amino acids and their derivatives. *Microbiology* **146**, 1775–1795.
- Saier, M. H., Beatty, J. T., Goffeau, A., Harley, K. T., Heijne, W. H. M., Huang, S., Jack, D. L., Jähn, P. S., Lew, K., Liu, J., et al.** (1999). The Major Facilitator Superfamily. *Journal of Molecular Biology and Biotechnology* **1**, 257–279.
- Schaffner, W. and Weissmann, C.** (1973). A Rapid , for Sensitive , the in Dilute and Specific of Method Protein Determination Solution. *Analytical biochemistry* **56**, 502–514.
- Schägger, H. and Von Jagow, G.** (1987). Tricine-sodium dodecyl sulfate-polyacrylamide gel electrophoresis for the separation of proteins in the range from 1 to 100 kDa. *Analytical biochemistry* **166**, 368–79.
- Schiller, D. and Morbach, S.** (2004). The C-Terminal Domain of the Betaine Carrier BetP of *Corynebacterium glutamicum* Is Directly Involved in Sensing K⁺ as an Osmotic Stimulus. *Biochemistry* **43**, 5583–5591.
- Schiller, D., Krämer, R. and Morbach, S.** (2004). Cation specificity of osmosensing by the betaine carrier BetP of *Corynebacterium glutamicum*. *FEBS letters* **563**, 108–12.
- Schiller, D., Ott, V., Krämer, R. and Morbach, S.** (2006). Influence of Membrane Composition on Osmosensing by the Betaine Carrier BetP from *Corynebacterium glutamicum*. *The Journal of biological chemistry* **281**, 7737–7746.
- Schmidt, T. G., Koepke, J., Frank, R. and Skerra, a** (1996). Molecular interaction between the Strep-tag affinity peptide and its cognate target, streptavidin. *Journal of molecular biology* **255**, 753–66.
- Schroers, A., Burkovski, A., Wohlrab, H. and Krämer, R.** (1998). The Phosphate Carrier from Yeast Mitochondria. *The Journal of biological chemistry* **273**, 14269–14276.
- Schulze, S., Köster, S., Geldmacher, U., Terwisscha van Scheltinga, A. C. and Kühlbrandt, W.** (2010). Structural basis of Na⁽⁺⁾-independent and cooperative substrate/product antiport in CaiT. *Nature* **467**, 233–6.
- Shaffer, P. L., Goehring, A., Shankaranarayanan, A. and Gouaux, E.** (2009). Structure and mechanism of a Na⁺-independent amino acid transporter. *Science* **325**, 1010–4.
- Shi, L., Quick, M., Zhao, Y., Weinstein, H. and Javitch, J. a** (2008). The mechanism of a neurotransmitter:sodium symporter--inward release of Na⁺ and substrate is triggered by substrate in a second binding site. *Molecular cell* **30**, 667–77.

- Shimamura, T., Weyand, S., Beckstein, O., Rutherford, N. G., Hadden, J. M., Sharples, D., Sansom, M. S. P., Iwata, S., Henderson, P. J. F. and Cameron, A. D.** (2010). Molecular basis of alternating access membrane transport by the sodium-hydantoin transporter Mhp1. *Science* **328**, 470–3.
- Skerra, A.** (1994). Use of the tetracycline promoter for the tightly regulated production of a murine antibody fragment in *Escherichia coli*. *Gene* **151**, 131–5.
- Smith, M. N., Crane, R. a, Keates, R. a B. and Wood, J. M.** (2004). Overexpression, purification, and characterization of ProQ, a posttranslational regulator for osmoregulatory transporter ProP of *Escherichia coli*. *Biochemistry* **43**, 12979–89.
- Sonoda, Y., Newstead, S., Hu, N.-J., Alguel, Y., Nji, E., Beis, K., Yashiro, S., Lee, C., Leung, J., Cameron, A. D., et al.** (2011). Benchmarking membrane protein detergent stability for improving throughput of high-resolution X-ray structures. *Structure* **19**, 17–25.
- Steger, R., Weinand, M., Krämer, R. and Morbach, S.** (2004). LcoP, an osmoregulated betaine/ectoine uptake system from *Corynebacterium glutamicum*. *FEBS letters* **573**, 155–60.
- Steiner-Mordoch, S., Soskine, M., Solomon, D., Rotem, D., Gold, A., Yechieli, M., Adam, Y. and Schuldiner, S.** (2008). Parallel topology of genetically fused EmrE homodimers. *The EMBO journal* **27**, 17–26.
- Sukharev, S. I., Blount, P., Martinac, B. and Kung, C.** (1997). Mechanosensitive channels of *Escherichia coli*: the MscL gene, protein, and activities. *Annual review of physiology* **59**, 633–57.
- Takatsuka, Y. and Nikaido, H.** (2009). Covalently Linked Trimer of the AcrB Multidrug Efflux Pump Provides Support for the Functional Rotating Mechanism. *Journal of bacteriology* **191**, 1729–1737.
- Tanford, C.** (1983). Translocation pathway in the catalysis of active transport. *Proceedings of the National Academy of Sciences of the United States of America* **80**, 3701–5.
- Tang, L., Bai, L., Wang, W. and Jiang, T.** (2010). Crystal structure of the carnitine transporter and insights into the antiport mechanism. *Nature structural & molecular biology* **17**, 492–6.
- Towbin, H., Staehelint, T. and Gordon, J.** (1979). Electrophoretic transfer of proteins from polyacrylamide gels to nitrocellulose sheets: Procedure and some applications.

- Proceedings of the National Academy of Sciences of the United States of America* **76**, 4350–4354.
- Tsai, C., Khafizov, K., Hakulinen, J., Forrest, L. R., Krämer, R., Kühlbrandt, W. and Ziegler, C.** (2011). Structural Asymmetry in a Trimeric Na⁺ / Betaine Symporter , BetP , from *Corynebacterium glutamicum*. *Journal of Molecular Biology* **407**, 368–381.
- Tsatskis, Y., Khambati, J., Dobson, M., Bogdanov, M., Dowhan, W. and Wood, J. M.** (2005). The Osmotic Activation of Transporter ProP Is Tuned by Both Its C-terminal Coiled-coil and Osmotically Induced Changes in Phospholipid Composition. *The Journal of biological chemistry* **280**, 41387–41394.
- Van der Heide, T. and Poolman, B.** (2000). Osmoregulated ABC-transport system of *Lactococcus lactis* senses water stress via changes in the physical state of the membrane. *Proceedings of the National Academy of Sciences of the United States of America* **97**, 7102–6.
- Van der Heide, T., Stuart, M. C. and Poolman, B.** (2001). On the osmotic signal and osmosensing mechanism of an ABC transport system for glycine betaine. *The EMBO journal* **20**, 7022–32.
- Watanabe, A., Choe, S., Chaptal, V., Rosenberg, J. M., Wright, E. M., Grabe, M. and Abramson, J.** (2010). The mechanism of sodium and substrate release from the binding pocket of vSGLT. *Nature* **468**, 988–991.
- Wood, J. M.** (1999). Osmosensing by bacteria: signals and membrane-based sensors. *Microbiology and molecular biology reviews* **63**, 230–62.
- Yamashita, A., Singh, S. K., Kawate, T., Jin, Y. and Gouaux, E.** (2005). Crystal structure of a bacterial homologue of Na⁺/Cl⁻-dependent neurotransmitter transporters. *Nature* **437**, 215–23.
- Zhao, Y., Terry, D., Shi, L., Weinstein, H., Blanchard, S. C. and Javitch, J. A.** (2010). Single-molecule dynamics of gating in a neurotransmitter transporter homologue. *Nature* **465**, 188–93.
- Zhao, Y., Terry, D. S., Shi, L., Quick, M., Weinstein, H., Blanchard, S. C. and Javitch, J. A.** (2011). Substrate-modulated gating dynamics in a Na⁺-coupled neurotransmitter transporter homologue. *Nature* **474**, 109–13.
- Ziegler, C., Morbach, S., Schiller, D., Krämer, R., Tziatzios, C., Schubert, D. and Kühlbrandt, W.** (2004). Projection structure and oligomeric state of the osmoregulated

sodium/glycine betaine symporter BetP of *Corynebacterium glutamicum*. *Journal of molecular biology* **337**, 1137–47.

Ziegler, C., Bremer, E. and Krämer, R. (2010). The BCCT family of carriers: from physiology to crystal structure. *Molecular microbiology* **78**, 13–34.

Danksagung

Ich danke Herrn Prof. Krämer herzlich für die freundliche und unerwartete Wiederaufnahme in seine Gruppe, die Überlassung des anspruchsvollen Themas und seine unermüdliche Diskussionsbereitschaft zu jeder Tageszeit sowie seiner grenzenlosen Zuversicht mit der er ja letztendlich Recht behalten hat.

Herrn Prof. Flügge danke ich für die freundliche Übernahme des Koreferats.

An erster Stelle der fakultativen Listung danke ich meiner Muse, meinem gleißenden Licht: Frau Dr. Julia Camps für alles. Ohne sie hätte ich wohl nicht den Wechsel von primär zu sekundär aktiv vollzogen.

Ich danke meinem Bruder Stefan für die wesentliche Aufwertung unseres technischen Equipments.

Desweiteren möchte ich mich herzlich bei dem gesamten technischen Personal der AG und des Instituts für stetige Unterstützung bedanken insbesondere bei: Ute Meyer, Anja Wittmann, Gabi Sitek und Eva Glees.

Natürlich sei auch unseren Sekretärinnen Claudia Beumers, Doro Grzelak und Judith Pinger für administrative Unterstützung gedankt.

Besonderer Dank gebührt auch allen Wissenschaftlern, die mich seit meinem Studium angeleitet haben: Dr. Martin Follmann, Dr. Kay Marin, Dr. Christian Schölz (FFM), Dr. David Parcej (FFM) und Prof. Robert Tampé (FFM).

Ich danke unseren Kollaborationspartnern die der zentralen Fragestellung dieser Arbeit zu einer herausragenden Bedeutung verholfen haben: Insbesondere genannt seien hier Prof. Christine Ziegler (FFM/Regensburg), Dr. Camilo Perez (FFM) und Rebecca Gärtner (FFM).

Desweiteren sei auch den single molecule FRET Kollaborateuren, Prof. Claus Seidel, Dr. Jakub Kubiak und Dr. Hugo Sanabaria (Düsseldorf) dafür gedankt, dass sie sich mit ihrer ausgefeilten Technik unserer Heterotrimere annehmen.

Danke auch an alle ehemaligen und aktuellen Mitglieder der AG für das tolle Arbeitsklima: Martin Catriona Sascha Phillip Ines Steffi Jens Jeanine Astrid Inga Vera Manaf Elena Caro Gerd Susanne Nina Kay Marc Boris Juri Frank Alex Alex Andi Natalie Anna Katja Dimitar und Allen die ich hier auf die Schnelle vergessen habe.

Natürlich danke ich im speziellen der Osmo Gang: Michael und Stan und seit neuestem auch Benni.

Danken möchte ich auch Jan für gutes Essen und viel französischen Rotwein aus Frankreich und Karin für die kompetente Unterstützung bei der Planung von Tagungsreisen.

Auch Anka und Mr. Pink sollen nicht unerwähnt bleiben

Am Ende bleibt nur noch meiner Familie zu danken: Opa für Logis, meinen Eltern für die Ermöglichung des Studiums und ausserdem dafür, dass mir immer die Möglichkeit zum notwendigen Ausgleich in solider Landarbeit gegeben ist.

Erklärung

Ich versichere, dass ich die von mir vorgelegte Dissertation selbständig angefertigt, die benutzten Quellen und Hilfsmittel vollständig angegeben und die Stellen der Arbeit – einschließlich Tabellen, Karten und Abbildungen –, die anderen Werken im Wortlaut oder dem Sinn nach entnommen sind, in jedem Einzelfall als Entlehnung kenntlich gemacht habe; dass diese Dissertation noch keiner anderen Fakultät oder Universität zur Prüfung vorgelegen hat; dass sie – abgesehen von unten angegebenen Teilpublikationen – noch nicht veröffentlicht worden ist sowie, dass ich eine solche Veröffentlichung vor Abschluss des Promotionsverfahrens nicht vornehmen werde.

Die Bestimmungen der Promotionsordnung sind mir bekannt. Die von mir vorgelegte Dissertation ist von Herrn Prof. Dr. Reinhard Krämer betreut worden.

(Markus Becker)